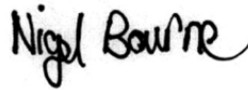**The Thesis Committee for Courtney Parker Cromer Certifies that this is the approved version of the following Thesis:**

Characterization of a recombinant chimeric yellow fever 17D vaccine - dengue-4 virus

Committee:

(signature)

Alan Barrett, PhD, Supervisor

(signature)

Nigel Bourne, PhD

(signature)

Alexander Freiberg, PhD

Dean, Graduate School

Characterization of a recombinant chimeric yellow fever 17D vaccine - dengue-4 virus

by

Courtney Parker Cromer B.S.

Thesis

Presented to the Faculty of the Graduate School of

The University of Texas Medical Branch

in Partial Fulfillment

of the Requirements

for the Degree of

Master of Science

The University of Texas Medical Branch
January 2018

This is dedicated to my family and those who believed in me.

Acknowledgements

I would like to acknowledge my mentor, Alan Barrett, and my thesis committee, Nigel Bourne and Alexander Frieberg, for their valuable advice and input. I would also like to acknowledge my lab mates and lab coordinator, without which none of this would have been possible. A special thanks to my parents and my husband, who kept me going when I thought that I couldn't keep going anymore, and for the sacrifices that they have made to get me to where I am today.

CHARACTERIZATION OF A RECOMBINANT CHIMERIC YELLOW FEVER 17D VACCINE -

DENGUE-4 VIRUS

Publication No._____

Courtney Parker Cromer, M.S.

The University of Texas Medical Branch, 2018

Supervisor: Alan D.T. Barrett

The disease dengue is caused by four genetically and serologically related virus termed dengue virus-1 to dengue virus-4 (DENV-1 to DENV-4) There are currently no licensed therapeutics, but there is a recently licensed recombinant live attenuated tetravalent vaccine, termed Dengvaxia™ by Sanofi Pasteur, available in some countries. This vaccine was based on Chimerivax™ technology where recombinant DNA technology was used to generate vaccine viruses based on a backbone of the yellow fever virus 17D (YFV-17D) vaccine virus with the structural components premembrane and envelope (prME) of a corresponding wild-type DENV. This thesis investigated the impact of viral chimerization on a YFV-17D infectious clone where the 17D prME genes were replaced with those of the sylvatic wild-type DEN-4 strain P75-215, hereafter termed YFV 17D/DENV-4 prME chimera. Viral RNA of 17D vaccine, wild-type DENV-4, and YFV 17D/DENV-4 prME chimera were compared by Next Generation Sequencing (NGS), which indicated that the YFV-17D/DENV-4 prME chimera has a similar genetic diversity profile to YFV-17D, exemplified by a low diversity profile across the genome. However, the YFV 17D/DENV-4 prME chimera exhibited lower diversity indices than that of YFV-17D in some gene regions, including C, prM, NS2B, and NS4B, 5'UTR. Compared to WT DENV-4, the YFV- 17D/DENV-4 prME chimera was less diverse, suggesting that chimerization lowers the genetic diversity of the virus. The phenotype of the YFV-17D/DENV-4 prME chimera was investigated in cell culture and animals. Multiplication kinetics indicate that the YFV-17D/DENV-4 chimera was functionally more like that of YFV-17D than that of DENV-4, while in vivo in interferon $\alpha\beta\gamma$ receptor deficient (AG129) mice the chimeric YFV 17D/DENV-4 prME virus was more virulent than either YFV-17D and DENV-4 parental viruses. It is hypothesized that the process of chimerization results in reduced genetic diversity indices of viruses, which may be linked attenuation of the virus, and may be important in development of chimeric flavivirus vaccine candidates. However, the chimera was not attenuated in the mouse model used and this may be due to the immunocompromised AG129 mouse model.

TABLE OF CONTENTS

List of Tables

List of Figures

List of Abbreviations

+ssRNA: positive single stranded ribonucleic acid

ADE: antibody dependent enhancement

AST: average survival time

B.C.: before Christ

C: capsid protein

CO_2: carbon dioxide

CPE: cytopathic effect

DC: dendritic cell

DENV: Dengue virus

DMEM: Dulbecco's modified Eagle medium

dNTP: deoxyribonucleotide triphosphates

E: envelope protein

ER: endoplasmic reticulum

ER: endoplasmic reticulum

FBS: fetal bovine serum

i.c.: intracranial

i.p.: intraperitoneal

i.v.: intravenous

IFN: interferon

JE: Japanese encephalitis

JEV: Japanese encephalitis virus

kB: kilobases

M: membrane protein

mL: milliliter

mm: millimeter

MOI: multiplicity of infection

NEAA: non-essential amino acids

NGS: next generation sequencing

NHP: non-human primate

nm: nanometer

NS: nonstructural

ORF: open reading frame

PBS: phosphate buffered saline

PDK: primary dog kidney

PFU: plaque forming units

polyA: poly adenine

RdRp: RNA dependent RNA polymerase

RPM: rotations per minute

s.c.: subcutaneous

SCID: severe immunodeficiency

TBEV: tick borne encephalitis virus

TLR: toll-like receptor

UTR: untranslated region

WHO: World Health Organization

WNF: West Nile fever

WNV: West Nile Virus

WRAIR: Walter Reed Army Institute of Research

WT: wild-type

YFV 17D: yellow fever virus 17D vaccine strain

YFV: Yellow fever virus

ZIKV: Zika virus

μg: microgram

μL: microliter

Chapter 1: Introduction

Flaviviruses

Flaviviruses are members of the genus *Flavivirus*, family *Flaviviridae,* which are small, icosahedral enveloped viruses that are approximately 50 nm in diameter (1). Flaviviruses have a positive-sense, single-stranded ribonucleic acid (+ssRNA) genome, which is typically about 11 kilobases (kB) in length (1). Yellow fever virus (YFV) is the prototypical member of the *Flaviviridae*, and the name *Flaviviridae* was derived from the Latin term *flavus*, which means yellow; this refers to the characteristic jaundice that is observed in patients that are infected with YFV. The *Flaviviridae* family includes major human pathogens, such as YFV, Japanese encephalitis virus (JEV), dengue virus (DENV), West Nile virus (WNV), tick borne encephalitis virus (TBEV), and Zika virus (ZIKV). These viruses cause a variety of disease presentations, ranging from hemorrhagic disease (e.g., YFV), to shock syndrome (e.g., DENV), febrile illnesses (e.g., DENV and ZIKV), encephalitic disease (e.g., WNV, TBE, and JEV), congenital/prenatal disease manifestations (e.g., ZIKV), and asymptomatic infections. There are currently no licensed antivirals available for any flavivirus, and there are only a few licensed vaccines available (see below in section 1.7). Many of the members of the genus *Flavivirus* are arthropod-borne viruses (or arboviruses). Arboviruses are transmitted by arthropods, such as mosquitoes or ticks, to vertebrate hosts, such as mammals). Many of these viruses infect and may cause pathology in the vertebrate host (1). As such, there are many natural vectors and reservoirs for flaviviruses. Due to the lack of availability of antivirals, and the

limited availability of vaccines, flaviviruses constitute an important public health threat in terms of both current and potential emerging infectious diseases.

CLASSIFICATION

The *Flaviviridae* family includes the genera *Flavivirus, Pestivirus, Hepacivirus*, and *Pegivirus* (1). The *Flavivirus* genus consists of over seventy viruses, including the prototypical YFV; more than 50 of the viruses in this genus have been demonstrated to infect humans. There are also a variety of other virus species in this genus, including insect-specific viruses and animal only viruses (2). Typically, these viruses are categorized into four separate groups: viruses with no known vector, tick-borne viruses, insect-specific viruses, and mosquito-borne viruses (2, 3). These can be further broken down into categories based on species of vector and phylogenetic relationships. These clusters are as follows: *Culex* species (ornithophilic, or bird loving) associated mosquito-borne flaviviruses, *Aedes* species (mammalophilic, or mammal loving) associated mosquito-borne flaviviruses, no known vector-like viruses, tick-borne flaviviruses, and no known vector specific lineage viruses (2). These can be further subdivided. For example, the pathogenic tick-borne viruses are typically associated with *Ixodes* species ticks, and the nonpathogenic are typically associated with *Ornithodorus* species ticks. The viruses that fall into the cluster of no known vector are usually those that infect either rodents or bats, and are thought to have diverged alongside the mosquito-borne flavivirus group, but have perhaps lost this relationship with the mosquito vector. These relationships are demonstrated in **Figure 1.1** (2). Additional studies have demonstrated that some flaviviruses can be broken down into eight serogroups, which are based upon cross-neutralization tests in cell culture with

14

polyclonal sera (4). These complexes are: the tick-borne encephalitis, Rio Bravo, JE, Tyuleniy, Ntaya, Uganda S, DEN, and Modoc complexes, plus 17 viruses that did not serologically cross-reactive with any of the complexes, including YFV (4). It is hypothesized that the genus *Flavivirus* has emerged from mammalian viruses which had no arthropod vectors, and that the mosquito-borne viruses originate from Africa (5).

STRUCTURE & GENOME

The flavivirus virion consists of the RNA genome, surrounded by capsid (C) protein and a lipid bilayer envelope that is obtained from the host cell (6). Located within this membrane are the viral proteins envelope (E) and membrane (M). The E and M proteins coat the surface of the virion, and both proteins contain portions that are transmembrane and membrane adjacent (6). The M protein is the mature version of the precursor viral protein, pre-membrane (prM), and is held in the membrane via two transmembrane alpha helices (7). The E protein is arranged in 90 homodimers in the mature form of the virion; that lie parallel to the surface of the virion in raft formations, forming a herringbone pattern (7). In mature virions, there are no physical interaction between either the E or M proteins with the C proteins (7). There are two dominant forms of the virion, mature (containing M protein) and immature (containing prM protein), but recent work has demonstrated the flaviviruses appear to have a range of conformational variants between these two extremes, with variable amounts of prM and/or M protein in various virions, and different presentations of the E protein (7, 8). The mature form of the virion appears to have a 'golf ball' like structure, and is smooth, while the immature or intermediate forms of the virion exhibit a 'rough' appearance (8). This change in appearance is due to differences in the conformation of the E protein of the virus.
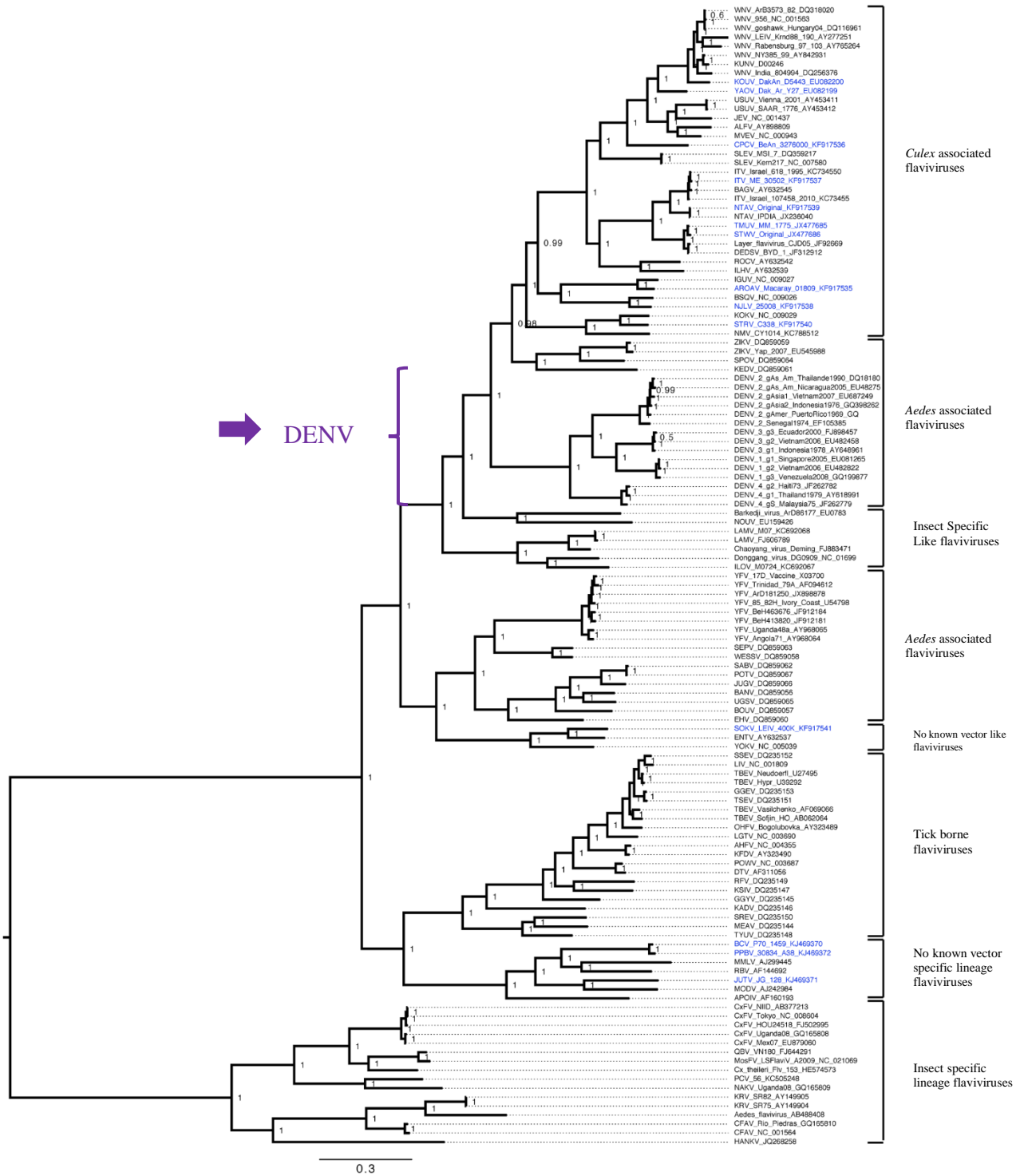
Figure 1.1. Phylogeny of flaviviruses and vector grouping, adapted from Moureau et al. 2015. The purple line and arrow is indicative the DENV grouping. DENV grouping has been specifically pointed out, as this is the predominant focus of this thesis.

At neutral pH, the E protein occurs in a dimeric form; these dimers lie parallel to the virion's surface, producing the smooth, 'golf ball' like structure (9). The rough appearance that is observed in the intermediate, immature form of the virion is caused by the formation of a trimer of E proteins, which are presented perpendicular to the virion's surface; this is induced by the low pH change that occurs upon viral entry, making the environment more acidic (9).

The genome contains a 5' untranslated region (UTR) with a 5' m^7G cap, and a 3' UTR with no polyA tail that flank a single, long open reading frame (ORF), which is approximately 3,500 amino acids in length and encodes the virus-encoded genes in the order 5'UTR -C-M(prM)-E-nonstructural protein 1(NS1)-NS2A-NS2B-NS3-NS4A-NS4B-NS5-3'UTR (10). These untranslated regions are thought to form secondary structures that are necessary for replication and translation of the viral genome (1). The 5' m^7G cap structure is required for the initiation of translation in the genus *Flavivirus* (1). The ORF is translated as one large polyprotein, that is co-and post-translationally processed to generate the three structural proteins and seven NS proteins (8). The NS proteins form the replication complex that are responsible for replication of the viral RNA genome and production of virions. In addition, the viral NS proteins contribute to antagonism of the host innate immune response (8, 11). Each of these individual proteins are cleaved via either host or viral proteases; the major host proteases are furin and signal-peptidase (12, 13). The genome is shown in **Figure 1.2.** Each of the virus-encoded proteins serves a variety of functions, some of which are poorly characterized. The C protein is responsible for encapsulating the viral genome; the prM protein has a dual function: it serves as a chaperone for the E protein and covers the fusion peptide to

prevent premature fusion of the viral particle with the host endoplasmic reticulum (ER) (12–14). It is also the precursor to the mature M protein found in virions, although prM is found in immature virus particles. The E protein is responsible for entry of the virus into cells and fusion with the membrane, and contains important epitopes that elicit neutralizing antibodies (12, 13, 15). NS1 and NS2A have many putative functions, but are mostly thought to be responsible for viral replication and assembly (12, 13). However, NS1 is unusual in that it is glycosylated (at two sites for YFV and DENV) and exist as dimers and hexamers inside the cell and secreted from cells, respectively.

NS1 is responsible for contributing to immune complex formation, immune evasion (via inhibition of the classical/lectin pathway of complement activation, as well as inhibition of toll-like receptor (TLR) signaling), and pathogenesis (via secretion of NS1 in to the circulation) (16). NS2A is thought to play other roles besides participation in the replication complex, such as virion assembly and contribution to the cytopathic effect (CPE) of the virus (17–19). The central region of NS2B is an important cofactor for the NS3 protease. The NS3 is a multifunctional enzyme and encodes a serine protease and helicase domains (including nucleoside 5' triphosphatase), and aids in RNA capping (20). NS4A is thought to be important in remodeling of the endoplasmic reticulum's (ER) membrane for replication, NS4B for host immune evasion/inhibition, and NS5 encodes a methyltransferase, which facilitates capping of the RNA, and the RNA dependent RNA polymerase (RdRp) domains (12, 13, 20). A summary of the functions of each of the viral proteins can be found in **Table 1.1**.

LIFE CYCLE

Flaviviruses enter the cell via receptor-mediated endocytosis; however, while putative receptor molecules have been proposed in many studies, none has yet to be confirmed by multiple groups. Examples of these receptors include, phosphatidyl-serine receptors for DENV, WNV, and YFV; heat-shock proteins for DENV and JEV; high-density lipoprotein receptors for DENV; and natural killer cell activating receptor proteins for DENV and WNV (14). In addition, co-receptor molecules have been identified that mediate non-specific binding of virus to cells, which include heparan sulfate (or other glycosaminoglycans) and C-type lectins (14). Once flaviviruses enter the cell via this receptor-mediated endocytosis, the endosome undergoes a pH change to an acidic pH that causes the trimerization of the E protein, which is irreversible (8). This, in turn, leads to the fusion of the viral membrane and the host's endosomal membrane (8). This allows the nucleocapsid, which encapsulates the genome, to be released into the cytoplasm of the host cell; the C and the RNA dissociate at this point, thus allowing the RNA genome to begin the replication process (8). Once the viral RNA is in the cytoplasm, it is co- and post-translationally processed by the viral and host proteases to yield the viral proteins (8). This process occurs on intracellular membranes; the polyprotein is then transitioned to the ER to undergo further processing, where the virus particles are assembled in the ER as immature particles containing prM (8). Subviral particles may also be produced in the ER; these are particles containing the E and prM proteins, but they do not have C protein or genomic RNA, hence making them non-infectious (8). The virus particle then moves to the trans-Golgi network, which allows the cleavage of prM to M, and maturation of the virion, allowing the virus particle to become infectious (8). The mature
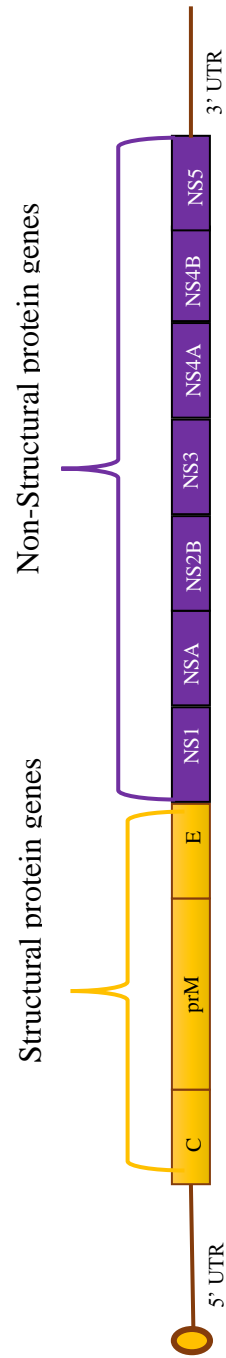
Figure 1.2 Schematic of the genome of flaviviruses. The ⬭ represents the m^{7}G cap.

virions (as well as subviral particles) are released from the cell via exocytosis (8). A depiction of the replication complex is shown in **Figure 1.3**.

DENGUE VIRUS

      The disease dengue is caused by four serologically and genetically distinct viruses termed dengue virus -1 to dengue virus-4 (DENV-1 to DENV-4). The transmission cycle involves *Aedes* species and primates; typically, the cycle is *Ae. aegypti* and humans. The disease has variable clinical manifestations, including dengue fever, dengue shock syndrome, and dengue hemorrhagic fever (DHF). There are thought to be 100 million clinical dengue (DEN) infections annually; of these, 2.1 million are thought to be severe DEN infections with 500,000 exhibiting DHF; 90%, or 450,000, occur in children (21). It is thought that infection elicits a life-time serologically specific immunity to the infecting serotype, as well as short term heterotypic cross DENV-immunity; for example, if someone is infected with DENV-1, they have life-time immunity to DENV-1, but only short-term immunity (months) to DENV-2, DENV-3, and DENV-4 (22). DEN is one of the fastest growing mosquito-borne diseases in the world today, with disease reported in at least 128 countries worldwide, and about one half of the world's inhabitants are now in jeopardy of being infected with DEN (23).

These mosquito-borne viruses are typically transmitted in one or a combination of three transmission cycles: sylvatic, human/endemic, and rural. The sylvatic cycle occurs in jungle or very sparsely populated areas, and typically occurs between monkey and various *Aedes* mosquito species, depending on the geographic region, with maintenance involving vertical transmission between mosquitoes and offspring (24). The rural transmission cycle occurs in a zone of emergence, in which there may be villages, or

humans may be entering jungle areas to hunt or search for food (24). In this transmission

cycle, mosquito species that are typically found in the sylvatic transmission cycle may

also be found in this zone of emergence, and the ability to infect humans with spill over

into human populations in this manner (24). The final documented transmission cycle is

that of the human/endemic cycle. This cycle typically occurs in urban environments, and

viral maintenance occurs via cycling between humans and mosquito species, with

teratogenic maintenance occurring again between mosquitoes and offspring (24).

History

Early descriptions of symptoms corresponding to illness like DEN have been found in

early Chinese literature, dating back to approximately 265 before Christ (BC) (25). In

these historical texts, the disease was referred to as 'water poison', which was due to its

seeming relationship with insects that seemed to associate with water (26). Symptoms of

this illness included rash, arthralgia, myalgia, fever, and hemorrhagic manifestations (26).

From this time period and region, the next occurrence of a similar disease occurs almost

seven centuries later, in the French West Indies and Panama; this occurs in the 1600s and

is described as an acute illness that exhibits long convalescence (25). Nearly a century

later, in the late 1700s, there were reports of a putative DEN pandemic occurring in

Batavia (which is present day Jakarta) as well as Cairo, Philadelphia, and Spain (26).

This appears to be the first demonstration of a wide-spread, global DENV distribution, or

at least a similar illness (26).

There is much discussion on the geographical origin of DENV. Some argue for an

African origin, due to the fact that this is also the origin of the current mosquito vector,

Aedes aegypti (26, 27). Some work, however, disputes this claim. Serological and

Protein	Function
Capsid (C)	Encapsulates virion and RNA
Premembrane/Membrane (prM/M)	E protein chaperone for folding, stabilization of virus during maturation, covers fusion peptide (preventing premature fusion)
Envelope (E)	Receptor binding, membrane fusion, neutralizing antibody induction
Nonstructural 1 (NS1)	RNA replication complex, immune complex formation, immune evasion, possible pathogenesis of virus
NS2A	Replication complex, virion assembly, and contribution to the cytopathic effect
NS2B	Replication complex, NS3 cofactor
NS3	Replication complex, serine protease, helicase, nucleoside triphosphatase, RNA capping
NS4A	Replication complex, endoplasmic membrane protein, ER remodeling
NS4B	Replication complex, endoplasmic membrane protein, immune evasion
NS5	Replication complex, RdRp, methyltransferase, RNA capping

Table 1.1. Each flavivirus protein and putative function.
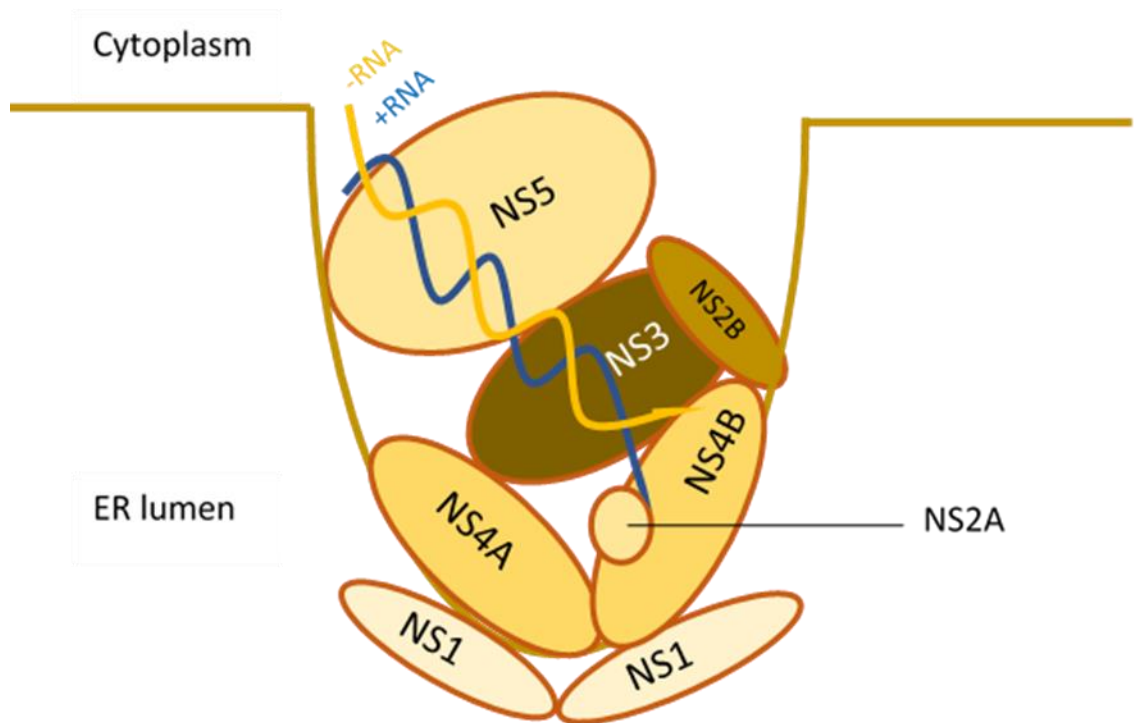
Figure 1.3 Flavivirus replication complex. Demonstrates the proposed alignment of NS proteins in the ER vesicle with NS1 on the lumen side and the other NS proteins on the cytoplasmic side of the ER. Note that NS4A and NS4B are transmembrane proteins

ecological work have demonstrated that the ancestral mosquito to *Aedes aegypti, Aedes aegypti formosus*, found in Africa, was comparatively insusceptible to infection with DENV (26, 28). This weakened the claim that DENV originated in Africa, alongside phylogenetic analyses, which indicated that an Asian DENV origin is more likely (26, 29). While the issue of the geographical origin of DENV has yet to be elucidated, it is widely accepted that the likely evolution pattern for DENV started with arboreal mosquitoes (25, 26). It likely originated as a virus in these mosquitoes, then adapting to primates in wooded environments (25). It is then hypothesized that DENV transitioned out of the forest and into a more peridomestic environment alongside human development (26).

Disease

DENV infections occur via the bite of an infected mosquito, which delivers the virus intradermally; it is thought that the virus will then infect dendritic cells (DCs) and macrophages (30). Once an individual is bitten by a female mosquito and is infected with DENV, there is an incubation period of 4-10 days where the virus multiplies before the onset of clinical symptoms. These clinical symptoms will then last about 2-7 days. In many cases, DENV infections cause a febrile, flu-like illness. However, in a minority of cases, infection proceeds into more severe illness. Typical symptoms of dengue fever include, but are not limited to, high fever (40°C/104°F), severe cephalgia, severe eye pain, general arthralgia, vomiting, rash, or swollen glands (23). Severe DEN is a highly dangerous and deadly complication of DENV infection, which is caused by plasma leakage, edema, respiratory distress, severe bleeding, and/or organ injury. Signs of severe DEN can begin to be observed approximately 3-7 days after the febrile-like symptoms,

alongside an overall decrease in temperature (below 38°C/100°F); these signs include abdominal pain, continued and prolonged emesis/vomiting, hyperventilation, bleeding gums, general fatigue, restlessness, and/or bloody emesis. After the appearance of these symptoms, the next 24 to 48 hours are critical for medical care as disease may progress to a fatal outcome without appropriate medical support. Other markers of severe DEN include: thrombocytopenia (low platelet count), increased liver enzymes, plasma leaking, and other signs of vascular dysfunction (30). There is currently no specific treatment for DEN fever, except for supportive care by health care professionals.

Animal Models

Animal model development for DENV has proven to be challenging, due to low-level or no detectable replication of clinical virus isolates in wild-type (WT) immunocompetent mice, as well as the presence of no clinical signs of disease in non-human primates (NHP) (30). Early models consisted of using intracranial (i.c.) inoculation of very high doses of mouse brain adapted neurovirulent DENV strains into suckling mice and/or adult mice that are immunocompetent (31–33). This method causes neurological disease and paralysis, but is not representative of DEN disease manifestations observed in humans. Prototypical WT mouse strains, such as BALB/c and C57BL/6 mice, do appear to demonstrate some low level DENV replication; these animals ultimately succumb to neurotropic associated outcomes, such as paralysis (34). Disease outcomes in these WT mice that may also appear like that of humans, including signs such as liver damage (exemplified by an increase in liver enzyme levels), rises in white blood cell (WBC) count, thrombocytopenia, and hematocrit increases (consistent with vascular dysfunction); however, this occurs once viral strains have been highly

mouse-adapted or when extraordinarily high virus inocula ($\geq 10^8$ FFU) are utilized (35, 36). Similarly, BALB/c mice appear to demonstrate DHF-like symptoms with very high doses of DENV (10^9 FFU) (37–39).

Other models include the use of mice deficient in interferon (IFN) αβγ receptors, known as AG129 mice (30). The first observation of peripheral DENV replication occurred in AG129 mice following intravenous (i.v.) or subcutaneous (s.c.) inoculation (30, 40). This model was further developed for studies using non-mouse-adapted DENV strains (30).   DENV infection of these mice causes neurological disease when mice are inoculated with a mouse brain-adapted DENV. More recent studies have demonstrated that AG129 models, which utilize non-mouse adapted DENV strains and are administered via intraperitoneal (i.p.) or i.v. inoculation, allows for an acute, disseminated virus infection and disease, and that these animals develop many of the clinical signs associated with human disease (41). Additionally, many studies have demonstrated that the results obtained when utilizing these mice and DENV are uniform and consistent (41–43). However, there is concern that the lack of all components of an immune response, at least IFN, does not allow a true model of DENV infection and disease progression. It is important to note that this AG129 model is meeting a need that has been ongoing for decades, and will potentially lead to a more representative model of human DENV disease.

Another common mouse model for DENV studies is that of severe combined immunodeficiency, or SCID, mice (44). These mice lack humoral and cellular immune cell responses, as they have B and T cell deficiencies, and are also used to generate humanized mouse models. In the case of DENV infection of SCID mice, mice are often

engrafted with tumor cells, and the virus in injected onto the engrafted cells; most of the virus infects these cells, which then allows the virus to spread to the brain, causing neurotropic disease and paralysis, as is seen in WT mice (44). SCID mouse models are traditionally used due to their ability to sustain external cellular grafts, thus making them ideal for studies with no appropriate animal model (30). This holds true for DENV, especially in studies regarding tropism and pathogenesis of DENV. Regarding humanized SCID DENV models, one method has been to engraft these mice with human progenitor cells; this is not a highly efficient process. There is often a strong immune response that prevents engraftment; thus, SCID mice were bred with nod-obese diabetic (NOD) mice, then with IL2RγKO mice, which helps to alleviate the immune response that prevents engraftment (30). By grafting these mice with CD34+ human cells, several human cell types, such as DCs, can be generated in the mouse, allowing the study of DENV infection (45, 46). Thus far, these mice have mimicked human infection, however, these models may not always be consistent.

A129 (IFNAR-/-) mice, or those mice lacking IFN αβ receptors, are another mouse model for DENV infection. These mice can exhibit a disease similar to that of humans via using high virus inocula or mouse-adapted DENV strains, and exhibit clinical signs that are similar to severe DEN disease (47). Other studies have shown that DENV-2 strains have been utilized at lower virus inocula to cause mortality in greater than 50% of animals (48). However, this model is not typically able to be infected with non-mouse adapted DENV strains, and, similar to AG129 mouse models, have deficient immune signaling. As such, there are concerns about its when mimicking human DEN disease and pathogenesis.

NHP models of DENV do not effectively recapitulate human disease either. When NHPs are inoculated via the s.c. route, there is viral replication, but it is much lower than that seen in humans, and is limited to tissues that are rich in lymphoid material, and exhibits different symptomology (i.e., lymphadenopathy, lymphocytosis, leukopenia) (49–51). Some NHPs, such as rhesus macaques (*Macaca mulatta*), occasionally display low platelet counts, like human disease, but there were no other clinical signs of DEN disease in these studies (49–51). When NHPs, rhesus macaques specifically, are inoculated with higher dosage than 10^5 PFU, via the i.v. route, hemorrhage and coagulopathies were observed, but not fever, malaise, or loss of appetite, which are characteristic of DENV disease in human cases (49–51).

DEN Vaccine Development

Vaccination is thought to be the most efficacious form of DEN disease prevention, due to the presence of many reservoirs and vectors in nature. This is especially true since the transmission cycle occurs almost exclusively through the bites of DENV-infected mosquitoes and humans. Most DENV infections are asymptomatic, and it is thought that this aids in the ever-growing spread and threat of DENV (52). These factors, along with the continuing geographic expansion of *Aedes* species mosquitoes that transmit DENV, as well as increasing urban populations in endemic regions, increased travel, and changing environmental conditions have intensified research into vaccination options for DEN. Since infection with DENV elicits a life-long, serologically specific immunity, there is a theoretical basis for successful vaccination strategies to lower DENV infections. However, there are many factors of DEN infection and pathogenesis that remain elusive, making it more challenging to discover an optimal vaccination strategy.

Furthermore, it is hypothesized that the vaccine should be tetravalent, containing all four

DENV serotypes, to ensure simultaneous immunity to all four DENVs and reduce risks

of adverse events.

There is evidence that secondary infections of DENV (i.e., primary infection by

one DENV serotype, followed by a secondary infection with a different serotype) may

cause more severe disease in some individuals than primary DENV infection. This is

hypothesized to be due to induction of DEN serotype cross-reactive, non- or weakly-

neutralizing antibodies that form virus-antibody complexes during secondary infections,

which are taken up in to cells of monocyte origin via Fc receptors on the surface of these

cell types. This has been termed Antibody Dependent Enhancement (ADE) (53). There

are a wide variety of DEN vaccine candidates that are in various stages of development,

ranging from early stages of investigation, to clinical trials, and even to licensing in one

instance. A table of these candidate vaccines can be found in **Table 1.2**. These vaccine

candidates are a mixture of empirically derived, live, attenuated vaccines (LAVs) to

recombinant, chimeric, LAVs, to inactivated vaccines, among others. The E protein is

thought to be an important component of induction of protective immunity; in particular,

induction of neutralizing antibodies. As such, most of the current vaccine candidates

contain at least some portion of the DENV E protein to stimulate the optimal immune and

antibody response to infection.

Dengvaxia

The most advanced candidate for DEN is Sanofi Pasteur's recombinant live-

attenuated, tetravalent, chimeric vaccine (trade name Dengvaxia™). This vaccine was

first licensed in Mexico in December 2015 and has been licensed in a total of 19

Vaccine	Vaccine Type
Live attenuated (Dengvaxia ™)	Recombinant live attenuated tetravalent vaccine; YFV-17D backbone with corresponding DENV serotype prM and E
Live attenuated (PDK-53 Vaccine/DENVax)	Recombinant live attenuated vaccine, DENV-2 PDK-53 virus with corresponding DENV serotype prM and E
Live attenuated (DENV-4 strain Δ30 Vaccine/TV003)	DENV-4 strain Δ30 (attenuated by 30 nt deletion in 3'UTR); with corresponding DENV serotype prM and E
E Protein Ectodomain Vaccine	Recombinant vaccine with N-terminal 400 amino acids of E protein
Purified Inactivated Vaccine	Inactivated by formalin
DNA Vaccine	DNA vaccine expressing prM and E of DENV-1 in a plasmid construct

Table 1.2. Vaccine candidates for DENV.

countries (Bolivia, Brazil, Cambodia, Costa Rica, El Salvador, Guatemala, Indonesia, Mexico, Paraguay, Peru, the Philippines, Singapore, Thailand, Honduras, Australia, Bangladesh**,** Argentina**,** and Venezuela) (54). It consists of a backbone consisting of YFV 17D, which is the vaccine strain of YFV, where the prM and E genes of 17D virus have been replaced with those each of the corresponding DENV serotypes (55, 56). Leading up to its licensure, extensive studies occurred to evaluate stability and safety of this candidate. The viruses contained within the vaccine were sequenced throughout the manufacturing and development process; this demonstrated stability of the genome, with no change between the premaster seed lots of the virus to the bulk seed lots (57). It was found that the chimeric vaccine viruses exhibited low level replication and viremia, and non-mosquito-competent when evaluating virus replication in *Aedes spp.* mosquitoes (58). Early *in* vitro characterizations demonstrated that immune cells and markers were activated, and the viruses were immunogenic (59). Studies in NHPs demonstrated that vaccine viruses exhibit low viremia but acceptable protectivity (60–62). Clinical trials of this vaccine indicate that while this vaccine does indeed prevent virologically confirmed dengue in DEN-immune individuals, there are concerns about the overall safety and efficacy of this vaccine for young age groups (particularly ages 2-5), possibly due to an ADE like phenomenon; additionally, the vaccine has limited use in dengue-naïve individuals and there seems to be inconsistent effectiveness of the vaccine among different serotypes of DENV with poor immunogenicity against DENV-2 (63–66).

DENVax

There are two other recombinant chimeric LAV viruses under development. One is by Takeda Pharmaceuticals, and this vaccine candidate consists of DENV-1, -3, and -4

prM and E regions inserted into the cDNA backbone of attenuated DENV-2 strain 16681 Primary dog kidney (PDK) passage 53 (67). This virus, termed DENV-2 PDK-53, was attenuated via extensive passing in PDK cell cultures at 32°C, and there appeared to be temperature sensitivity, small plaque size (which is often correlated with flavivirus attenuation), moderate monocyte infectivity and growth, loss of neurotropism and virulence for suckling mice, and low viremia in monkeys when compared to non-PDK passaged DENV-2 strain 16681 virus (68). DENV-2 16681 PDK53 virus was then investigated as a LAV by studying its effects in ten volunteers; five of these volunteers were flavivirus naïve, and five were immune to JEV, but presumably to no other flaviviruses (68). After receiving 1 mL of the candidate vaccine virus by the s.c. route, all ten of the vaccine recipients demonstrated neutralizing antibody responses to DENV-2, and exhibited no obvious signs of adverse reactions, hence making it interesting to investigate farther (68). This vaccine virus was then used as material to generate infectious cDNA clones for this strain and its parental strain, DENV-2 16681 (69). It was found that there were no amino acid mutations in the C, prM, or E regions of the cDNA and resulting virus, making this an ideal candidate for chimeric viruses that expressed the structural genes of other flaviviruses (69). The next step was to generate these chimeric viruses, with a backbone consisting of the attenuated DENV-2 16681 PDK-53 with the prM and E genes of WT DENV-1, DENV-3, and DENV-4 (67). This resulted in viruses that had attenuation markers similar to that of DENV-2 PDK-53 *in vitro*, as well as a lack of neurovirulence in newborn mice (67). This tetravalent vaccine virus formulation is known as DENVax (70). The four DENVax viruses were studied in cynomolgus macaques (*Macaca fascicularis*) that were infected by the s.c, route; these vaccine viruses proved to be well-tolerated, with

low viremia levels and protection demonstrated (70). These viruses were then studied in AG129 mice, and it was found that they were safe, elicited neutralizing antibody responses, and provided significant protection (71). DENVax is currently in phase III clinical trials.

TV003

The other vaccine candidate consists of cDNA clones of DENV-4 strain Δ30 with a 30-nucleotide deletion in the 3'UTR, and was developed by the U.S. National Institutes of Health (72–74). This approach to attenuation is important because the 3' UTR of the flavivirus genome is thought to contain important sequences and secondary RNA structures important for replication of the virus men (75). Nucleotide numbers 10,478-10,507 were removed from the genome of DENV-4 (72, 75). When properties of DENV-4 Δ30 were examined, it was found the virus was viable but had reduced multiplication in both mammalian and mosquito cells, and plaque morphology was fainter than observed with the WT parental DENV-4 (75). When examined further in monkeys, viremia was noted less frequently in those infected with DENV-4 Δ30 when compared to parental DENV-4, and a moderate antibody response was observed (75). Additional studies were undertaken in humans and monkeys to assess safety. This virus has been shown to be attenuated for rhesus monkeys and exhibited decreased replication and maintained immunogenicity, suggesting its usefulness as a candidate for vaccine studies in humans (72). In a phase I study 20 human volunteers were given 5 $\log_{10}$ PFU of virus in the deltoid region, and it was found that the virus could efficiently infect humans, but produced few clinical symptoms (most common was an asymptomatic, transient rash in those with detectable viremia); however, viremia levels were low, and a neutralizing antibody response was noted, even in those with non-detectible viremia; (72). Following

this, a phase II clinical trial was performed, in which three doses (10^3 PFU, 10^2 PFU, and 10^1 PFU) were inoculated into humans, with 20 recipients per dose and 4 placebo recipients (74). This study discerned that the virus was tolerated by all recipients at all doses, with the most common adverse event once again being the transient, asymptomatic rash that was observed in the phase I study (74). There was a tentative relationship observed between the highest dose here (10^3 PFU) and increased serum alanine aminotransferase (ALT) levels in a few individuals (74). The viremia observed seemed to indicate no significant clinical symptoms; a neutralizing antibody response was observed, and the 3'UTR deletion was stable after replication in humans (74). This backbone of a 3' UTR deletion mutant was utilized to develop a tetravalent formulation, with a corresponding deletion in each of the other DENV serotypes, DENV-1, -2, and -3. This combination was proven to be non-reactogenic, and to be immunogenic and stable (76). As was observed with the two prior studies, the most common adverse event was the transient, asymptomatic rash, although it occurred in more recipients (approximately 64%) (76). There was a potent neutralizing antibody response, as well as acceptable viremia, and the virus seemed to be stable and safe after injection into humans, with the caveat regarding the rash (76). Several combinations of these tetravalent formulations were tested, and the one that was deemed the most promising option to move forwards was termed TV003, which demonstrated the most promising results regarding immunogenicity and safety (76). All prior studies have been performed in flavivirus naïve populations, and TV003 was recently tested in populations who were flavivirus seropositive prior to receiving the vaccine. Once again, the most common adverse event was rash, which was mostly mild (53). Following one dose (0.5 mL) of this tetravalent

mixture, 87% of recipients had neutralizing antibodies to all four DENV serotypes and 76% were viremic (53). In summary, this tetravalent virus combination has proven to be highly effective and shows great promise as a putative DEN vaccine in the future. TV003 is currently in phase III clinical trials. Alongside this tetravalent vaccine candidate that has been constructed, this methodology and these viruses may represent candidates for chimeric vaccines that may carry structural components of other flaviviruses.

Non-live dengue vaccine candidates

The Walter Reed Army Institute of Research (WRAIR) has developed a purified inactivated virus candidate by formalin inactivating each of the four DENV serotypes; this is currently being tested in phase I/II clinical trials, but shows promise due to lack of reactivity and enhanced immunogenicity (77). This vaccine is a tetravalent formation, and was inspired by successes with other inactivated flavivirus vaccines, such as the inactivated JEV vaccine Ixiaro™ (77). Other DEN vaccine candidates being studied include a recombinant, truncated E protein component (N-terminal 400 amino acids), which is produced in *Drosophila* S2 cells, and is currently being evaluated by Merck & Company (52, 78, 79). It has been shown to be effective at protection in mouse and NHP studies (78, 79). There is also a monovalent DNA vaccine being studied by WRAIR and the U.S. Naval Medical Research Center, which has the prM and E gene of DENV-1 (80). Initial testing suggests reactogenicity and safety (80).

These are only a handful of the DEN vaccine candidates under clinical investigation. As can be seen, there are many options for vaccine development. However, there are still many hurdles to overcome in the race for an optimal DENV vaccine. While Dengvaxia™ has been licensed in 19 countries to date, the concerns about its safety and

36

use in all age groups causes some concerns regarding its efficacy, and allows for a continuation of the search for an ideal DENV vaccine. Safety, reactogenicity, immunogenicity, cost-effectiveness, route of inoculation, ease of use, and durability of the immune response to the vaccine are just a few factors that are important to be elucidated and examined before moving forward (52).

Yellow Fever

YFV is found extensively throughout tropical regions in Africa and South America. It is spread via sylvatic and urban transmission cycles (81). As is common with many arboviruses, human events (travel, etc.) have allowed YFV to expand beyond these traditional areas, and outbreaks have occurred in other non-traditionally infected YFV areas, such as North America, Europe, and the Caribbean prior to introduction of the vaccine in the late 1930s (82).

History

Yellow fever (YF) was a plague to many areas of the globe in the early nineteenth century. Occasionally known as "yellow jack" due to the flags that would be flown on ships where YF outbreaks occurred, it was a widely feared disease with great health and economic impact (83). In the late 1800s, Patrick Manson hypothesized that the presence of a "germ or virus", but also suggested that it may require time outside of the human host to be infectious (83). During and after the Spanish-American War, where YF was a notorious problem, U.S. surgeon general George Sternberg arranged for a "Yellow Fever Commission", which was headed by Walter Reed (83). This commission famously demonstrated that mosquitoes were responsible for the transmission of YF, and that the responsible agent was filterable (83). Upon the opening of the Panama Canal in 1912,

large world-wide populations were suddenly more susceptible to YF infection, resulting in the Rockefeller Foundation's International Health Commission goal to eradicate YF (83). On this team was Dr. Hideyo Noguchi, a Japanese scientist whom had risen to fame by discovering spirochetes in brains of patients; he suspected that spirochetes were responsible for YF (83). The team from the Rockefeller foundation, including Dr. Noguchi, was sent to Ecuador to combat YF; while there, Noguchi found spirochetes in the livers of 'yellow fever' patients, passed these to guinea pigs, and published suggesting he had found the cause of YF, calling it *Leptospira icteroides* (83). Some years later, in 1926, Max Theiler, along with Andrew Watson Sellards, demonstrated the *L. icteroides* was serologically identical to that of *L. icterhemorrhagica*, which was the cause of Weil's disease; this occurred after extensive production of a vaccine of Noguchi's making, and during a time of question regarding Noguchi's yellow fever work (83).

Post-World War I, the Rockefeller Foundation continued its work for the eradication of yellow fever, moving to Africa to investigate the differences between YF in Africa and South America (83). In June 1927, a blood sample from a 28-year-old African named Asibi, who was suffering a mild case of yellow fever, was taken and injected into a rhesus macaque (83). This macaque had been imported from India, as the African green monkeys that were in the region did not become ill (83). The monkey was susceptible, and infection was established in a laboratory host for the first time; after more studies, it was found that serum from humans with YF immunity could protect monkeys from infection, and that immune sera from patients with the South American YF virus infection could protect from the African YF (83). This suggested that one vaccine could confer global protection, and that it was unlikely that inactivated virus would suffice for vaccination (83).

An alternative strain of yellow fever, from Dakar, Senegal, was obtained from a patient named Francoise Mayali; Mayali was found to have a fever, and his blood, when injected into a rhesus monkey, produced severe YF, although Mayali's case was mild (83). This later became known as the 'French strain'; the team working with the sample found that the virus could be frozen without decaying, and was able to transport tissues and samples for further examination (83). A few vaccine candidates were generated via formalin and phenol-preserved livers, but they were inactivated, and it became clear that a live, attenuated vaccine would be the best vaccine candidate (83). Max Theiler was aware of studies with herpes virus and rabies virus that attenuated viruses could be generated via passaging in non-native tissues; he inoculated mice i.c. with YFV strains and discovered multiplication occurred, as well as that if passaging continued, viscerotropism decreased when the mouse-passaged virus given to monkeys (83). The first attenuated strain was generated, although it had increased neurotropism (83). In 1931, the French strain, which had been attenuated via passage over 100 times in mouse brain, was administered in a clinical trial as a vaccine, mixed with human serum and given in multiple doses; this was the Rockefeller Foundations standard for a while, used in the Western Hemisphere and England (83). The strain was further developed by coating the virus particle with oil or egg yolk, freeze-drying, and vaccinating via scarification; this was used by France and its African colonies, typically along with smallpox, during the 1940s-1950s (83). However, both vaccines, based on the French strain, had demonstrated higher than average cases of post-vaccinal neurologic effects in children. In 1932, Theiler and Eugen Haagen cultivated YFV in mouse and chicken embryo tissues; however, extensive passaging of both Asibi and French strains failed to alter the observed neurotropism (83). Consequently, nervous

tissue was removed from the embryonic tissue, and at the 100th subculture of chicken embryo with nervous tissue (176th in chicken embryo all together), the Asibi strain failed to kill mice when injected by the i.p. route (83). Altogether, the Asibi strain was passed 18 times in mouse embryo, 58 times in minced whole chick embryo, and 100 times in minced whole chick embryo without nervous tissue; at this point, it acquired the optimal characteristics of attenuation and immunogenicity after 176 passages (84). Thus, the live attenuated 17D vaccine was generated empirically in the 1930s by Max Theiler. This virus was found to be highly attenuated, with decreased viscerotropism, neurotropism, and a loss of vector competence (84). This became the vaccine of choice in the early 1940s and has remained so. There are two substrains of 17D vaccine used today; 17D-204, which was derived at the 204th passage of Asibi and 17DD derived at passage 198 of 17D. The original 17D virus has been lost so it is difficult to directly identify those mutations responsible for the attenuation of 17D. Thus, mutations found in 17D have been interpreted by comparison of Asibi with 17D-204 and 17DD vaccine strains. There are a total of 20 amino acid substitutions shared by 17D-204 and 17DD substrains that are not present in the Asibi strain. Nine of these are in the structural genes, with eight out of nine in the E, and 1 in the M. There are 11 amino acid substitutions in the non-structural genes, one in NS1, four which are in NS2A, one in NS2B, one in NS3, one in NS4A, one in NS4B, and two in NS5, as well as four silent mutations in the 3'UTR. These amino acid differences are shown in **Table 1.3**. While the exact mechanism of attenuation of YFV 17D remains unknown, recent studies have suggested that it is partially due to decreased viral diversity of the RNA population in the 17D virus, and a high-fidelity RdRp (85, 86). Despite its empirical

discovery, YFV 17D has proven to be a highly stable, high effective vaccine that has been

utilized for decades with over 700 million doses of vaccine distributed since 1938.

Animal Models

It was a struggle for many years to find a suitable laboratory model of YFV, and

thus YFV 17D vaccine. A variety of animal models are now available for YF disease

modeling, as well as for use in YFV 17D testing. NHPs are natural hosts and reservoirs for

YFV infection in areas where the WT YFV is endemic. NHP species from Africa exhibit

very little, if any, clinical disease, except for fever and viremia, while some NHP species

from South America have a lethal disease and show more promise for animal studies (81).

The initial work with YFV and safety testing of YFV 17D vaccine was performed in rhesus

macaques from Thailand (81). When infected with wild-type YFV, macaques often exhibit

severe disease, which greatly models human infection (81). NHP models are vital to the

evaluation of vaccine safety (e.g. safety, viscerotropism and neurotropism), neurotropism),

on both new vaccine candidates, as well as new batches of seed lots of the already establish

YFV 17D.

Another valuable model for YFV studies are mice. Although mice are not naturally

infected with YFV, as was observed with DENV mouse models, virus adaptation for mouse

infection, as well as direct i.c. inoculation into suckling mice were early small animal

models to study YFV (81). These i.c. studies often cause severe and fatal disease, and as

such, are often used to study attenuated viruses, vaccine candidates, or putative treatments

for disease (81, 87). The AG129 mouse model has been an important model to study YFV

infections, including live attenuated vaccine strains. These animals have increased

vulnerability to wild-type YFV, as observed with DENV, and serve as a model of

viscerotropism (i.e., infection of the liver here) (88, 89). A129 mice also exhibit viscerotropic and neurotropic disease manifestations, although this may be dependent on viral strain, route of inoculation, and dosage (90). A129 and AG129 mouse strains are both useful for studying safety and replication kinetics of YFV vaccines (81). Peripheral inoculation of AG29 mice with YFV 17D results in a lethal infection, hence making them useful for the study of potential antiviral therapies at biosafety level 2, as well as vaccine challenge studies; WT YFV Asibi strains have been utilized previously, and cause a rapidly disseminated, lethal infection (81, 88, 89).

Another model that has been used for studies of YFV is the Syrian golden hamster (*Mesocricetus auratus*), which is susceptible to infection with YFV strains that have been adapted to hamsters (91–93). The disease manifestations are like that of humans, and this model may be used for countermeasure evaluations (81, 91). While this model does have difficulty efficiently growing primary virus isolates, there are studies that have suggested that hamsters may be used for comparative studies of naturally attenuated YFV strains and more virulent strains (via high dosage), as well as utilizing the recently developed STAT2 knockout hamster (82, 94, 95).

Overall, there are several viable options for animal models for the study of not only WT YFV, but YFV 17D and other putative vaccine candidates as well. The typically order of evaluation includes study in mouse or hamster models to ensure that there is no neurotropism via direct i.c inoculation, followed by NHP studies (81).

Nucleotide	Gene	Amino Acid	Asibi	17D-204 and 17DD
854	M	36	Leu	Phe
1127	E	52	Gly	Arg
1482		170	Ala	Val
1491		173	Thr	Ile
1572		200	Lys	Thr
1870		299	Met	Ile
1887		305	Ser	Phe
2112		380	Thr	Arg
2193		407	Ala	Val
3371	NS1	307	Ile	Val
3860	NS2A	118	Met	Val
4007		167	Thr	Ala
4022		172	Thr	Ala
4056		183	Ser	Phe
4505	NS2B	109	Ile	Leu
6023	NS3	485	Asp	Asn
6876	NS4A	146	Val	Ala
7171	NS4B	95	Ile	Met
10142	NS5	836	Glu	Lys
10338		900	Pro	Leu
10367	**3'UTR**	–	Thr	Cys
10418		–	Thr	Cys
10800		–	Gly	Ala
10847		–	Ala	Cys

Table 1.3. Common amino acid coding changes and nucleotide changes in 3'UTR of YFV-17D-204 and 17DD vaccine viruses compared to WT YFV-Asibi.

Chimeric Flavivirus Vaccines

Chimeric flaviviruses have been investigated as candidate vaccines based on swapping genes between viruses via reverse genetics. The focus has been on using attenuated vaccine backbone, particularly that of the YF 17D vaccine virus, to swap the prM and E genes of different flaviviruses for those of 17D virus. Such chimeric viruses have shown great promise as vaccine candidates, and some have been licensed. Specifically, chimeric 17D-DEN and 17D-JE viruses where the 17D prM and E genes have been replaced with the corresponding genes of WT DENV-1 to DENV-4 (e.g. Dengvaxia™; see section 1.7.1 above) and the live attenuated JE vaccine strain SA14-14-2 (Imojev™).

1.10.1 Japanese Encephalitis Virus Vaccine (Imojev™)

One of the earliest flaviviral chimeric viruses developed is that of JEV (96). This virus has the backbone of the C and NS proteins of YFV 17D and the prM and E genes of the SA14-14-2 JEV virus and was subsequently termed ChimeriVax-JE™ (97). It was found that this chimeric virus has the specificity (antigenically) of JEV, and was attenuated in mice when inoculated via the i.c. route (97). Further studies demonstrated that this virus was able to replicate efficiently in multiple mammalian cell types, the nucleotide sequences were comparable to the parental vaccine strains, was found to be genetically stable over passaging, and the virus was attenuated in multiple mouse models (suckling ICR WT mice and C57/BL6 WT mice), and induced protective immunity against JEV challenge (96). This virus was shown to be less neurovirulent than YFV 17D in mouse and NHP models (96–99) and attenuation appeared to be due to the presence of the SA14-14-2 JEV E protein (97, 100).

This became known as ChimeriVax-JE™. After the pre-clinical studies were performed, clinical studies were undertaken. An early, randomized, double blind study compared the safety and immunogenicity of the chimeric virus to that of YFV 17D. A single dosage of $5_{log}10$ PFU and $4_{log}10$ PFU were inoculated into healthy flavivirus naïve and YFV immune volunteers by the s.c. route (101). There were cases of mild, transient reactions at the injection site and flu-like symptoms in each treatment group, but there was no significant difference between each group (101). Nearly all recipients of either virus dosage and flavivirus status developed a temporary, low level viremia, like that of YFV 17D (101). There was 100% seroconversion to ChimeriVax™-JE neutralizing antibody in both dosage groups and flavivirus exposure statuses; hence suggesting that this virus was similar to that of YFV 17D (101). A double-blind, phase II clinical trial was then performed in 99 adults; these vaccine recipients received two virus doses by the s.c. route with varying dosages of the virus (from 1.8 $\log_{10}$ PFU to 5.8 $\log_{10}$ PFU) to perform further efficacy and safety analyses (102). Overall, the vaccine was well received and tolerated, with no significant differences in adverse events (flu-like illness and injection site response) between the various treatment groups; viremias were short and low-grade, and a neutralizing antibody response was generated in 94% of vaccine recipients (102). The second dose, which was administered 30 days after the original vaccination appeared to have no boosting effect (102). Another study examining immune memory in those who had received the vaccine nine months prior, and which were challenge with an inactivated mouse-brain JEV vaccine, demonstrated that an enhanced immune response occurred, and that it had lost mosquito competence (102). ChimeriVax™-JE appeared to be safe and effective, and was licensed under the name

Imojev™ in 2012, and is currently licensed in Australia, the Philippines, Malaysia, and Thailand.

West Nile Virus Chimeric Vaccine

WNV was first introduced to the United States in 1999, and then spready rapidly across North America, causing disease in birds, horses, and humans, who are dead end hosts (103). WNV causes asymptomatic disease in 80% of cases; about 20% of cases are West Nile fever, which is a flu-like illness, and less that 1% of cases are neurological diseases. Since ChimeriVax™ technology had been utilized to successfully generate a single dose, live attenuated vaccine again JEV (at least in clinical trials), and JEV is in the same serocomplex as WNV, it was hypothesized that the same technology could be utilized for a WNV chimeric vaccine virus candidate. In early studies, the prM and E genes of YFV 17D were replaced with that of WNV strain NY99 (103). This work demonstrated that this chimera did not have the neurotropic properties typically exhibited with WNV infections and was less neurovirulent than YFV 17D in mouse (ICR WT mice) and cynomolgus monkey models (103). Additional attenuating point mutations were then inserted into the E gene (at positions 107, 138, 176, and 280) in order to reduce virulence; this resulted in ChimeriVax-West Nile02, which had further reduction in neurovirulence (103). Preclinical studies in mice doses ranging from 0.89 $\log_{10}$ PFU to 6.51 $\log_{10}$ PFU given by the i.p. route; rhesus monkey studies utilized virus given by the i.c. route, with dosages from 4.99 to 5.07 $\log_{10}$ PFU (103). The mice that were vaccinated. were challenged with WT WNV and were protected in some instances; similarly, macaques that were challenged by the i.c. route were also protected (103).

Approximately half of the macaques exhibited subclinical disease after the challenge, but this was thought to be due to the aggressive challenge (103).

A second set of studies were performed utilizing ChimeriVax-WN02, which has point mutations in the E gene (E107, E336, and E440), and rhesus macaques were used to test the attenuated phenotype of the virus. It was found that skin and lymphoid tissues (lymph nodes and spleen) were major replication sites (104). These macaques were challenged with $5\log_{10}$ PFU by the s.c. route, and viremia was low-grade and short-lived and neutralizing antibodies were detected in about 40% of animals (104). The virus was found to be safe in animals ((104). A randomized, double-blind clinical trial study was also performed at this time; healthy volunteers received $5.0\log_{10}$ PFU of ChimeriVax-WN02, and a second group received a lower dose of $3.0\log_{10}$ PFU (104). Viremia was observed, but low-grade and short lived, although the higher dosage had significantly higher viremia than the low dosage (104). Many of the vaccine recipients had at least one adverse event, but this incidence seemed to be similar across active and placebo groups; there was no relationship between viremia and severity of these events (104). This study demonstrated that the vaccine virus induced high neutralizing antibody responses and antigen specific CD8+ T cells, which produced IFN-γ, as well as WNV specific CD4+ T cells in greater than 80% of subjects (104). Follow up Phase II clinical trials indicated that the vaccine was well-tolerated and immunogenic in multiple age groups (105, 106). In the phase II study, recipients were immunized with approximately $3\log_{10}$ PFU to $5\log_{10}$ PFU, based upon their group; greater than 96% of vaccine recipients seroconverted, viremia was low-grade and short-lived, and neutralizing antibody responses were generated, hence proving the immunogenicity of ChimeriVax-WN02

(105). In 2006, an equine vaccine based on this ChimeriVax™ technology was licensed and marketed under the name Prevenile (107).

Quasispecies Theory and Next Generation Sequencing

Unlike DNA polymerases that have proof reading functions, the RdRp is error prone and so RNA viruses generate high rates of mutations within the genome during replication (108). As such, RNA virus populations do not exhibit a single genotype; rather they are a collection of sequences that have shared features with variable mutations possible in each virus' genome (109). This variability within the genome gives rise to populations of viral RNAs that are sometimes termed quasispecies. Like other RNA viruses, flaviviruses tend to generate viral RNA populations that have a wide amount of diversity, or quasispecies populations. There are a wide variety of reasons for the phenomenon. The RdRp is the enzyme that is responsible for the replication of the RNA. The fidelity, or the inherent error rate, of this enzyme determines that amount of errors, or mutations, that occur during the replication process. Flaviviruses have RdRp's with low-fidelity (about 10^{-4} mutations per nucleotide), hence the RdRp lacks proofreading abilities and generates high mutation rates (86). Flaviviruses also have rapid viral replication kinetics, as well as the ability to quickly generate large viral populations, allowing further errors to occur. In addition, viruses must respond to host selection pressures, such as tissue and cellular tropisms and alterations in host. In particular, flaviviruses, such as YFV and DENV must replicate in both mosquitoes and vertebrate hosts; thus, although mutations are generated in the viral RNA population, the virus has constraints and only allows mutations that able it to replicate in both mosquito and vertebrate hosts. Quasispecies theory for viruses was generated from studies trying to explain how life evolved in the

precellular RNA world (108, 110). It is based on classical theories of population genetics, and examines the results of the error-prone replication and large population sizes, which is often seen in viruses, making this a useful theory to study RNA viruses (108). Viral quasispecies theory states that the error rates for RNA virus replication are high, which in turn leads to a diverse mutant population that has variable fitness (or the ability to reproduce and survive) within any given system (108, 111). If too many mutations that are deleterious occur in this population, then the virus may lose fitness, as the virus replication abilities may become decreased; this is called error catastrophe (109, 111). However, if the population stabilizes then the viral population becomes more homogenous, has fewer mutations, and undergoes a fitness decrease, as the viral population has now lost the advantage of quick adaptation to host and environmental pressures (112). An example is the process of plaque picking of viruses. Quasispecies diversity has been shown to have implications on virulence and attenuation of viruses. For example, poliovirus has been shown to have less quasispecies and be less virulent when a virus with a high fidelity RdRp is selected (109, 112). The YFV 17D vaccine virus is thought to be attenuated in part due to decreased viral diversity across the entire genome and hypothesized to be due to 17D vaccine having a high fidelity RdRp that introduces few mutations (85, 113). Therefore, quasispecies theory is important in the investigation of attenuation and virulence of viruses, as well as pathogenesis. The role of mutational robustness and quasispecies diversity for flaviviruses is in the early stages of investigation. Next generation sequencing (NGS) allows an in-depth examination of viral RNA populations via insertion of fluorescently labeled deoxyribonucleotide triphosphates (dNTPs) into the template strands during cycles of DNA synthesis; as the fluorophores are excited, a signal is generated that can be read

(114). NGS is different than other sequencing methods because it sequences millions of fragments in a parallel fashion; this allows analysis of the population of RNAs that are present in viral samples, as well as the small variants not detectable by previously used methods, in addition to the consensus sequence that represents the dominant sequence in a population. Variability can be measured using Shannon's entropy, which is the measurement of absolute variability that is found at each site in the full genome of the virus in question, or the average unpredictability in a random variable (85). This ranges from highest diversity (meaning that all four nucleotides are occurring at equal proportions in the population), to 0 (meaning the entire viral RNA population is homogeneous and only one of the four nucleotides is found at a specific position). RNA viral populations often exhibit these differences via single nucleotide variants (SNVs), which are nucleotide positions in the genome where the nucleotide is different to that of the consensus (or predominant) sequence. As one might expect for RNA viruses, there are many SNVs and their detection depends in part on the number of reads by NGS and the proportion of the population at a particular nucleotide position that have nucleotide different to the consensus nucleotide at that position. Consequently, the focus is on SNVs that represent $\geq$1% of the nucleotides at a particular position. By utilizing NGS to investigate SNVs and Shannon entropy calculations, the viral population can be examined to elucidate the roles that viral diversity plays on infectivity and virulence. An excellent example of the role that viral diversity plays on infectivity and virulence of RNA viruses is that of WT YFV Asibi versus YFV 17D. Studies have demonstrated that YFV Asibi, which is the parental strain of YFV 17D, has high diversity indices across the entire genome, while YFV 17D lacks diversity and exhibits a much more stable genotype across the genome, with much less viral diversity

50

demonstrated (85). This is hypothesized to be one reason that YFV 17D is attenuated (85).

Other studies hypothesize that YFV 17D has a more stable RdRp than that of YFV Asibi,

hence allowing less errors to be inserted into the genome, hence stabilizing the quasispecies

via loss of introduction of single nucleotide variants (86).

Chapter 2: Thesis Rationale

The global importance of DENV is clearly demonstrated in its global range, economic burden, and occasional severe disease manifestations. The ChimeriVax™ technology has been used to successfully generate effective, licensed vaccines for flaviviruses, including Dengvaxia™ that has varying effectiveness for each DENV serotype, and effectiveness also varies based on previous flavivirus and DENV seropositivity status upon vaccination.

While this vaccine has been successful, the contribution of chimerization to the attenuated phenotype remains unknown. This is important as the other live attenuated vaccine candidates, DENVax and TV003, are also chimeric flaviviruses. Recent studies have suggested that the ability of RNA viruses to generate quasispecies populations are important to virus attenuation; a study has suggested YFV 17D is at least in part attenuated due to a lack of quasispecies diversity (85). The objective of the studies undertaken was to investigate why ChimeriVax™ is attenuated, since the WT DENV prM and E genes are present in the 17D backbone, and to investigate the contribution of chimerization on virulence and infectivity. It is hypothesized that the process of flavivirus chimerization results in decreased viral diversity and virulence. Two Specific Aims are proposed. In Specific aim 1, the impact of viral chimerization on genetic diversity and viral replication will be investigated. In Specific aim 2, the virulence phenotype of the chimera YFV 17D/DENV-4 prME will be investigated in a mouse model. For this project, a chimeric YF 17D virus with the DENV-4 prM and E genes from DENV-4 P75-215, a sylvatic DENV-4 strain, developed in the Barrett lab (and not the Sanofi

Dengvaxia™ DENV-4 component will be used to investigate the putative role of the E

protein in the genotype and phenotype of a chimera.

Chapter 3: Materials and Methods

Cell Types

 Cell types utilized in these studies were Vero, A549, and C6/36 cells. Vero cells were derived from African green monkey (*Cercopithecus aethiops*) kidneys, in the 1960s (115). Cells were maintained in Dulbecco's modified Eagle medium (DMEM), supplemented with 10% heat inactivated, filter sterilized fetal bovine serum (FBS), and 1% L-glutamine, non-essential amino acids (NEAA), and penicillin-streptomycin. Vero cell stocks were maintained in liquid nitrogen, and when ready to use, thawed at 37°C, and incubated in 10% DMEM at 37°C and 5% CO_2 until confluent in a $25cm^2$ vented flask. Cells were passaged as the cells become approximately 80% confluent. Vero cells double in number about every 24 hours, and have no effective IFN response. They have been utilized for many years for virology studies, and are shown be effective at allowing viral replication and maintenance, as well as being the cells utilized for plaque assay titrations.

 A549 cells were isolated from a human alveolar cell carcinoma, and are found to have an efficient IFN response, making them useful for immunological and virologic studies. These cells were maintained in DMEM supplemented with 8% FBS, and 1% L-glutamine, NEAA, penicillin-streptomycin, and are maintained at 37°C in 5% CO_2. Cells were stored in liquid nitrogen, and when ready to use, thawed at 37°C and incubated in 5% DMEM at 37°C in 5% CO_2 until confluent. A549 cells grow slowly, and were monitored daily until 70% confluency, when subculture was performed. A549 cells were utilized due to the presence of an intact interferon signaling system when compared to

Vero cells. This was chosen because interferon signaling has been shown to play a vital role in the host anti-viral response.

C6/36 cells were maintained at 28°C in DMEM supplemented with 10% or 2% FBS, and 1% L-glutamine, NEAA, penicillin-streptomycin, sodium pyruvate, and 5% tryptose phosphate broth. These cells were derived from *Aedes albopictus* whole larva. Cells are stored at liquid nitrogen, and thawed at 37°C when ready to use. They are then incubated in 10% or 2% FBS, and 1% L-glutamine, NEAA, penicillin-streptomycin, sodium pyruvate, and 5% tryptose phosphate broth, at 28°C until 80% confluent, at which time subculture is performed. These cells grow slowly, and were subcultured approximately once per week. These cells have shown to be useful for multiplication of flaviviruses, and can replicate these viruses to high titers.

Virus

Viruses were obtained from laboratory virus stocks. DENV-4 P75-215 was originally obtained from the World Reference Center for Emerging Viruses and Arboviruses at UTMB. The strain was isolated from *Ae. niveus s. l.* mosquitoes, which were found in the Gunong Besut forest reserve of Malaysia in late 1974 (116). Virus was passaged a total of 18 times, in a combination of baby hamster kidney (BHK-21), Vero, and C6/36 cells prior to and during the studies in this thesis. During the studies, the virus was passaged in either Vero or C6/36 cells at passages 16, 17, or 18. YFV 17D utilized in the studies were generated from an infectious clone via in-vitro transcription and electroporation from a cDNA backbone. YFV 17D infectious clone RNA was electroporated into *E. coli* MC-1061 cells, then maintained in Vero cells. YFV 17D-204 (YF-Vax by Sanofi Pasteur) vaccine strain virus that was utilized in animal studies was

obtained from a direct sample of YFV 17D-204 vaccine obtained from laboratory stocks

of vaccine and was not passage prior to use in animal studies.

The chimeric YFV 17D/DENV-4 prME was generated prior to the studies

undertaken in this thesis by other members of the Barrett lab. Briefly, RNA was extracted

from DENV-4, and RT-PCR was performed on prM and E genes, with a primer based at

the end of the C gene and a reverse primer based at the start at the NS1 gene. The PCR

product was cloned into a pGEM-T vector, and junction regions were sequenced to

generate primers for cloning into YFV 17D. A YFV 17D infectious clone underwent site-

directed mutagenesis, and SfoI and BsiWI sites were inserted, and this was transformed

and grown in MC 1061 bacterial cells; colonies were screened by digestion with the SfoI

and BsiWI restriction sites. PCR of the prM and E genes in the pGEM-T SfoI site was in

the forward primer, and BsiWI site in the reverse primer, and this was cloned into the

YFV 17D infectious clone. The resulting virus was sequenced to show restriction sites

and ensure the virus genomic sequence was accurate. DNA was then linearized, in-vitro

transcribed, and electroporated into BHK-21 cells. For viruses generated using in-vitro

transcription and electroporation, virus RNA was electroporated into 75cm^2 flasks of

Vero cells at approximately 80% confluency, and monitored for approximately five days,

or until CPE was observed. Virus was harvested from cell culture supernatant, spun at

1500 RPM for 5 minutes at 4°C, then aliquoted and stored at -80°C. Viruses used in

animal studies was concentrated using 50 kDa molecular weight cut-off Amicon filters

via collecting cell culture supernatant (50 mLs per filter), spinning at 1500 RPM at 4°C,

for approximately 30 minutes and resuspending in a volume of 1 ml. A schematic of the

cDNA of the YFV 17D/DENV-4 prME is shown in **Figure 3.1**.

Plaque Assay Titration of Viruses

All virus titers were obtained via plaque assay titration in Vero cells. Six-well plates of Vero cells were grown to about 80% confluency in DMEM supplemented with 10% FBS. When cells were confluent, virus samples were thawed at 37°C, vortexed to mix, and put on ice. Ten-fold virus dilutions were performed, ending at 10^{-6}. Virus dilutions were mixed, placed on ice, and six-well plates were washed with phosphate buffered saline (PBS). PBS was removed, and 200 microliters (μL) of virus was applied to each well. Six-well plates were rocked to ensure virus was spread evenly across cell monolayer and cells did not dry out. After 30 minutes incubation at room temperature, four milliliters (mL) of agar overlay (a 1:1 mixture of 2% agar and 2X MEM) was added to each well. Plates were incubated for four days at 37°C with 5% CO_2. On day 5 post-infection, a 1:1 solution of 2% agar and 2X MEM with 2% neutral red was added to allow visualization of plaques, and plaques were counted. Only wells with 10-100 plaques were used to calculated virus titer, using the following equation: reciprocal of the virus dilution x number of plaques x5.

Multiplication Kinetics

Multiplication kinetics of viruses were undertaken at a multiplicity of infection (MOI) of 0.1. Vero or A549 cells were grown in 12-well plates to approximately 80% confluency. Once cells were confluent, media was removed from cells and they were washed with PBS to remove any cell culture media and FBS. Cells from three wells were trypsinized and counted. The cell count of each well was averaged, and total cell count was calculated in order to calculate quantity of virus needed for the MOI of 0.1. Cells were infected, and virus was adsorbed while rocking for 30 minutes. PBS was used to

wash wells three times to remove residual virus. Two mLs of DMEM supplemented with 2% FBS was added to each well. There were three wells with virus for each time point taken: 0, 24, 36, 48, 60, and 72 hours post infection. Cells were checked for CPE at each time point, harvested (four 500 µL aliquots), and stored at -80°C until plaque assay titration. Statistical analysis was performed on growth curves, which had an n=3 for each time point per virus, via a two-way repeated measures ANOVA with a Tukey's post-hoc test. An alpha value of 0.05 was used.

In-Vitro Transcription and Electroporation

Virus was rescued from infectious clones by in-vitro transcription of an infectious clone template via an exogenous SP6 promoter. The first step was to linearize the template of the infectious clone by taking approximately 4 microgram (µg)/mL of starting template and mixed with buffers and cut utilizing specific restriction enzymes that are engineered into infectious clone models. Specifically, YFV 17D utilized in these studies has an Xhol1 restriction site, and the YFV 17D/DENV-4 prME has BsiWI and SfoI restriction sites. This digestion mixture was incubated at 37°C for two to three hours. Subsequently, 5 µL of 20 mg/mL proteinase K was added and incubated at 37°C for one hour. DNA was then extracted via two phenol-chloroform extractions followed by a single chloroform extraction. The DNA was ethanol precipitated, and in-vitro transcription performed, using linearized template, specific buffers for the promoter, and a nucleotide triphosphate mix; and incubated for two and a half hours at 37°C. A small sample of the reaction mix was run on a gel to ensure the presence of viral RNA. A 75cm^2 flask of Vero cells was trypsinized, washed once with PBS, and counted using a standard hemocytometer and the cell count calculation described in section 3.4. Cells

were washed twice more in PBS, then 6.8 x 10^6 cells put into electroporation cuvettes and transcribed RNA is added. The cuvettes are put in a Bio-Rad gene pulser that was used at 1.5 kV, infinite ohms, and 25 μF to perform the electroporation, shocking twice. Following electroporation, the solution was kept at room temperature for10 minutes, and the mixture transferred to a 75cm^2 filter top flask with DMEM supplemented with 10% FBS. Cells were observed daily, and CPE was monitored. Virus was harvested when approximately 80% CPE occurred, which typically occurred approximately 5 days post infection.

NGS Analysis

Viral RNA was extracted from Vero cells using a Qiagen Viral RNA kit, and viral RNA is then sent to the UTMB Next Generation Sequencing Core for NGS analysis. Deep sequencing was performed on an Illumina HighSeq 1500 instrument by the UTMB Next Generation Sequencing Core. Once data were received from the core, a large data file containing the information for each of the RNA reads, called a bam file, was processed further. This file was converted to a fastq file via Picard tools, and alignment and processing undertaken. Files were then processed to remove PCR duplicates and downsampled to the same number of reads per virus to ensure an accurate comparison of viruses based on coverage. R studio was then used to analyze viral population diversity and variability. Variability was measured via Shannon's entropy, which is a probability measurement of diversity. This ranges from highest diversity (meaning all four nucleotides we are examining are occurring equally), to 0 (meaning only one of the four nucleotides is occurring). Other programs were used to analyze the variant population
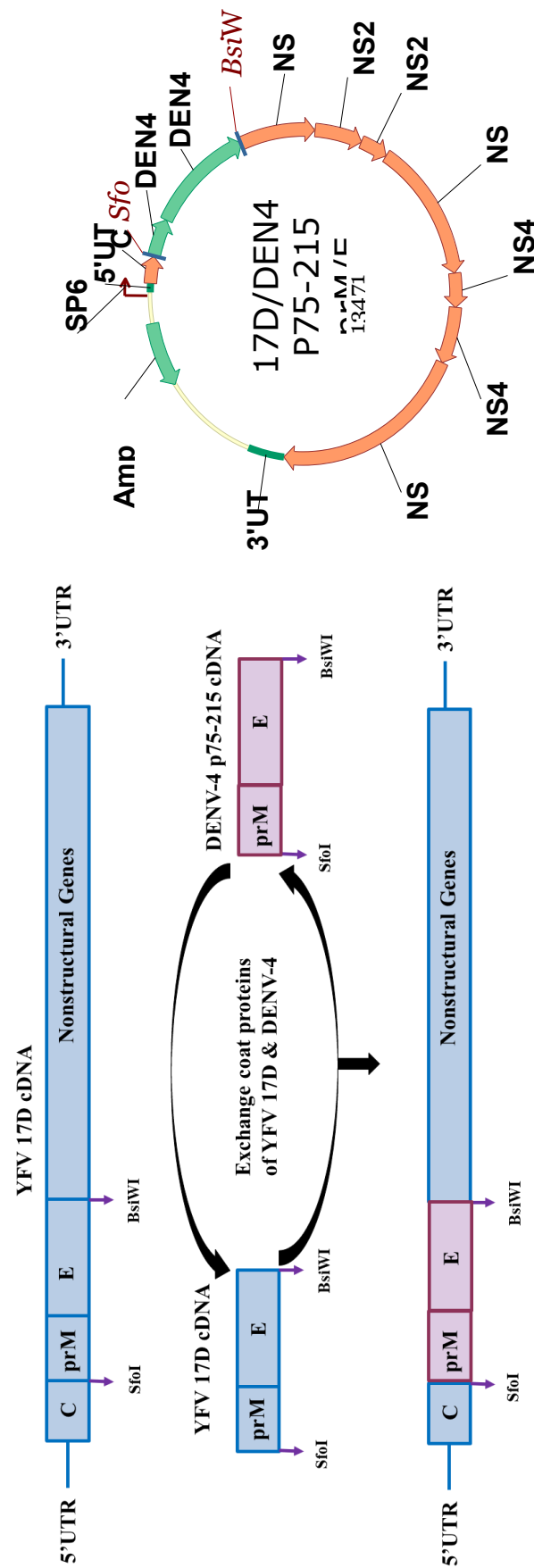
Figure 3.1 Schematic of YFV 17D/DENV-4 prME virus with restriction enzymes

60

present in each sample via Vphaser software, with a cutoff of 1% used, (i.e., only Single Nucleotide Variants (SNVs) greater than 1% of the population at a particular nucleotide position are analyzed. The pipeline analysis for NGS data is shown in **Figure 3.2**. Statistical analysis comparing the diversity of the three viruses was performed via a one-way ANOVA with Kruskal-Wallace post-test for non-parametric data. The alpha was 0.05.

Animal Studies

Animal studies utilized eight-week-old AG129 mice (provided by Nigel Bourne from a colony maintained by Dr. Nigel Bourne), which are deficient in IFN α, β, and γ receptors. Animals were monitored daily for signs of illness, and if observed, were humanely euthanized. If no disease was observed, animals were humanely sacrificed at day 28 post infection. A second group of five animals, 10 weeks old, were utilized to confirm the initial results of the chimeric YFV 17D/DENV-4 prME results.

In a second study, AG129 mice were utilized again, at eight weeks old, and received all inoculations i.p. Serum samples were taken at day three post infection, and animals were monitored for signs of illness daily. If illness was observed, animals were humanely euthanized. Serum samples were taken at three days post infection and were used to test for viremia by plaque infectivity assay. Liver and brain tissues were homogenized in MEM supplemented with 2% FBS, using a Beadbug microtube homogenizer. Samples were spun at 8,000 rotations per minute (RPM) to clarify, then aliquoted and stored at -80°C until viral load testing via plaque assay.
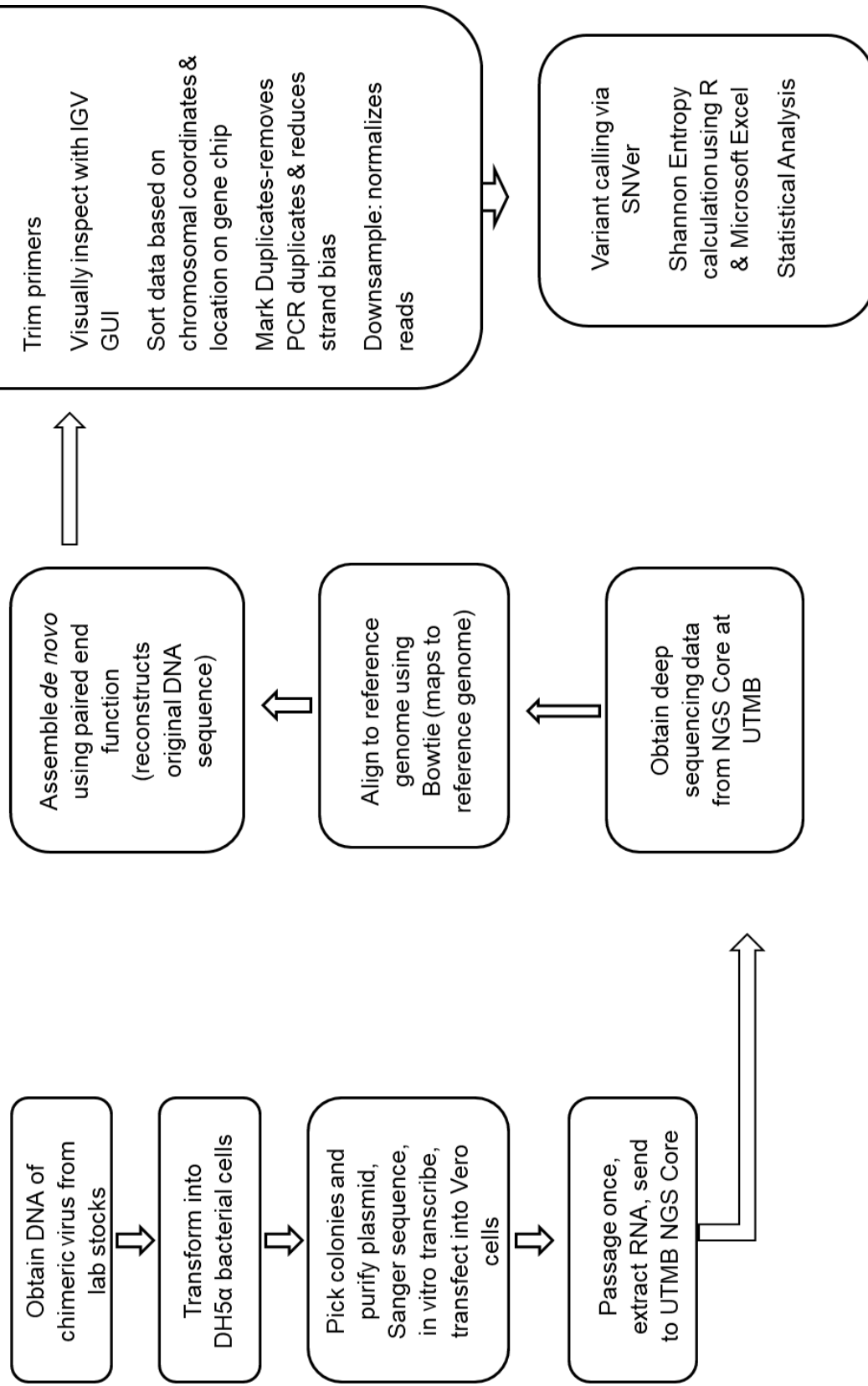
Figure 3.2 NGS analysis pipeline.

Chapter 4: Results

Multiplication Kinetics in Vero cells

To determine whether or not the virus' replication machinery has been compromised by chimerization, multiplication kinetic studies were performed. The rationale was the premise that while there were no changes in the viral nonstructural replication machinery genes, the changes that occurred in the structural proteins (i.e. prM and E) may have affected entry. If entry was altered, then this would in turn alter the replication kinetics and multiplication efficiency of the virus. Multiplication kinetics were performed in triplicate at an MOI of 0.1 (Figure 4.1A). The results indicate that YFV 17D infectious clone multiplies most efficient of the three viruses in the study. DENV-4 P75-215, a wild-type sylvatic strain, multiplies slightly less efficiently and slightly slower than YFV 17D infectious clone, although both viruses multiply to approximately the same peak infectivity titer (6 $\log_{10}$ PFU) (i.e., 48 hours for YF 17D infectious clones vs. 72 hours for DENV-4 P75-215). The chimeric virus, YFV 17D/DENV-4 prME multiplied the slowest of the three viruses. Furthermore, the chimera took longer to get to a titer level similar to YFV 17D infectious clone or DENV-4 P75-215. The differences between overall curves were tested using a two-way ANOVA with a Tukey's post-hoc test. This demonstrated YFV 17D infectious clone was multiplication was significantly different from both DENV-4 P75-215 and YFV 17D/DENV-4 prME, with $P<0.05$.

Viruses that were plaque titrated in Vero cells exhibited the following phenotypes. Typically, DENV-4 P75-215 plaques were large, ≥ 2 millimeters (mm), YFV 17D had small plaques (≤ 2 mm), and YFV 17D/DENV-4 prME had a mixed plaque phenotype

(data not shown). NGS analysis demonstrated only one viral population in YFV 17D/DENV-4 prME (see below), and no plaque purification was performed.

A549 Multiplication Kinetics

Multiplication kinetics in A549 cells were performed in triplicate as described in section 3.4, at an MOI of 0.1 (Figure 4.1B). These results indicate that YFV 17D infectious clone multiplies more efficiently and faster than either DENV-4 P75-215 or the chimeric YFV 17D/DENV-4 prME. YFV 17D infectious clone reaches the highest infectivity titer (approximately 6.1 $\log_{10}$ PFU) of the three viruses. DENV-4 prME multiplies less efficiently than YFV 17D infectious clone, but slightly better than YFV 17D/DENV-4 prME and reaches a slightly higher infectivity titer than YFV 17D/DENV-4 prME in this cell line (approximately 4 $\log_{10}$ PFU). The chimeric virus, YFV 17D/DENV-4 prME, multiplied least efficiently of the three viruses, reaching a maximum infectivity titer of approximately 4 $\log_{10}$ PFU. Overall, DENV-4 P75-215 and the chimeric YFV 17D/DENV-4 prME appear to have reduced multiplication kinetics when compared to YFV 17D infectious clone in both cell lines (**Figure 4.1B**). Significance was demonstrated with a P<0.005. The differences between overall curves were tested using a two-way ANOVA with a Tukey's post-hoc test. This demonstrated that all curves were significantly different from one another, with P<0.05.

Next Generation sequencing of viruses: Shannon Entropy Comparison

The three viruses were subjected to NGS to analyze the population of viral RNAs in each virus. In order to generate statistically significant data, the virus samples from the same virus preparation of each of the three viruses were compared on two different NGS runs, one was undertaken in 2015 and one in 2017. The data for both individual runs are

shown below with labels of "2015" and "2017", respectively, plus the pooled average data. In the 2015 NGS run, the number of reads, or coverage, for each virus is as follows. YFV 17D infectious clone had a coverage of 4100.232. DENV-4 P75-215 had a coverage of 4816.704, and YFV 17D/DENV-4 prME had a coverage of 8308.273. This was then downsampled to the lowest value of YFV 17D infectious clone, and the post downsampling coverages were as follows. The YFV 17D infectious clone coverage remained the same, DENV-4 P75-215 had a coverage of 4101.365, and YFV 17D/DENV-4 prME had a coverage of 4099.708. The same procedure was performed in the 2017 NGS run. The initial coverages were: YFV 17D infectious clone (42,839.88), DENV-4 P75-215 (29,869.54), and YFV 17D/DENV-4 prME (7,494.581). Post downsampling, the coverage for YFV 17D/DENV-4 prME was 7376.028, YFV 17D infectious clone was 7385.0667, and DENV-4 P75-215 had a coverage of 7381.415. Overall, as described in detail below, both runs demonstrated very similar data, namely that the results obtained are reproducible.

Comparison of Shannon's Entropy of YFV 17D Infectious Clone, DENV-4 P75-215 and YFV 17D/DENV-4 prME viruses

Diversity is low across the entire genome of YFV 17D infectious clone (**Figure 4.2**). There were no areas of distinctly high diversity in any genome location in either runs for the 17D vaccine virus.

The diversity indices for DENV-4 P75-215 vary widely across the entire genome, with peaks of high diversity occurring in each gene, in both NGS runs (**Figure 4.3**). This is typical of what one would expect with a RNA virus, due to the poor proof-reading capability of the RdRp (117).

65

The Shannon entropy diversity indices for YFV 17D/DENV-4 prME were similar to that of YFV 17D infectious clone (**Figure 4.4**). Interestingly, there are peaks of high diversity at nucleotide position 257 in the E gene for both NGS runs. This is a non-coding change in both instances. However, excluding this high diversity point, the prM/E region of the chimeric virus appears to be much less diverse than that of parental DENV-4 P75-215 prM/E region, and appears to have a genotype more like that of YFV 17D infectious clone. To compare the Shannon's Entropy data for the three viruses, the average Shannon's Entropy of each gene was compared for the three viruses. **Table 4.1a** represents the average Shannon's entropy calculated for the 2015 NGS run, **Table 4.1 b** represents the average Shannon's entropy for the 2017 NGS run. **Table 4.1 c** is the pooled average Shannon's entropy for both NGS runs. **Figure 4.5** represents the graphical Average Shannon's entropy for each virus run, as well as a graphical representation of the pooled average data of the two NGS runs. A Friedman's non-parametric test was performed with an alpha of 0.05, with a Dunn's post-hoc test, in order to see if the average entropies of the two NGS Runs were significantly different. It was found that they were different; however, this may be attributed to variation in read numbers (coverage) in the two NGS runs (4100 vs 7495 reads for 2015 and 2017 runs, respectively). However, the trends are similar between the two NGS runs, demonstrating that there is decreased diversity of the chimeric YFV 17D/DENV-4 prME compared to DENV-4 P75-215 (**Table 4.1, Figure 4.5**). DENV-4 prME appears to have the highest diversity all across the genome. YFV 17D infectious clone has the lowest diversity indices all across the genome, when compared to YFV 17D/DENV-4 prME and DENV-4 P75-215. The YFV 17D/DENV-4 prME virus has genes/regions that have lower diversity

than that of YFV 17D infectious clone, namely the C, prM, NS2B, and NS4B, although with slightly higher Shannon Entropy diversity indices in the E region (0.0026 vs 0.0035) in the 2015 NGS run (**Table 4.1a).** In the 2017 NGS run, the Shannon's entropy values were demonstrated to be higher in all viruses, but this may be attributed to NGS differences in coverage and runs. It was found that prM, NS1, NS4B, and NS5 all had lower average Shannon's entropy values than either YFV 17D or DENV-4 P75-215 (**Table 4.1b**). Pooled data of the average Shannon's entropy demonstrated that DENV-4 had the highest entropy in all instances. YFV 17D and YFV17D/DENV-4 prME each had instances of lowest and intermediate diversity (**Table 4.1c**). It was discovered that YFV 17D/DENV-4 prME had lower average entropy than YFV 17D in the prM, NS1, and NS4B genes (**Table 4.1c).** Statistical analyses of the three viruses determined that YFV 17D/DENV-4 is significantly different from DENV-4 P75-215 (P<0.0001), and is not significantly different from YFV 17D (P=0.7887). YFV 17D and DENV-4 P75-215 are significantly different from one another (P<0.001) (**Figure 4.2, 4.3, 4.4**).

Single Nucleotide Variant Population Analysis

The NGS data were also analyzed for Single Nucleotide Variants (SNVs) using a cutoff of variants that occurred in instances greater than 1% of the population and had no strand bias. When looking at the overall variant population of YFV 17D infectious clone, very few variants were observed in any position of the genome (**Figure 4.6)** while variants occurred at many positions of the DENV-4 P75-215 genome (**Figure 4.6**). YFV 17D/DENV-4 prME has very few variants occurring in the genome, with the variant occurring at E gene nucleotide 257 occurring at 45 and 20 percent (2015 vs 2017 NGS run), respectively; this variant is non-coding (**Figure 4.6**). **Figure 4.7** demonstrates the
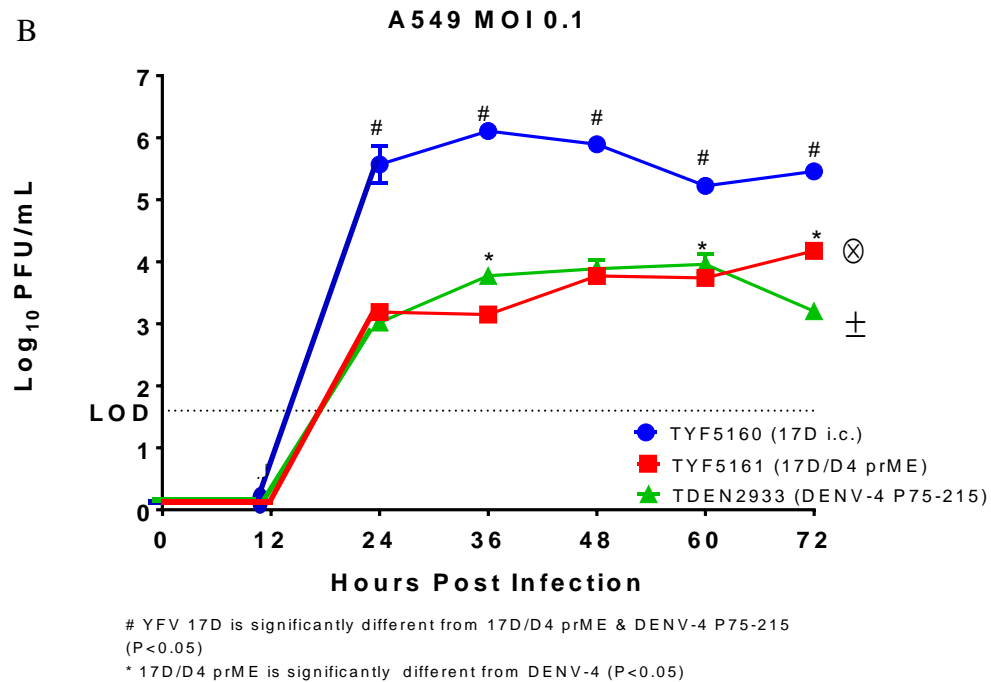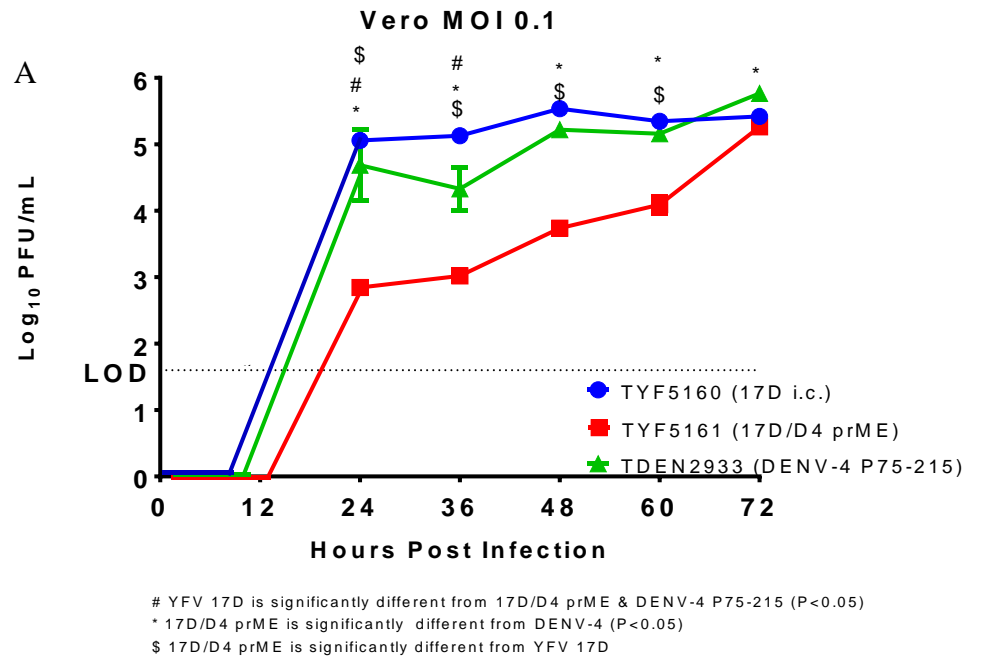
Figure 4.1. Replication kinetics performed in triplicate in Vero and A549 cells at MOI 0.1. Curves were analyzed for statistical differences in both cell lines. A. Vero cells demonstrated significant differences between all three viruses, with P<0.05. B. A549 cells demonstrated significant differences between YFV 17D infectious clone and DENV-4 P75-215, as well as YFV 17D infectious clone and YFV 17D/DENV-4 prME, with P<0.05.
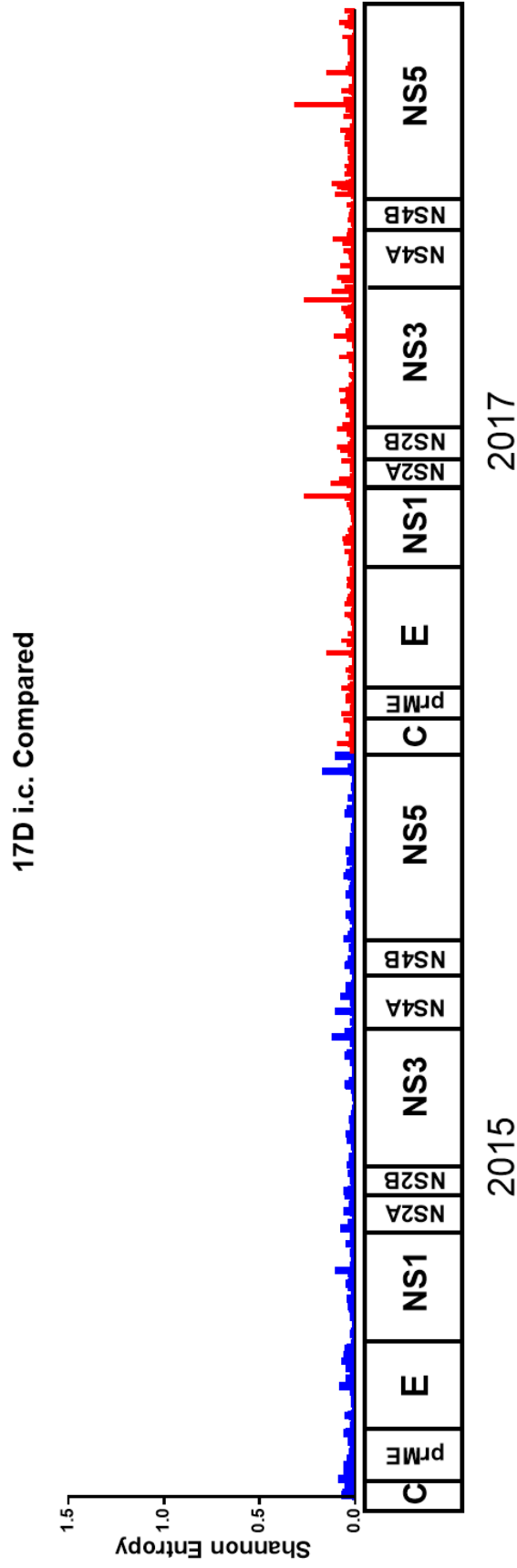
Figure 4.2. YFV 17D infectious clone diversity for two NGS runs of the same sample, as demonstrated by Shannon's entropy.

overall variant percentage of each virus and demonstrates that DENV-4 P75-215 has the most variants occurring, while YFV 17D infectious clone has very few, and YFV 17D/DENV-4 prME has few, with the one non-coding variant at E257 occurring at high frequency. When observing the variants that occur in greater than 1% of the viral variant population, **Figure 4.8a** shows where each variant occurs in the genome for the sample run in 2015, and **Figure 4.8b** shows where each variant occurs in the genome for the sample run in 2017. **Figure 4.8a** showed that in the 2015 run, many of the variants that were observed in greater than 1% of the population occurred in DENV-4 P75-215. Nearly every area of the genome, except for the 3'UTR, demonstrated the presence of at least one variant in the DENV-4 P75-215 population. YFV 17D infectious clone had only two variants occurring in greater than 1% of the population, and one of these was in the 3'UTR, and thus was non-coding. The other variant occurred in NS5. The chimeric YFV 17D/DENV-4 prME demonstrated that there were two variants that occurred: one in NS2A, and another at a high percentage (45%) in the E, which was E257, and was non-coding. **Figure 4.8b** demonstrated the NGS variants over 1% were occurring most frequently in DENV-4 P75-215, similar to what was observed in the 2015 NGS run (**Figure 4.8a**). In this NGS run (**Figure 4.8b),** there were variants greater than 1% occurring in every area of the genome of DENV-4 P75-215. YFV 17D infectious clone demonstrated no coding change variants occurring in greater than 1% of the population, only changes in the 3'UTR. YFV 17D/DENV-4 prME demonstrated that there were few variants occurring in the population, with four total. One occurred in the 3'UTR, one in the NS2A region, one in the NS3 region, and there was a high frequency (20%) of the E257 non-coding change in this instance as well as the 2015 NGS run. Similar to
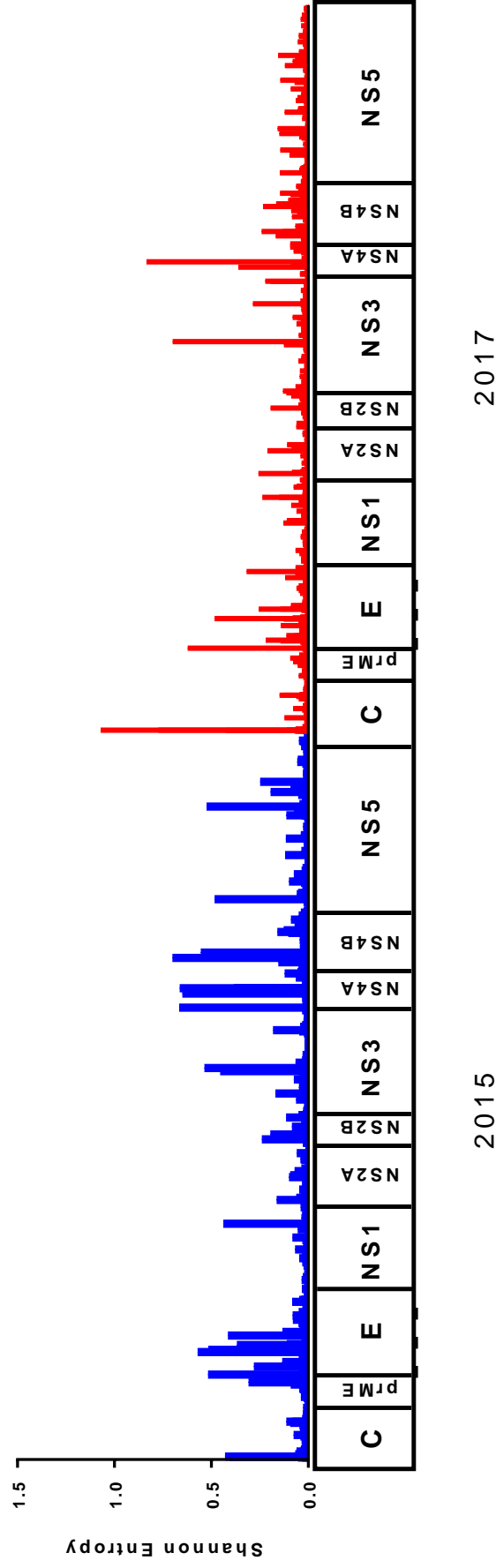
Figure 4.3. DENV-4 P75-215 diversity for two NGS runs of the same sample, as demonstrated by Shannon's entropy.
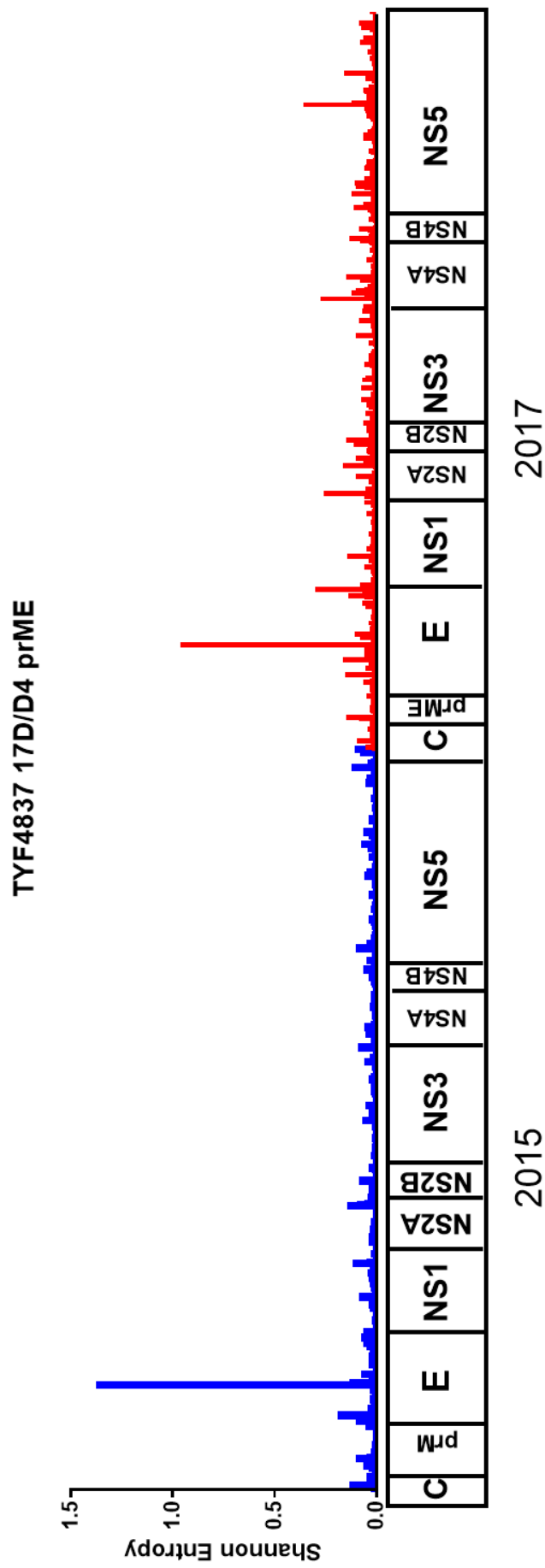
Figure 4.4. YFV 17D//DENV-4 prME diversity for two NGS runs of the same sample, as demonstrated by Shannon's entropy.

observations with average Shannon's entropy, the 2017 NGS run appeared to have more variants observed at greater than 1% of the population; this is hypothesized to be due to NGS differences based on read coverage. These data demonstrated that there was a decreased variant population in YFV 17D/DENV-4 prME, compared to that of DENV-4 P75-215, and that it appeared to have a variant population more similar to that of YFV 17D. Table **4.2** summarizes the variants occurring in the 2015 NGS run, and **Table 4.3** summarizes that of the 2017 NGS run.

Animal Studies

In order to analyze the *in vivo* effects, and to characterize the phenotype of the chimeric YFV 17D/DENV-4 prME compared to parental YFV 17D and DENV-4, animal studies were undertaken utilizing AG129 mice, which are the current standard for flavivirus research (118). All animals were inoculated via the i.p route. In the first animal study, DENV-4 P75-215 was administered by the i.p. route in a volume of 200 µL to a group of five eight-week-old AG129 mice at a dose of 2.5 x10^6 PFU. All virus inocula were back titrated to confirm virus titer and to demonstrate that virus titer was accurate (data not shown). YFV 17D infectious clone was administered to a group of five animals at a dose of 3.5 x 10^5 PFU. YFV 17D vaccine virus (17D-204) was administered to a group of three mice, with the same amount and dosage received as the of YFV 17D infectious clone. YFV 17D/DENV-4 prME was given to five animals at a dose of 1.2 x 10^6 PFU. Control AG129 animals (n=5) were inoculated with vehicle only (PBS). Varying virus inocula were utilized due to previous studies that suggested YFV 17D would be lethal at doses higher than used here, and that pathological changes could be observed using chosen DENV doses (88, 89, 119). Doses were also chosen based on

variable infectivity and titer of each virus used (88, 89, 118). Initial animal study results in AG129 mice are shown in **Figure 4.9** (weight change) and **Figure 4.10** (survival). Weight change (**Figure 4.9**) began approximately two days post infection in YFV 17D/DENV-4 prME animals. Those animals receiving DENV-4 P75-215 lost some weight at approximately day two post infection. YFV 17D infectious clone animals began exhibiting weight loss at day 10 post infection, and rapidly declined. Animals receiving YFV 17D vaccine were stable, and only began to demonstrate weight loss at approximately day 16 post infection. Control animals did not exemplify significant weight loss.

Clinical disease manifestations of DEN consist of a febrile, flu-like illness. However, in a minority of cases, infection proceeds into more severe illness. Symptoms of DEN fever include high fever (40°C/104°F), severe cephalgia, severe eye pain, general arthralgia, vomiting, rash, or swollen glands (23). Severe DEN is caused by plasma leakage, edema, respiratory distress, severe bleeding, and/or organ injury. Signs of severe DEN can include an overall decrease in temperature (below 38°C/100°F), as well as abdominal pain, continued and prolonged emesis/vomiting, hyperventilation, bleeding gums, general fatigue, restlessness, and/or bloody emesis (30).

YFV 17D/DENV-4 prME inoculated animals began succumbing to infection at day six post infection (four out of five mice were euthanized), and the remaining animal succumbed to infection at day seven post infection (**Figure 4.10**). The average survival time (AST) was 5.8 ± 0.4 days. The one animal which received DENV-4 P75-215 and succumbed to disease did so at day 20 post infection. Animals receiving YFV 17D infectious clone succumbed to disease at day 14 post infection (1/5), another at day 15

post infection, a third at day 16 post infection, a fourth at day 17 post infection, and the remaining animal succumbed at day 20 post infection. The AST for this group was 16.5 $\pm$ 1.0 days. Three of the five animals who received YFV 17D vaccine succumbed to infection at day 22, and the other two animals survived until the termination of the study. The AST was 22.0 $\pm$ 1.2 days.

In order to confirm results obtained with the chimeric YFV 17D/DENV-4 prME, an additional group of five, 10-week-old AG129 mice were inoculated with virus by the i.p. route. Three animals received 1.4 x 10^6 PFU in a 100µL volume and two animals received 2.8 x 10^6 PFU in a 200 µL volume. The rationale behind using different volumns of virus inoculum was due to altered virus titers of each of the different viruses, allowing normalization of virus concentration, as well as to determine if the amount of virus would alter infectivity and lethality of the virus.The weight loss of these animals is shown in **Figure 4.11**. These animals began to exhibit weight loss at approximately day three post infection. The survival curve is shown in **Figure 4.12,** which showed that two out of five animals succumbed at day seven post infection, with the other three animals succumbing at day eight post infection. The virus was lethal in all animals at differing doses, with animals with a lower dose succumbing later in the time course, indicating that this may be a dose dependent phenomenon. The AST from this study was 7.6 $\pm$ 1.0 days. Serum samples taken at day three post infection were checked for viremia. **Figure 4.13** demonstrates the serum viremia levels; this showed that the animals receiving YFV 17D infectious clone had detectable viremia three days post infection; two of these animals had no detectable viremia (below 2.0 x 10^2 FFU/mL), one had viremia of 2.0 x 10^3 ffu/mL, and two at 2.4 x 10^3 FFU/mL. All three of those receiving YFV 17D vaccine had

no detectable viremia. Those receiving DENV-4 P75-215 had three out of five animals with detectable viremia, between 1.0×10^3 and 2.4×10^3 PFU/ml, as did the group of 8-week-old animals infected with YFV 17D/DENV-4 prME virus with infectivity titers ranging between 1.3×10^3 and 1.6×10^3 PFU/ml. The 10-week-old animals that were challenged with YFV 17D/DENV-4 prME virus exhibited no detectable viremia on day three post infection (i.e., ≤ 50 PFU/ml). Samples were collected at day three post infection due to studies suggesting this was the peak viremia (118). There was detectable virus in the brains of the 8-week-old animals infected with YFV 17D/DENV-4 prME, in three of the animals which succumbed at day five post infection (5.4, 4.3, and 5.2 $\log_{10}$ PFU/g), and one at day six post infection (4.7 $\log_{10}$ PFU/g). There was virus in the brain of one 10-week-old animal with a viral titer of 5.7 $\log_{10}$ PFU/g at day seven post infection; mice inoculated with DENV-4 P75-215 exhibited no detectable viral load in the brain ($\leq 3.1 \log_{10}$ PFU/g), except for the one animal that succumbed to infection on day 20 post infection (4.3 $\log_{10}$ PFU/g) (**Figure 4.14**). Animals receiving the YFV 17D-204 vaccine strain, exhibited viremia, in one out of three animals, with 4.5 $\log_{10}$ PFU/g detected; this animal succumbed at day 22 post infection (**Figure 4.14**). The animals receiving YFV 17D infectious clone virus displayed variable viral loads in the brain. Two animals in this group exhibited a brain viral load of 5.4 and 5.2 $\log_{10}$ PFU/g; however, all other animals demonstrated much lower brain viral loads, with one animal displaying 4.3 $\log_{10}$ PFU/g and another at 4.7 $\log_{10}$ PFU/g; these both occurred at day 17 post infection (**Figure 4.14**). No animals demonstrated detectable virus in the liver ($\leq 3.1 \log_{10}$ PFU/g) (**Figure 4.15**).

A second experiment was undertaken to confirm the data of the first study and utilized the same 8-week-old AG129 animal model and virus was administered by the intraperitoneal route. Overall, the results demonstrated a similar pattern to the prior study. 17D infectious clone was administered at 1.05×10^6 PFU in a 100µL volume. The chimeric virus, YFV 17D/DENV-4 prME was administered at a dose of 1.4×10^6 PFU in a 100 µL volume. In addition, two groups of animals received different doses of DENV-4 P75-215. One group of five mice received a dose of 2.0×10^7 PFU in a volume of 100 µL while the second group of five animals received a dose of 3.6×10^6 PFU in a volume of 100 µL. Animals receiving YFV 17D infectious clone began to show weight loss at approximately day 10 post infection (**Figure 4.16**). Those receiving YFV 17D/DENV-4 prME began exhibiting weight loss at day three post infection, while those receiving the higher dose of DENV-4 P75-214 (2×10^7 PFU) showed some weight loss around day four post infection; those receiving the lower dose (3.6×10^6 PFU) exhibited some weight loss around day 12 post infection (**Figure 4.16**). The animals receiving YFV 17D infectious clone began to succumb to disease on day 15 post infection, and all animals had succumbed by day 19 post infection, with an AST of 15.6 ± 0.9 days (**Figure 4.17**).

Animals inoculated with YFV 17D/DENV-4 prME began to die on day six post infection, and all animals had succumbed by day nine post infection; the average AST was 7.2 ± 0.6 days (**Figure 4.17**). Those animals who received the 3.6×10^6 PFU of DENV-4 P75-215 began to succumb to disease on day 15 post infection (one animal), another on day 16 post infection, a third on day 26, with the other two animals surviving until study termination; the AST was 17.5 ± 3.8 days (**Figure 4.17**). Those animals inoculated with 2×10^7 PFU of DENV-4 P75-215 began to show clinical signs of illness

on day nine post infection, including one animal succumbing, with three others

succumbing by day 14 post infection, with one animal surviving until the termination of

the study, and an AST of 12.0 days. **Figure 4.18** incorporates the results from all the

studies to show that the trends for each virus are confirmed in all studies; it also shows

pooled average data from the animal experiments based on dosage, demonstrating the

survival curves of animals were similar in each study, and that there was a significant

difference in the curves of the animal/virus groups; statistics were performed via a

Mantel-Cox test (P<0.0001).

A

	Shannon Entropy		
	YFV 17D Mean Entropy	Dengue 4 Mean Entropy	17D/DENV4 prM/E	
C	0.0034	0.0037	0.0033	⬅
prM	0.0028	0.0032	0.0027	⬅
E	0.0026	0.0052	0.0035	⬅
NS1	0.0028	0.0037	0.0028	
NS2A	0.0027	0.0038	0.0028	
NS2B	0.0027	0.0029	0.0026	⬅
NS3	0.0023	0.0037	0.0024	
NS4A	0.0024	0.0064	0.0025	
NS4B	0.0027	0.0052	0.0025	⬅
NS5	0.0026	0.0035	0.0026	

B

	Shannon Entropy		
	YFV 17D Mean Entropy	Dengue 4 Mean Entropy	17D/DENV4 prM/E	
C	0.0054	0.0057	0.0058	
prM	0.0058	0.0057	0.0054	⬅
E	0.0053	0.0071	0.0065	
NS1	0.0055	0.0094	0.0052	⬅
NS2A	0.0053	0.0072	0.0054	
NS2B	0.0061	0.0060	0.0062	
NS3	0.0055	0.0072	0.0055	
NS4A	0.0053	0.0097	0.0056	
NS4B	0.0047	0.0087	0.0044	⬅
NS5	0.0057	0.0066	0.0055	⬅

Green: Lowest Diversity   Black: Intermediate Diversity   Red: Highest Diversity

C

	Shannon Entropy		
	YFV 17D Mean Entropy	Dengue 4 Mean Entropy	17D/DENV4 prM/E	
C	0.0044	0.0047	0.0045	
prM	0.0043	0.0044	0.0040	⬅
E	0.0039	0.0062	0.0050	
NS1	0.0042	0.0065	0.0040	⬅
NS2A	0.0040	0.0055	0.0041	
NS2B	0.0044	0.0044	0.0044	
NS3	0.0039	0.0054	0.0039	
NS4A	0.0039	0.0081	0.0040	
NS4B	0.0037	0.0069	0.0035	⬅
NS5	0.0041	0.0050	0.0041	

Green: Lowest Diversity   Black: Intermediate Diversity   Red: Highest Diversity

Table 4.1. Average Shannon's entropy of the three viruses. Panel A is the data from 2015, panel B is the data from 2017, and panel C is the pooled average data from both experiments. Yellow arrows are indicative of areas where YFV 17D/DENV-4 prME has lower Shannon entropy than YFV 17D.
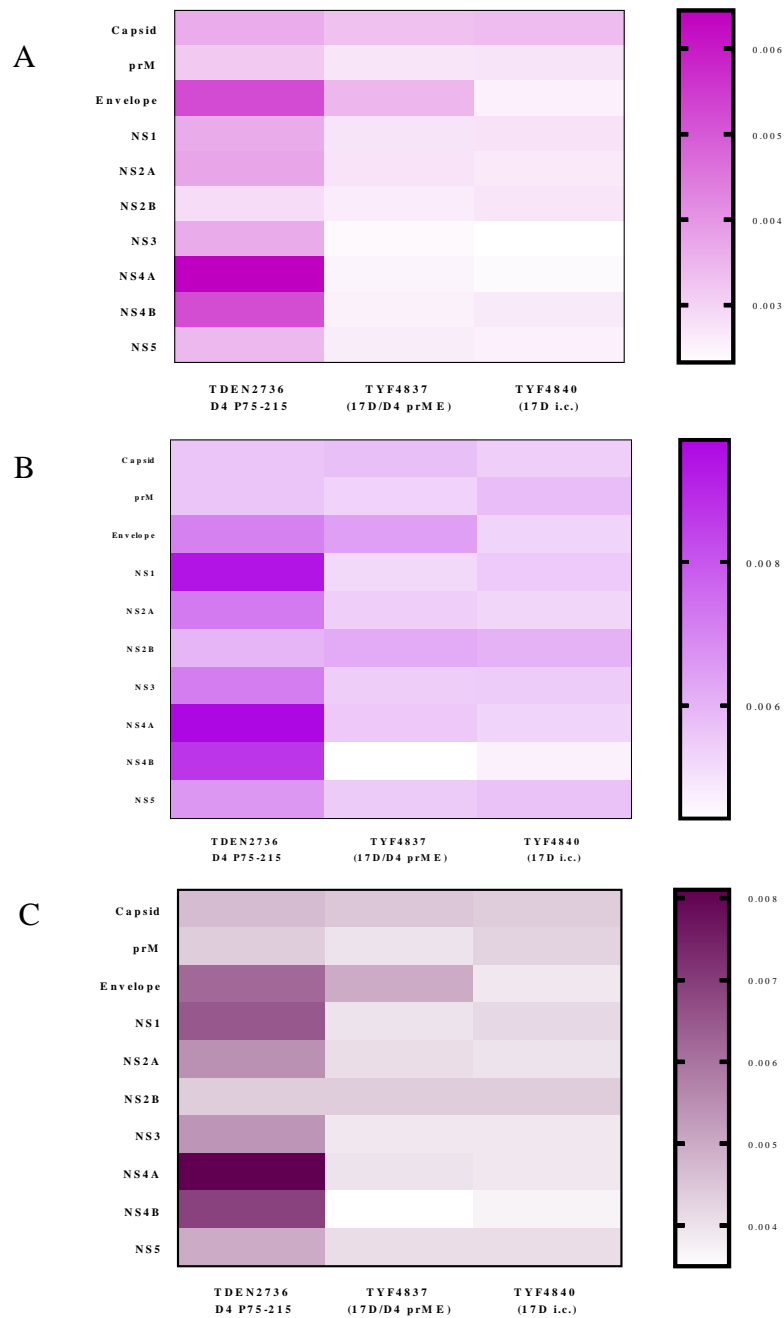
Figure 4.5. Average Shannon's entropy heatmap of the three viruses for two NGS runs of the same sample. Panel A demonstrates the 2015 NGS run, panel B the 2017 NGS run, and panel C the pooled average data of the two studies. Panels A and B were significantly different (P<0.05).
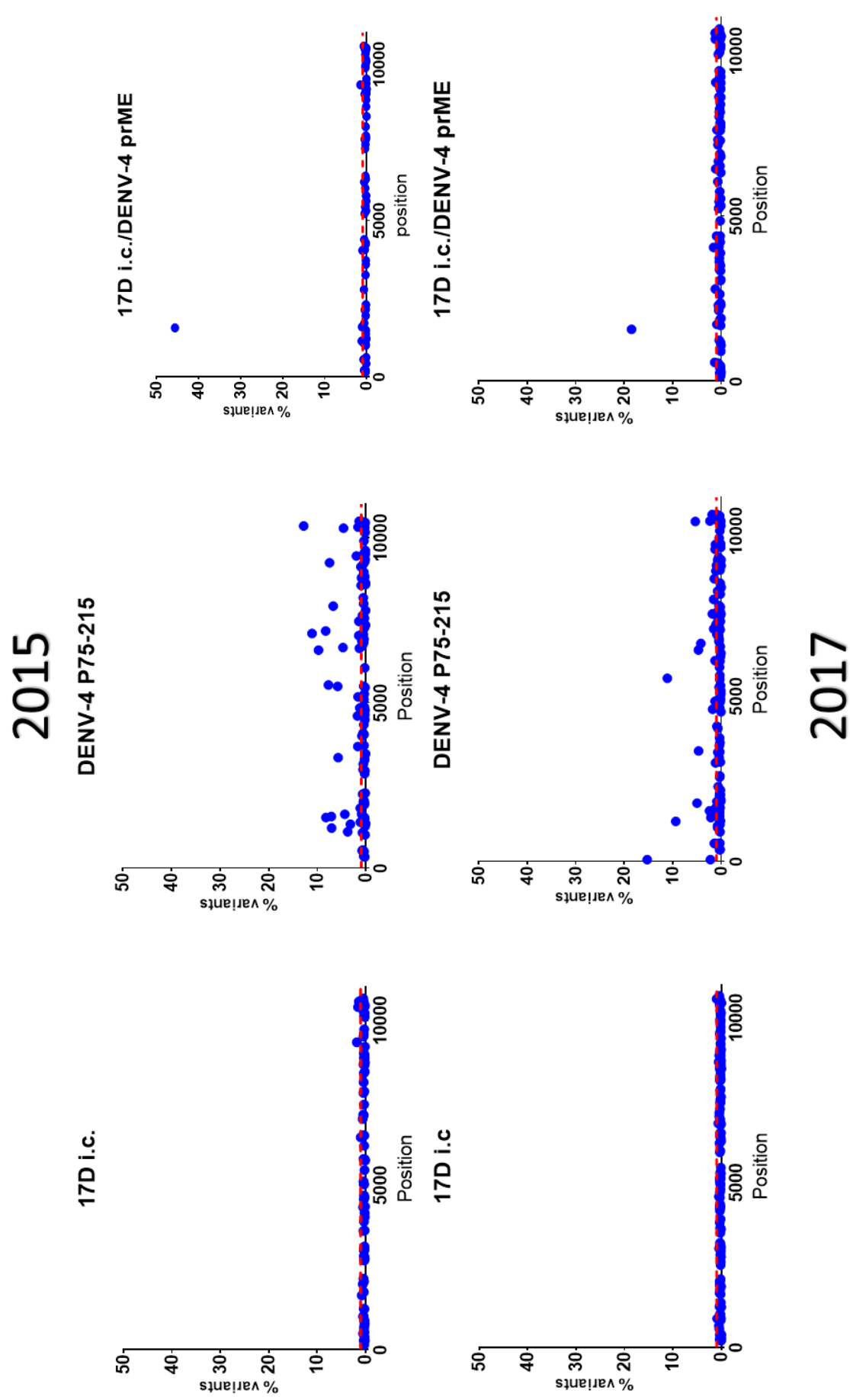
Figure 4.6. Variant population of each virus for two NGS runs of the same sample. The red dashed line represents the 1% cut off used to analyze variants occurring in greater than 1% of the population.

Variant Percentage 2015

Variant Percentage 2017

Figure 4.7. Overall variant percentage for each virus.

Figure 4.8b. Variants occurring in greater than 1% of the population for 2017 NGS run.

Figure 4.8a. Variants occurring in greater than 1% of the population for 2015 NGS run.

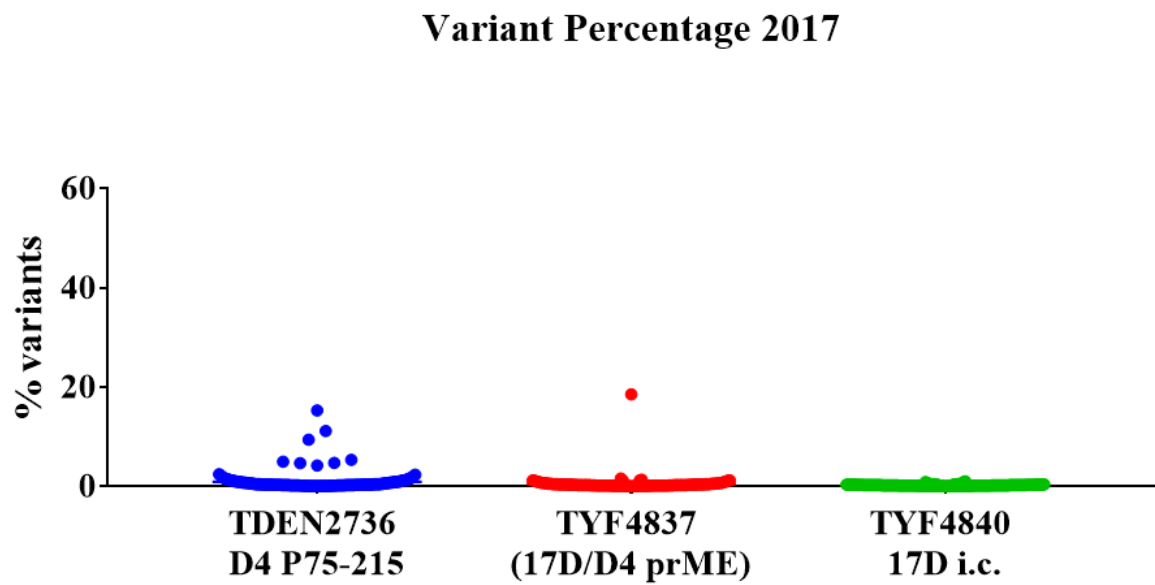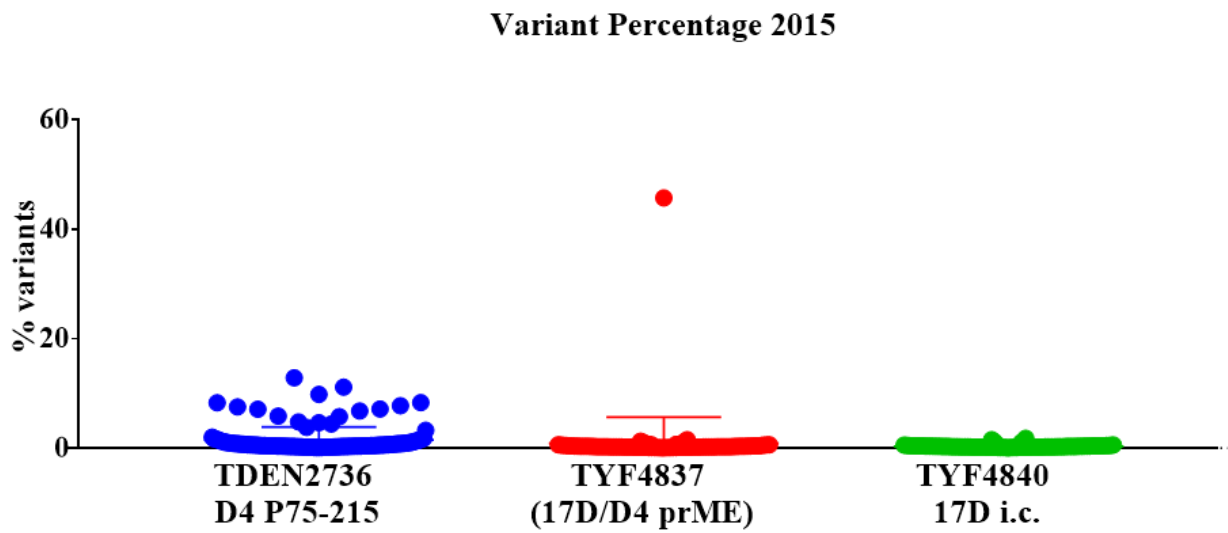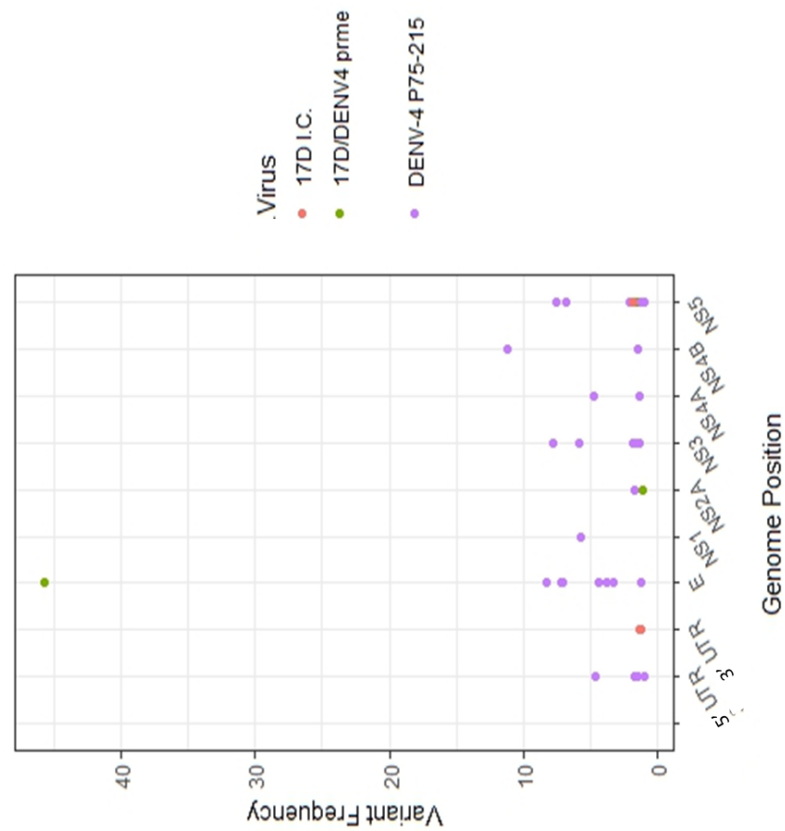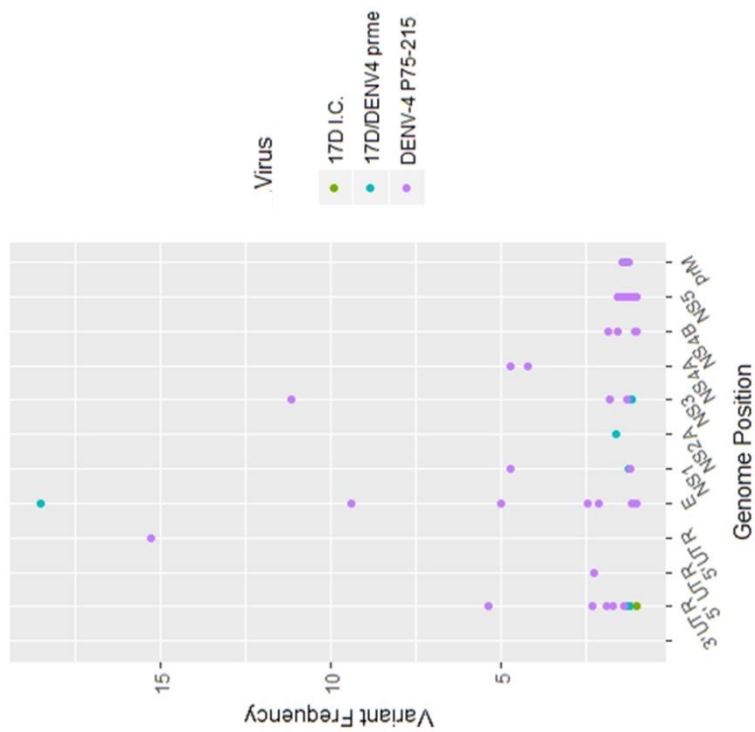| Virus	Nucleotide Position	Polyprotein #	Codon Location	Coding?	Genome Position	Variant	Consensus	Variant Percentage
17D/DENV4 prme	1137	379	3	no	E	A	G	1.257
17D/DENV4 prme	1560	520	3	no	E	A	G	45.68
17D/DENV4 prme	1591	531	1	lys-glu	E	G	A	1.175
17D/DENV4 prme	4038	1346	3	no	NS2A	C	A	1.058
17D/DENV4 prme	9335	3112	na	na	NS5	IA	d	1.546
DENV-4 P75-215	1087	363	1	gln-stop	E	T	C	3.802
DENV-4 P75-215	1199	400	2	thr-ile	E	T	C	7.109
DENV-4 P75-215	1312	438	1	stop-gln	E	C	T	3.246
DENV-4 P75-215	1377	459	3	no	E	A	G	1.196
DENV-4 P75-215	1518	506	3	leu-glu	E	G	A	8.268
DENV-4 P75-215	1549	517	1	lys-glu	E	G	A	7.151
DENV-4 P75-215	1617	539	3	no	E	C	T	4.388
DENV-4 P75-215	1801	601	1	ala > thr	E	A	G	1.218
DENV-4 P75-215	3329	1110	2	gln-arg	NS1	G	A	5.758
DENV-4 P75-215	3665	1222	2	ile-thr	NS2A	C	T	1.702
DENV-4 P75-215	4589	1530	2	tyr-phe	NS3	T	A	1.787
DENV-4 P75-215	4831	1611	na	na	NS3	IA	d	1.303
DENV-4 P75-215	5169	1723	3	no	NS3	T	C	1.665
DENV-4 P75-215	5485	1829	1	gln-stop	NS3	T	C	5.853
DENV-4 P75-215	5528	1843	2	ser-leu	NS3	T	C	7.747
DENV-4 P75-215	6638	2213	2	leu-pro	NS4A	C	T	1.38
DENV-4 P75-215	6660	2220	3	no	NS4A	T	C	4.777
DENV-4 P75-215	7022	2341	2	leu-ser	NS4B	C	T	1.514
DENV-4 P75-215	7086	2362	3	no	NS4B	G	A	11.14
DENV-4 P75-215	7452	2484	3	no	NS4B	C	T	1.508
DENV-4 P75-215	7475	2492	2	cys-tyr	NS5	A	G	1.192
DENV-4 P75-215	7913	2638	2	leu-pro	NS5	C	T	6.774
DENV-4 P75-215	8537	2846	2	stop-leu	NS5	T	A	1.024
DENV-4 P75-215	9101	3001	1	ile-thr	NS5	C	T	1.08
DENV-4 P75-215	9224	3075	2	arg-gln	NS5	A	G	7.529
DENV-4 P75-215	9428	3143	2	arg-lys	NS5	A	G	2.024
DENV-4 P75-215	10269	3423	3	tyr-stop	3' UTR			4.656
DENV-4 P75-215	10303	3435	1	lys-glu	3' UTR			1.67
DENV-4 P75-215	10383	3461	2	val-ala	3' UTR			1.017
DENV-4 P75-215	10481	3494	2	thr-lys	3' UTR			1.418
17D I.C.	9332	3111	na	na	NS5	IA	d	1.783
17D I.C.	10559	3520	na	na	3'UTR			1.352
17D I.C.	10559	3520	na	na	3'UTR			1.217

Table 4.2. Variants occurring in greater than 1% of the population for 2015 NGS run.

Virus	Nucleotide Position	Polyprotein #	Codon Location	Coding?	Genome Position	Variant	Consensus	Variant Percentage
17D/DENV4 prme	559	187	1	asp>tyr	prM	T	G	1.372
17D/DENV4 prme	1559	520	2	no	E	G	A	18.51
17D/DENV4 prme	2780	927	2	gln>pro	NS1	C	A	1.233
17D/DENV4 prme	4037	1346	2	his>pro	NS2A	C	A	1.605
17D/DENV4 prme	6415	2139	1	no	NS3	C	G	1.15
17D/DENV4 prme	9034	3012	1	no	NS5	A	G	1.145
17D/DENV4 prme	10344	na	na	na	3'UTR	C	T	1.23
17D/DENV4 prme	10515	na	na	na	3'UTR	A	G	1.209
17D/DENV4 prme	10531	na	na	na	3'UTR	C	A	1.237
DENV-4 P75-215	40	na	na	na	5'UTR	C	T	15.28
DENV-4 P75-215	41	na	na	na	5'UTR	T	C	2.254
DENV-4 P75-215	532	178	1	ser>pro	prM	C	T	1.45
DENV-4 P75-215	533	178	2	ser>leu	prM	T	C	1.245
DENV-4 P75-215	1199	400	2	thr>ile	E	T	C	9.397
DENV-4 P75-215	1312	438	1	stop>gln	E	C	T	2.141
DENV-4 P75-215	1377	459	3	no	E	A	G	1.005
DENV-4 P75-215	1518	506	3	no	E	G	A	2.439
DENV-4 P75-215	1609	537	1	no	E	T	C	1.148
DENV-4 P75-215	1750	584	1	ile>val	E	G	A	4.996
DENV-4 P75-215	2966	989	2	ile>thr	NS1	C	T	1.202
DENV-4 P75-215	3329	1110	2	gln>arg	NS1	G	A	4.694
DENV-4 P75-215	4589	1530	2	tyr>phe	NS3	T	A	1.789
DENV-4 P75-215	4831	1611	1	na	NS3	IA	d	1.293
DENV-4 P75-215	5528	1843	2	ser>leu	NS3	T	C	11.14
DENV-4 P75-215	6063	2021	3	na	NS3	IA	d	1.287
DENV-4 P75-215	6381	2127	3	val>gly	NS4A	G	A	4.73
DENV-4 P75-215	6580	2194	1	phe>leu	NS4A	C	T	4.217
DENV-4 P75-215	7022	2341	2	leu>ser	NS4B	C	T	1.572
DENV-4 P75-215	7160	2387	2	tyr>cys	NS4B	G	A	1.067
DENV-4 P75-215	7466	2489	2	leu>pro	NS4B	C	T	1.02
DENV-4 P75-215	7475	2492	2	cys>tyr	NS4B	A	G	1.839
DENV-4 P75-215	7913	2638	2	leu>pro	NS5	C	T	1.583
DENV-4 P75-215	8537	2846	2	stop>leu	NS5	T	A	1.443
DENV-4 P75-215	8771	2924	2	leu>ser	NS5	C	T	1.125
DENV-4 P75-215	8939	2980	2	na	NS5	IA	d	1.005
DENV-4 P75-215	9428	3143	2	arg>lys	NS5	A	G	1.27
DENV-4 P75-215	9572	3191	2	leu>pro	NS5	C	T	1.217
DENV-4 P75-215	10269	na	na	na	3'UTR	G	T	5.357
DENV-4 P75-215	10283	na	na	na	3'UTR	T	C	2.333
DENV-4 P75-215	10383	na	na	na	3'UTR	C	T	1.398
DENV-4 P75-215	10384	na	na	na	3'UTR	G	A	1.689
DENV-4 P75-215	10481	na	na	na	3'UTR	A	C	1.892
17D I.C.	10559	na	na	na	3'UTR	IT	d	1.013

Table 4.3. Variants occurring in greater than 1% of the population for 2017 NGS run.
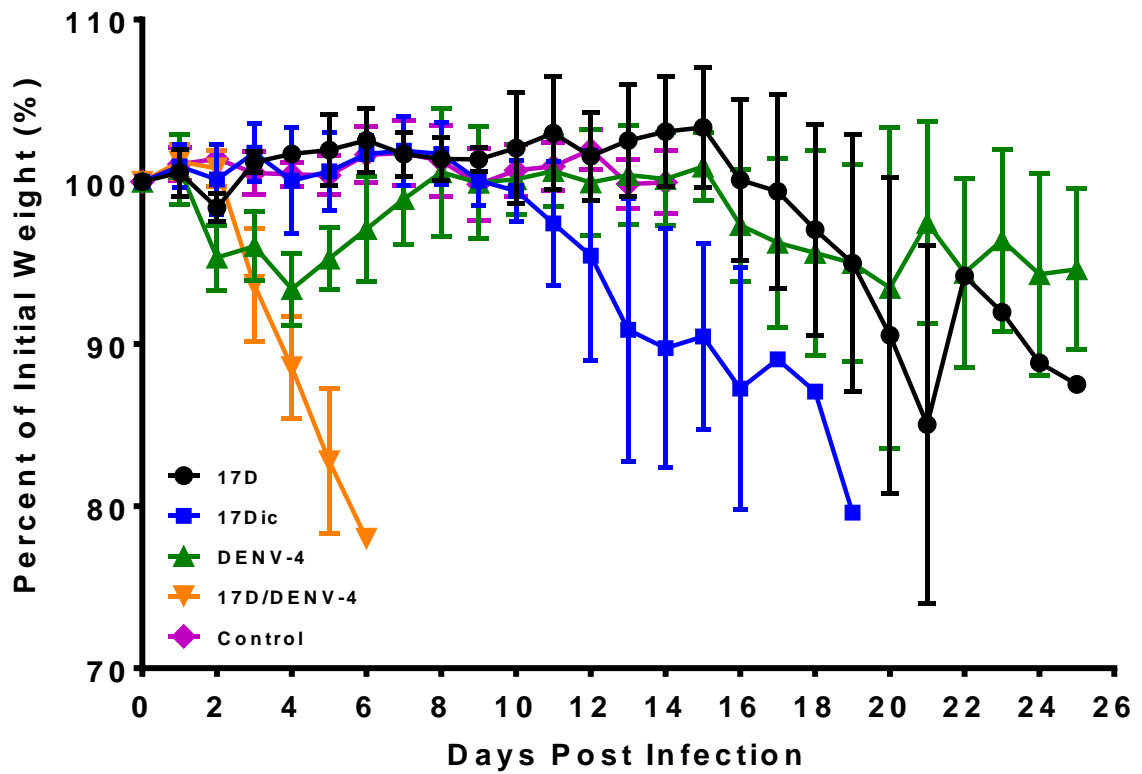
Figure 4.9. Weight loss of animals in experiment #1 with AG129 mice.
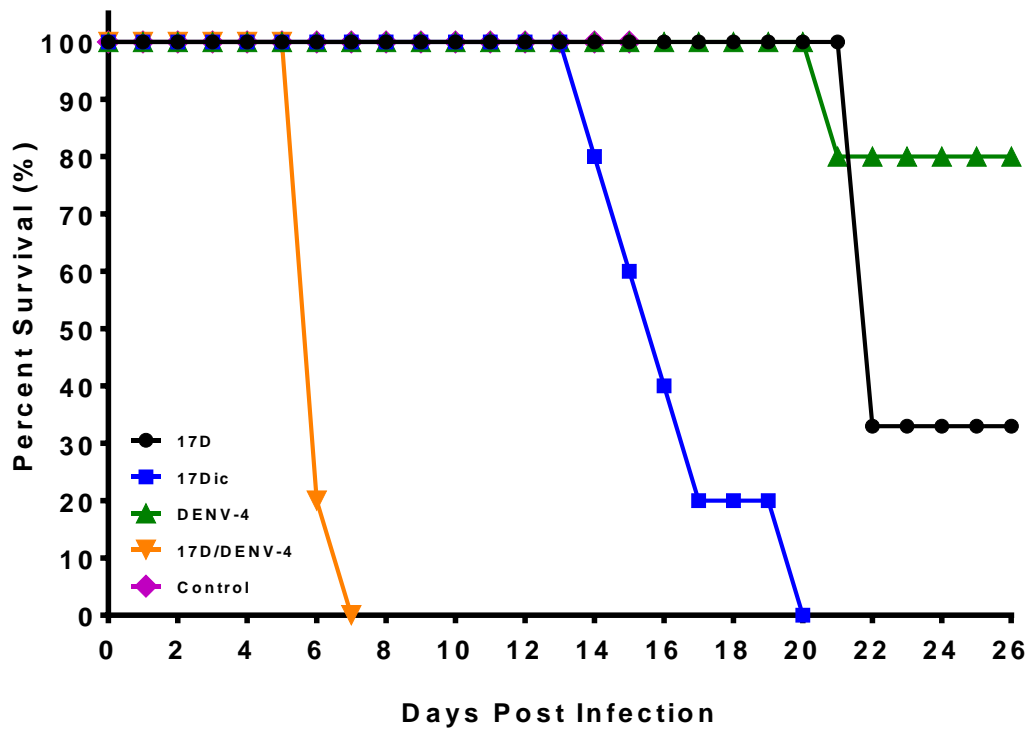
Figure 4.10. Survival curves of first AG129 mouse study.
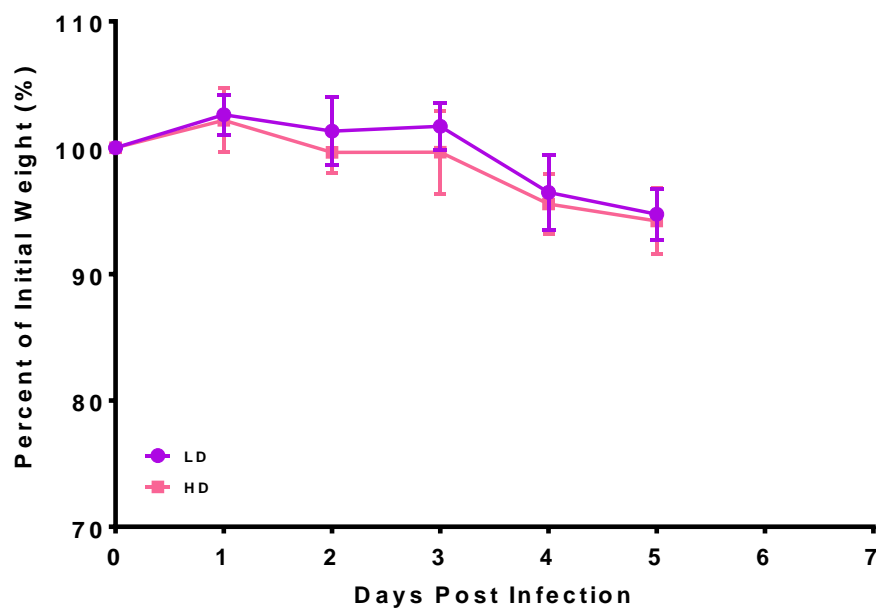
Figure 4.11. Weight loss of 10-week-old AG129 mice administered with YFV 17D/DENV-4 prME virus. LD is low dose 1.4 x 10^6 PFU in a 100µL volume HD is high dose: 2.8 x 10^6 PFU in a 200 µL volume
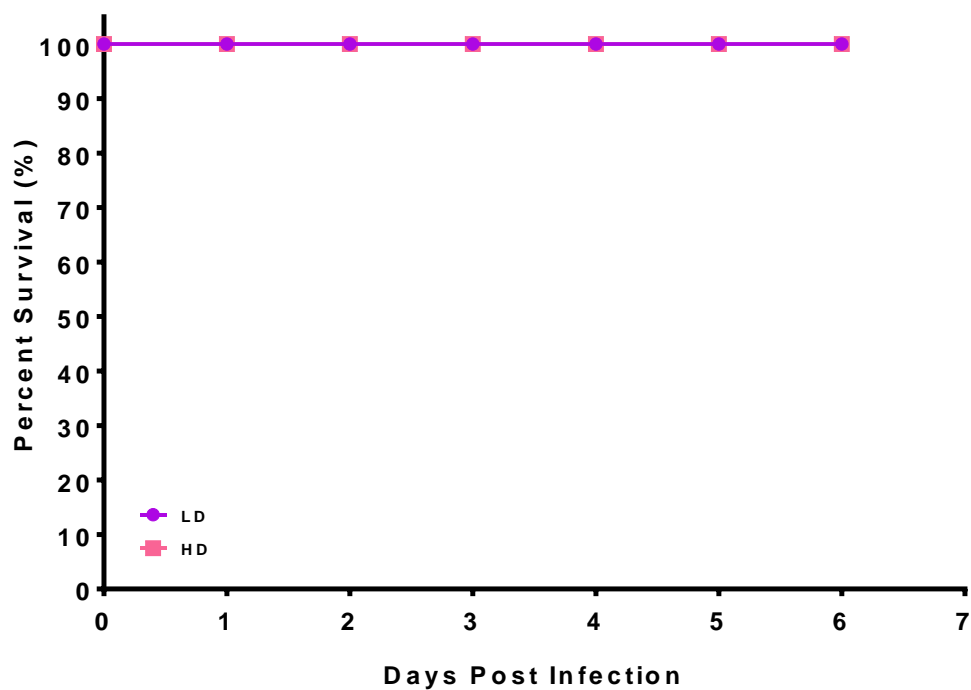
Figure 4.12. Survival curve of 10-week-old AG129 mice administered with YFV 17D/DENV-4 prME virus. LD is low dose 1.4 x 10^6 PFU in a 100µL volume HD is high dose: 2.8 x 10^6 PFU in a 200 µL volume
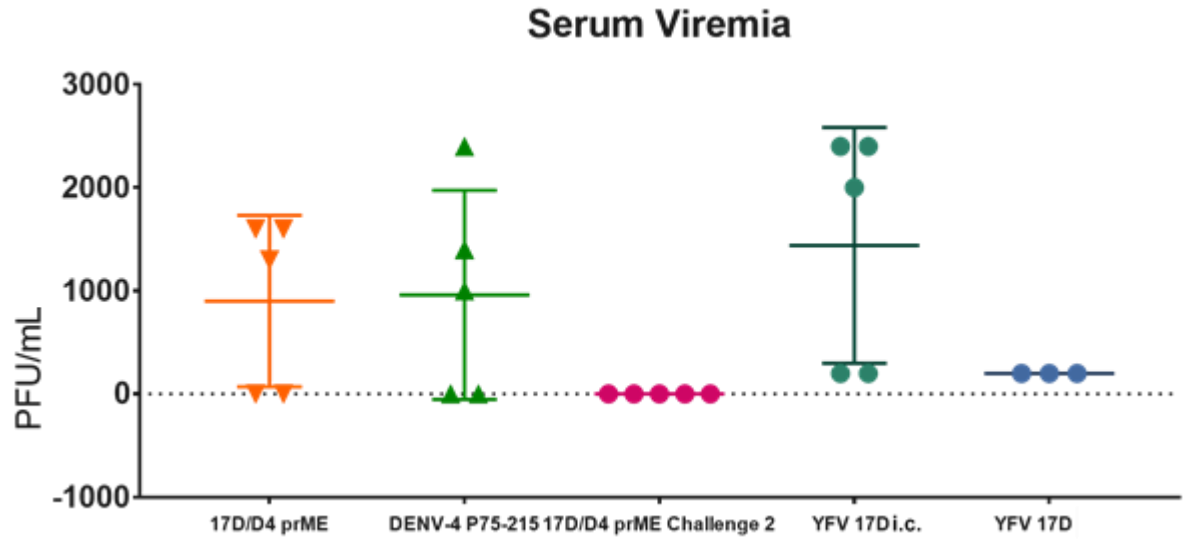
Figure 4.13. Viremias from day three post infection in experiment #1.
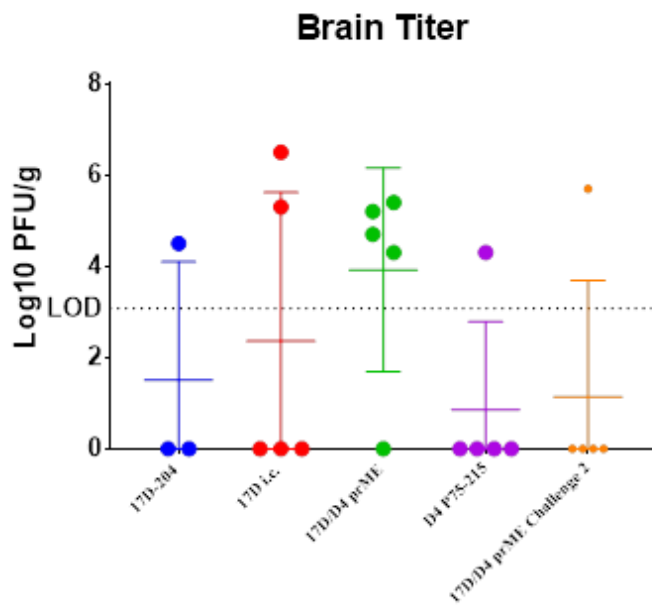
Figure 4.14. Brain titers of viruses of AG129 mice from experiment #1.
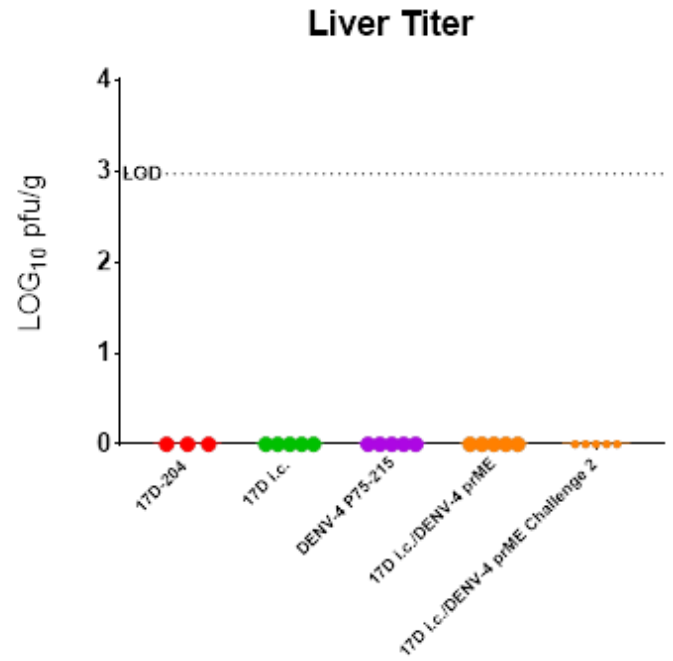
Figure 4.15. Liver titers of viruses of AG129 mice. In experiment #1
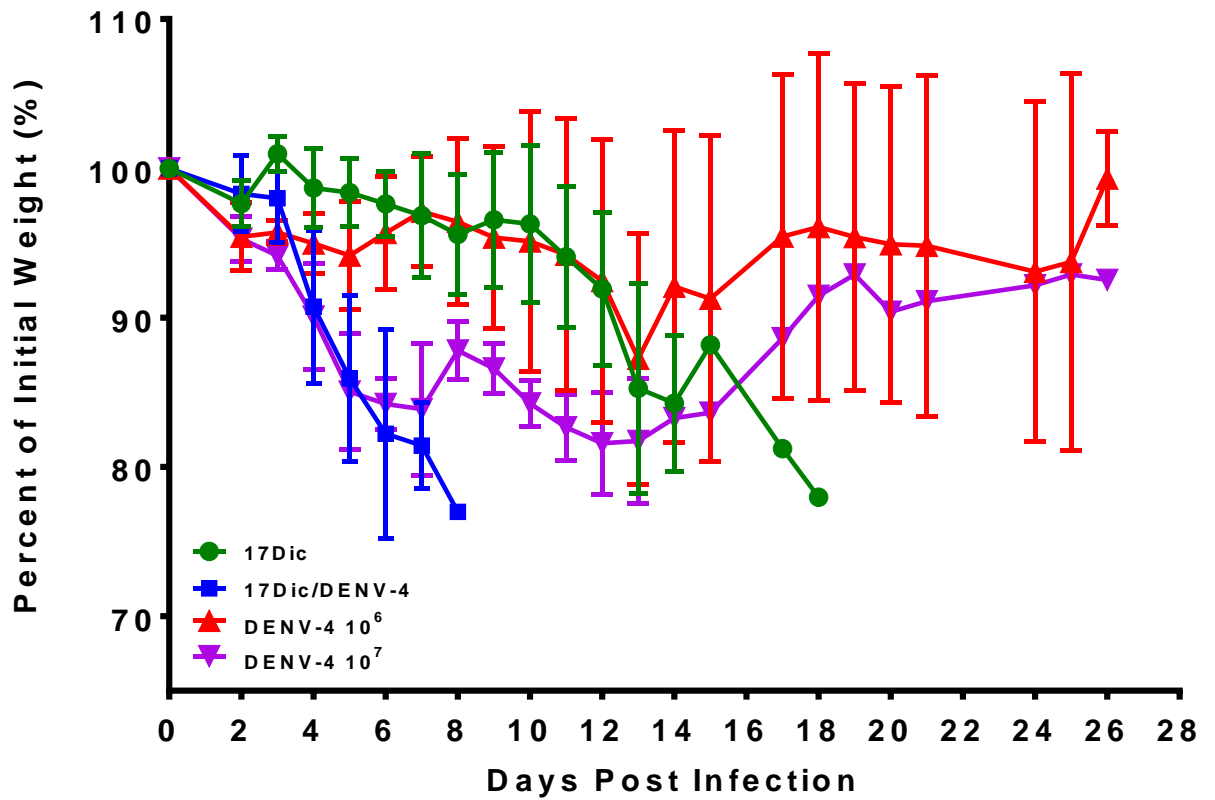
Figure 4.16. Weight loss of second AG129 mouse study. Virus titers used as follows: 17D i.c. was at 1.05×10^6 PFU, 17D ic/DENV-4 at 1.4×10^6 PFU, DENV-4 10^6 at 3.6×10^5 PFU, & DENV-4 10^7 at 1.4×10^7 PFU.
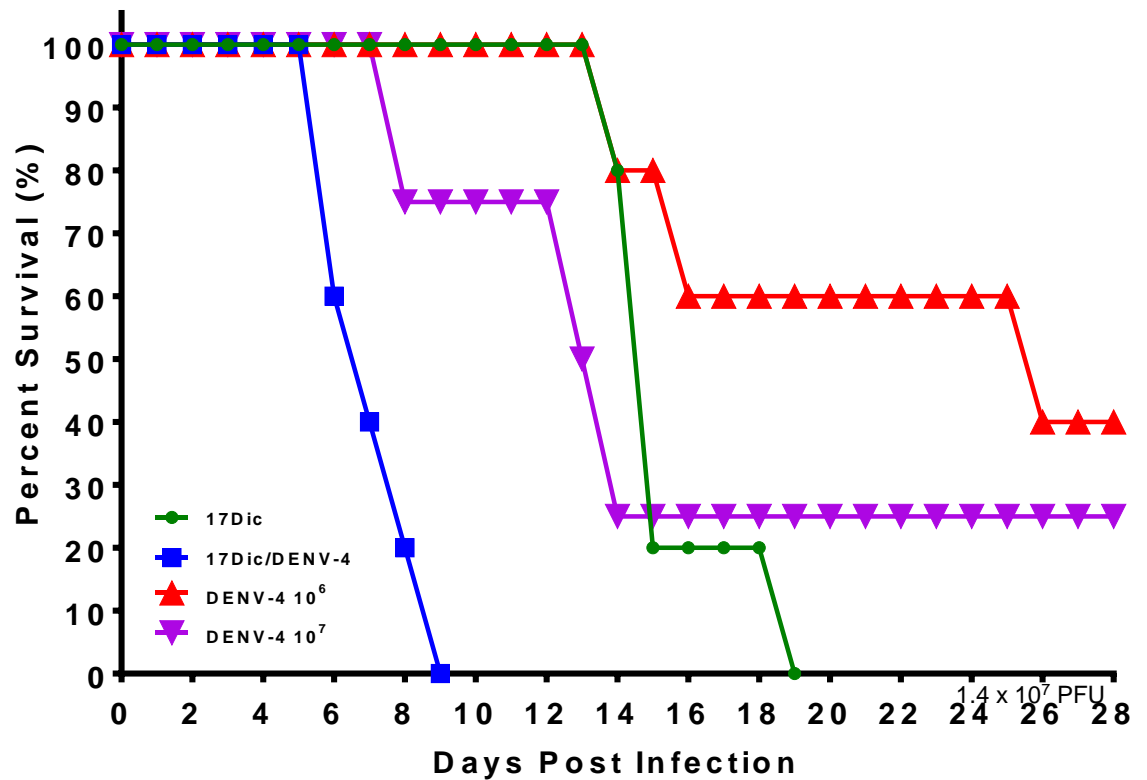
Figure 4.17. Survival curves of second AG129 mouse study. Virus titers used as follows: 17D i.c. was at 1.05×10^6 PFU, 17D ic/DENV-4 at 1.4×10^6 PFU, DENV-4 10^6 at 3.6×10^5 PFU, & DENV-4 10^7 at 1.4×10^7 PFU.
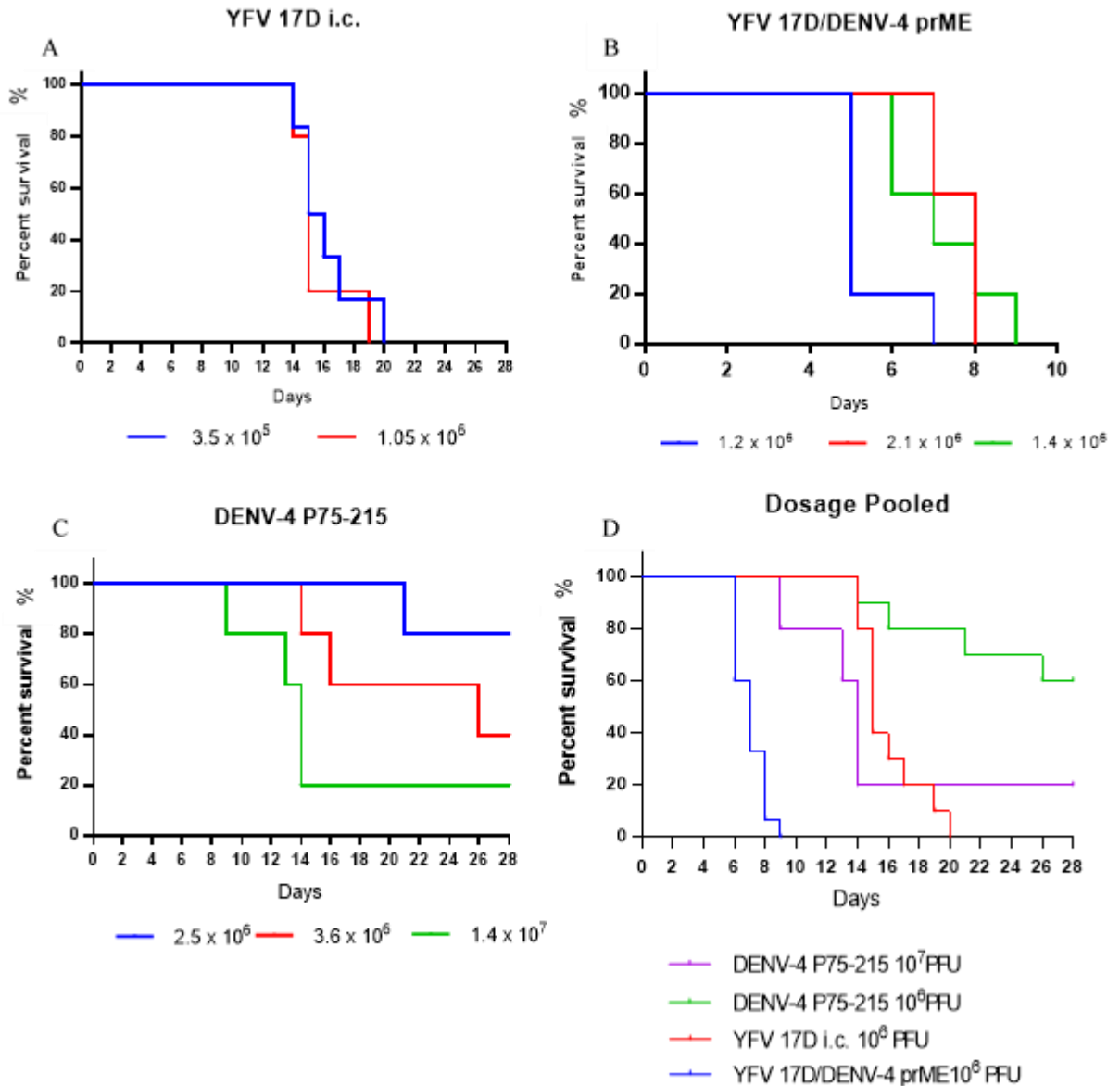
Figure 4.18. Comparisons of each animal study. Panel A demonstrates the YFV 17D infectious clone survival curves, showing that the curves are not significantly different (P=0.5497). Panel B demonstrates the YFV 17D/DENV-4 prME curves, showing that the curves are slightly different statistically (P=0.0143), but the trend is the same in all three studies. Panel C shows the comparison of the DENV-4 P75-215 comparisons, with the curves not statistically significant (P=0.0587). Panel D shows the pooled average animal data from all studies based on dosage, which demonstrates that there are significant differences between the curves (P<0.0001).

Chapter 5: Discussion

Flaviviruses have been considered a major public health threat for many years, and currently, there are very few licensed vaccines available. Many studies since the early 1990s have found use for ChimeriVax™ technology to develop flavivirus vaccine candidates (61, 65, 97, 101). The studies reported in this thesis utilized a methodology similar to that of ChimeriVax™, by generating a chimeric YFV 17D/DENV-4 prME virus, but using different restriction sites and donor DENV-4 prM/E sequences, and showed that the chimerization of this virus had variable effects of the genotype and phenotype of the virus. Notably, the diversity profile of this chimeric virus was like that of YFV 17D, and much less diverse than that of DENV-4 P75-215 (**Figure 4.2, Figure 4.3, Figure 4.4, Table 4.1**). This suggests that the hypothesis that chimerization results in decreased diversity was correct. Examination of the variant population by NGS (**Figure 4.6, 4.7, 4.8a, 4.8b,** and **Table 4.2, 4.3**) demonstrated that YFV 17D had a very low percentage of SNVs occurring in the population, in any area of the genome, as was shown by Beck et al (85). DENV-4 P75-215 had an average of 30 SNVs occurring in the population across the entire genome, as expected for a wild-type RNA virus, while YFV 17D/DENV-4 prME had a variant population that looked more like that of YFV 17D, with very few SNVs, with an average of 6 SNVs, occurring across the genome, with the exception of one region of high incidence, E257, which was a non-coding change and was confirmed in two NGS runs.

Surprisingly, the diversity of the DENV-4 prM/E genes in the chimera was higher than that of 17D prM/E as both 17D and the chimera had the same RdRp. This could indicate that this region is refractory to genetic diversity changes, hence making it more

difficult to attenuate. Further, the DENV samples studied demonstrated high diversity across the genome; analysis suggests that chimerization is reducing diversity in the regions of the genome containing DENV genes. This may lead to the suggestion that it may need further attenuation in this region. However, the diversity was lower than that of wild type DENV-4 P75-215. This further correlates with the hypothesis that the chimerization process does result in reduced genetic diversity but cannot be explained based on the role of the fidelity of the RdRp alone. The regions that were present in the YFV 17D/DENV-4 prME chimera that had lower diversity than YFV 17D (C, prM, NS2B, NS4B) support this theory. Viral multiplication kinetics performed in Vero cells indicated that all three viruses (YFV 17D, DENV-4 prME, and YFV 17D/DENV-4 prME) multiplied significantly different from each other at 12, 24, and 36 hours post infection (**Figure 4.1**). YFV 17D/DENV-4 prME was significantly different from DENV-4 P75-215 and YFV 17D at 48 and sixty hours post infection, while only 17D/DENV-4 prME was significantly different from DENV-4 P75-215 at 72 hours post infection (**Figure 4.1**). YFV 17D/DENV-4 P75-215 replicated significantly less efficiently than either of its parental viruses (YFV 17D and DENV-4 P75-215).

In A549 cells, the differences were more dramatic, where viral multiplication kinetics showed significant differences with YFV 17D the most efficient compared to DENV-4 P75-215 and YFV 17D/DENV-4 prME at all time points (**Figure 4.1**). DENV-4 P75-215 was found to be significantly different from YFV 17D/DENV-4 prME at 36, 60, and 72 hours post infection (**Figure 4.1**); thus, multiplication differences cannot be explained based on the swapping of the prM/E region of 17D for DENV-4. Since YFV 17D/DENV-4 prME and DENV-4 share the same prM and E genes, the observation that

they do not replicate as efficiently in A549 cells is likely due to an impairment in cellular entry resulting in virus replicating less efficiently in A549 cells due to the low MOI needing multiple rounds of replication so amplifying differences in multiplication kinetics. These results confirm the efficient multiplication of YFV 17D in Vero cells (85, 120). Interestingly, the data demonstrate the chimeric YFV 17D/DENV-4 prME virus has decreased multiplication efficiency when compared to that of its parental viruses (YFV 17D and DENV-4 P75-215, indicating that chimerization reduces the phenotypic property of the ability to multiply in cell culture, at least with the cell types used. Further studies would be needed to understand the mechanism for this difference.

In vivo studies were utilized to examine the virulence phenotype of the chimeric YFV 17D/DENV-4 prME virus compared to parental viruses (**Figure 4.9, 4.10, 4.11, 4.12, 4.16, 4.17**). These studies demonstrated that YFV 17D infectious clone, as well as YFV 17D vaccine virus, had the phenotype previously reported (88, 89). Average survival times for YFV 17D vaccine virus indicated that animals had an AST of approximately 18 days in previous literature, while the data in these studies suggest that the AST was 22 days (89). Furthermore, DENV-4 P75-215 resulted in expected lethality and disease for previously reported DENV-4 strains that were lethal in AG129 mice, except that the virus had an extended mean survival time compared to published DENV-4 strains (41–43). Average survival times for previous studies, in the literature, indicate that most animals survived until the termination of the study, with deaths occurring by day 10-15 post infection. The data obtained in this thesis indicated similar patterns, with most deaths occurring by day 15 (41–43). The chimeric YFV 17D/DENV-4 prME virus demonstrated very interesting results. Due to the decreased diversity of the virus and the

decreased viral multiplication in cell culture, it was predicted that this virus would be attenuated *in vivo*. However, the chimeric virus had the most virulent phenotype of the three viruses examined. Specifically, it had a much shorter mean day to death than the other two viruses (9 versus 20 days)

Brains and livers were examined in order to determine the presence of virus in these organs, and viremia samples from three days post infection of animals were also examined (**Figure 4.13, 4.14, 4.15**). The liver samples showed no detectable virus. This was not surprising, as it was not anticipated any of the viruses to have viscerotropic manifestations in the liver; thus, the chimera did not have an apparent change in tropism of 17D virus. The brain samples demonstrated irregular detection of virus, but there were no significant patterns in titration levels, groups, day of harvest, etc. The viremia samples presented similar data to that of the brains, albeit with much lower titer's detected. The viremia data indicated that some of the animals receiving YFV 17D infectious clone had low but detectable viremia. Two of the five animals which received YFV 17D infectious close were below the limit of detection, one of the five animals had a viremia of 2.0×10^3 ffu/mL, and two of the five animals had titers of 2.4×10^3 ffu/mL. Those which received YFV 17D 204 vaccine virus had no detectable viremia of day post-infection. Animals which received DENV-4 P75-215 exhibited detectable viremia with titers between 1.0×10^3 and 2.4×10^3 PFU/mL. All three of the mice infected at with YFV 17D/DENV-4 prME had detectable viremia, with the titers ranging between 1.3×10^3 and 1.6×10^3 PFU/mL. These values are comparable to previous studies performed in AG129 mice with similar viruses. Thus, the viremias on day 3 post-infection of chimeric YFV 17D/DENV-4 prME were similar to DENV-4 P75-215 virus, and not 17D infectious

clone or 17D-204 vaccine virus. However, viremias were not measured at later time points and it is possible that replicating virus would have been detectable in 17D infected mice and could be compared to YFV 17D/DENV-4 prME; albeit the chimera infected mice died by day 9 post infection.

The data fit into the current paradigm of RNA quasispecies, and the impact that this phenomenon plays on viral diversity and infectivity, except for the chimeric YFV 17D/DENV-4 prME. The data suggest the virus could be more pathogenic and this could be due to or the virus altered its genotype *in vivo* due to selection pressure in the mouse. The virus obtained from animal studies would need to be analyzed via NGS to address this hypothesis. The results of the NGS analysis shows that the chimeric virus is indeed less diverse than the DENV-4 P75-215 virus, even though it does have the prM and E genes of this virus. Thus, the process of chimerization, combined with the backbone of YFV 17D and the structural components of WT DENV-4 P75-215, does indeed cause a loss of viral diversity. This may be important moving forward, because this process may be able to be used to generate less diverse, possibly attenuated, viruses as effective candidate vaccines. This current paradigm suggests that the loss of diversity also results in a loss of virulence of the virus (109). However, the animal data are contradictory to this paradigm developed for poliovirus. It was originally anticipated that this would hold true for our chimeric virus considering the results obtained in the diversity analyses and the multiplication kinetics. Currently, there are no published results for the analysis of AG129 studies utilizing viruses generated using ChimeriVax™ technology.

The studies described in this thesis are, to the authors knowledge, the first of their type, and thus examine an important phenomenon. Animal studies of chimeric viruses

utilizing NHPs seemed to demonstrate safety and efficacy, with none of the puzzling results that were obtained with our AG129 studies (62, 96, 99, 103). There are possible reasons to explain why the chimeric YFV 17D/DENV-4 prME exhibits reduced diversity, but seems to have enhanced virulence when compared to that of its parental YFV 17D and DENV-4 P75-215 viruses. One possible reason for this phenomenon is that the backbone of YFV 17D, which contains the YFV 17D RdRp, which mediates a more efficient replication process of the virus *in vivo*, due to its putative high fidelity RdRp (86). Another possibility, which may be combined with the theory of a higher fidelity RdRp, is the possibility that the prM and E regions inserted into the YFV 17D backbone results in more efficient entry of the virus in to cells *in vivo*, hence allowing enhanced replication. A more simplistic explanation is that this is partially due to the lack of IFN response in AG129 mice, hence allowing a more severe infection to occur. Yet another option is that the chimerization process does decrease the diversity of the chimeric YFV 17D/DENV-4 virus, but it is not enough of a genetic change to fully attenuate it. There are nine amino acid differences in the structural region of YFV 17D that differ from virulent YFV Asibi (85) . There have been studies done on ChimeriVax-JE™, trade name Imojev, which demonstrated that there were certain markers that could be used to explain virulence and attenuation (98). This lends to the idea that perhaps further attenuation is necessary of this chimeric virus, possibly in the prM and/or E regions, to lead to a discernable *in vivo* attenuation.

Overall conclusions from this work lead to the following propositions. The lower diversity of YFV 17D/DENV-4 prME compared to that of DENV-4, and even YFV 17D in some regions, do indeed suggest that the process of viral chimerization results in

reduced viral diversity. However, when this was tested *in vivo*, it was discovered that the chimera was virulent, and killed mice faster and to a higher degree than either parental virus, YFV 17D or DENV-4 P75-215. The results of the multiplication kinetics show that the chimeric YFV 17D/DENV-4 prME replicates less efficiently in both Vero and A549 cells, with a significant decrease in multiplication when compared to YFV 17D and DENV-4 P75-215 viruses. This suggests that the chimerization process must be impacting replication efficiency somehow; however, the presence of low level viremia and tissue titers indicate that the virus is replicating. The animal studies indicate that the structural prM and E genes of DENV-4 P75-215 cause increased virulence compared to both parental viruses, hence leading to the theory that it may need further attenuation, perhaps via point mutations in the prM and E regions. The data from the multiplication kinetics and the animal studies demonstrate that there is a difference in replication capacity *in vivo* and *in vitro*. This further lends to the theory that perhaps the chimera needs to be further attenuated in order to see changes both *in vitro* and *in vivo*.

Future studies would seek to further attenuate the chimera, possibly via site directed mutagenesis of the prM and E regions initially, to examine the role of these changes on viral diversity and *in vivo* attenuation. The paradoxical results of the *in vitro* data, which demonstrate decreased diversity and multiplication in Vero and A549 cells, may be further clarified via performance of single cell PCR to examine replication efficiency of the viruses. If there is a possible problem with entry in to cells, this may be elucidated by electron microscopy, ELISA assays, or binding assays. Further animal studies may be performed to investigate the role of viral chimerization on diversity and pathogenicity. Samples from *in vitro* multiplication kinetic curves, as well as serum and

homogenized tissue samples may be examined by NGS to see if diversity changes once the virus has infected cells in cell culture or animals plus it would be useful to assess immune activation and cytokine presence via Bioplex assays. This work would be vital to the development of highly safe and effective countermeasures for flaviviruses, and perhaps may be able to be applied to other RNA viral populations as well.

References

1. **Simmonds P**, **Becher P**, **Bukh J**, **Gould EA**, **Meyers G**, **Monath T**, **Muerhoff S**, **Pletnev A**, **Rico-Hesse R**, **Smith DB**, **Stapleton JT**, **Consortium IR**. 2017. ICTV virus taxonomy profile: Flaviviridae. J Gen Virol **98**:1161–1162.
2. **Moureau G**, **Cook S**, **Lemey P**, **Nougairede A**, **Forrester NL**, **Khasnatinov M**, **Charrel RN**, **Firth AE**, **Gould EA**, **De Lamballerie X**. 2015. New insights into flavivirus evolution, taxonomy and biogeographic history, extended by analysis of canonical and alternative coding sequences e0117849. PLoS One **10**.
3. **Kuno G**, **Chang GJ**, **Tsuchiya KR**, **Cropp CB**, **Kuno G**, **Chang GJ**, **Tsuchiya KR**, **Karabatsos N**. 1998. Phylogeny of the Genus Flavivirus Phylogeny of the Genus Flavivirus **72**:72–83.
4. **Calisher CH**, **Karabatsos N**, **Dalrymple JM**, **Shope RE**, **Porterfield JS**, **Westaway EG**, **Brandt WE**. 1989. Antigenic relationships between flaviviruses as determined by cross-neutralization tests with polyclonal antisera. J Gen Virol **70**:37–43.
5. **Osorio JE**, **Brewoo JN**, **Silengo SJ**, **Arguello J**, **Moldovan IR**, **Tary-Lehmann M**, **Powell TD**, **Livengood JA**, **Kinney RM**, **Huang CYH**, **Stinchcomb DT**. 2011. Efficacy of a tetravalent chimeric dengue vaccine (DENVax) in cynomolgus macaques. Am J Trop Med Hyg **84**:978–987.
6. **Schweitzer BK**, **Chapman NM**, **Iwen PC**. 2009. Overview of the Flaviviridae With an Emphasis on the Japanese Encephalitis Group Viruses. Lab Med **40**:493–499.
7. **Smit JM**, **Moesker B**, **Rodenhuis-Zybert I**, **Wilschut J**. 2011. Flavivirus cell entry and membrane fusion. Viruses **3**:160–171.
8. **Mukhopadhyay S**, **Kuhn RJ**, **Rossmann MG**. 2005. A structural perspective of the flavivirus life cycle. Nat Rev Microbiol **3**:13–22.
9. **Bressanelli S**, **Stiasny K**, **Allison SL**, **Stura EA**, **Duquerroy S**, **Lescar J**, **Heinz FX**, **Rey FA**. 2004. Structure of a flavivirus envelope glycoprotein in its low-pH-induced membrane fusion conformation. EMBO J **23**:728–738.
10. **Westaway EG**, **Brinton MA**, **SYa G**, **Horzinek MC**, **Igarashi A**, **Kaariainen L**, **Lvov DK**, **Porterfield JS**, **Russell PK**, **Trent DW**. 1985. Flaviviridae. Intervirology **24**:183–192.
11. **Lubick KJ**, **Robertson SJ**, **McNally KL**, **Freedman BA**, **Rasmussen AL**, **Taylor RT**, **Walts AD**, **Tsuruda S**, **Sakai M**, **Ishizuka M**, **Boer EF**, **Foster EC**, **Chiramel AI**, **Addison CB**, **Green R**, **Kastner DL**, **Katze MG**, **Holland SM**, **Forlino A**, **Freeman AF**, **Boehm M**, **Yoshii K**, **Best SM**. 2015. Flavivirus Antagonism of Type I Interferon Signaling Reveals Prolidase as a Regulator of IFNAR1 Surface Expression. Cell Host Microbe **18**:61–74.
12. **Bollati M**, **Alvarez K**, **Assenberg R**, **Baronti C**, **Canard B**, **Cook S**, **Coutard B**, **Decroly E**, **de Lamballerie X**, **Gould EA**, **Grard G**, **Grimes JM**, **Hilgenfeld R**, **Jansson AM**, **Malet H**, **Mancini EJ**, **Mastrangelo E**, **Mattevi A**, **Milani M**, **Moureau G**, **Neyts J**, **Owens RJ**, **Ren J**, **Selisko B**, **Speroni S**, **Steuber H**,

        Stuart DI, **Unge T**, **Bolognesi M**. 2010. Structure and functionality in flavivirus NS-proteins: Perspectives for drug design. Antiviral Res **87**:125–148.

13. **Helenius A**. 1995. Alphavirus and flavivirus glycoproteins: Structures and functions. Cell **81**:651–653.
14. **Perera-Lecoin M**, **Meertens L**, **Carnec X**, **Amara A**. 2013. Flavivirus entry receptors: An update. Viruses **6**:69–88.
15. **Gromowski GD**, **Barrett ND**, **Barrett ADT**. 2008. Characterization of dengue virus complex-specific neutralizing epitopes on envelope protein domain III of dengue 2 virus. J Virol **82**:8828–8837.
16. **Muller DA**, **Young PR**. 2013. The flavivirus NS1 protein: Molecular and structural biology, immunology, role in pathogenesis and application as a diagnostic biomarker. Antiviral Res **98**:192–208.
17. **Takamatsu Y**, **Morita K**, **Hayasaka D**. 2015. A Single Amino Acid Substitution in the NS2A Protein of Japanese Encephalitis Virus Affects Virus Propagation *In Vitro* but Not *In Vivo*. J Virol **89**:6126–6130.
18. **Voßmann S**, **Wieseler J**, **Kerber R**, **Kümmerer BM**. 2015. A basic cluster in the N terminus of yellow fever virus NS2A contributes to infectious particle production. J Virol **89**:4951–65.
19. **Wu R-H**, **Tsai M-H**, **Tsai K-N**, **Tian JN**, **Wu J-S**, **Wu S-Y**, **Chern J-H**, **Chen C-H**, **Yueh A**. 2017. Mutagenesis of Dengue Virus Protein NS2A Revealed a Novel Domain Responsible for Virus-Induced Cytopathic Effect and Interactions between NS2A and NS2B Transmembrane Segments. J Virol **91**:e01836-16.
20. **Peterson L**, **Barrett A**. 2009. Arthropod-Borne Flaviviruses, p. 1173–1214. *In* Clinical Virology, Third Edition.
21. **Guilarde AO**, **Turchi MD**, **Jr. JBS**, **Feres VCR**, **Rocha B**, **Levi JE**, **Souza VAUF**, **Boas LSV**, **Pannuti CS**, **Martelli CMT**. 2008. Dengue and Dengue Hemorrhagic Fever among Adults: Clinical Outcomes Related to Viremia, Serotypes, and Antibody Response. J Infect Dis **197**:817–824.
22. **Osorio JE**, **Partidos CD**, **Wallace D**, **Stinchcomb DT**. 2015. Development of a recombinant, chimeric tetravalent dengue vaccine candidate. Vaccine **33**:7112–7120.
23. **World Health Organization (WHO)**. 2016. WHO | Dengue and severe dengue. Who.
24. **Chen R**, **Vasilakis N**. 2011. Dengue-Quo tu et quo vadis? Viruses **3**:1562–1608.
25. **Gubler DJ**. 1997. Epidemic dengue/dengue haemorrhagic fever: a global public health problem in the 21st century. Dengue Bull **21**:1–14.
26. **Vasilakis N**, **Weaver SC**. 2008. Chapter 1 The History and Evolution of Human Dengue EmergenceAdvances in Virus Research. Elsevier Inc.
27. **Christophers SR**. 1960. Aëdes Aegypti (L.) The Yellow Fever Mosquito: Its Life History, Bionomics and Structure. Cambridge University Press.
28. **SMITH CEG**. 1956. The history of dengue in tropical Asia and its probable relationship to the mosquito Aedes aegypti. J Trop Med Hyg **59**:243–251.
29. **Wang E**, **Ni H**, **Xu R**, **Barrett a D**, **Watowich SJ**, **Gubler DJ**, **Weaver SC**. 2000. Evolutionary relationships of endemic/epidemic and sylvatic dengue viruses. J Virol **74**:3227–3234.
30. **Zompi S**, **Harris E**. 2012. Animal models of dengue virus infection. Viruses

4:62–82.

31.	**SABIN AB**. 1952. Research on dengue during World War II. Am J Trop Med Hyg **1**:30–50.

32.	**Schlesinger RW**. 1977. Dengue viruses. Virol Monogr 1–132.

33.	**Raut CG**, **Deolankar RP**, **Kolhapure RM**, **Goverdhan MK**. 1996. Susceptibility of laboratory-bred rodents to the experimental infection with dengue virus type 2. Acta Virol **40**:143–146.

34.	**Shresta S**, **Kyle JL**, **Beatty PR**, **Harris E**. 2004. Early activation of natural killer and B cells in response to primary dengue virus infection in A/J mice. Virology **319**:262–273.

35.	**Chen HC**, **Lai SY**, **Sung JM**, **Lee SH**, **Lin YC**, **Wang WK**, **Chen YC**, **Kao CL**, **King CC**, **Wu-Hsieh BA**. 2004. Lymphocyte activation and hepatic cellular infiltration in immunocompetent mice infected by dengue virus. J Med Virol **73**:419–431.

36.	**Chen H-C**, **Hofman FM**, **Kung JT**, **Lin Y-D**, **Wu-Hsieh BA**. 2007. Both virus and tumor necrosis factor alpha are critical for endothelium damage in a mouse model of dengue virus-induced hemorrhage. J Virol **81**:5518–26.

37.	**Blaney JE**, **Johnson DH**, **Manipon GG**, **Firestone C-Y**, **Hanson CT**, **Murphy BR**, **Whitehead SS**. 2002. Genetic Basis of Attenuation of Dengue Virus Type 4 Small Plaque Mutants with Restricted Replication in Suckling Mice and in SCID Mice Transplanted with Human Liver Cells. Virology **300**:125–139.

38.	**Paes M V.**, **Pinhão AT**, **Barreto DF**, **Costa SM**, **Oliveira MP**, **Nogueira AC**, **Takiya CM**, **Farias-Filho JC**, **Schatzmayr HG**, **Alves AMB**, **Barth OM**. 2005. Liver injury and viremia in mice infected with dengue-2 virus. Virology **338**:236–246.

39.	**Souza DG**, **Fagundes CT**, **Sousa LP**, **Amaral FA**, **Souza RS**, **Souza AL**, **Kroon EG**, **Sachs D**, **Cunha FQ**, **Bukin E**, **Atrasheuskaya A**, **Ignatyev G**, **Teixeira MM**. 2009. Essential role of platelet-activating factor receptor in the pathogenesis of Dengue virus infection. Proc Natl Acad Sci U S A **106**:14138–43.

40.	**Johnson AJ**, **Roehrig JT**. 1999. New Mouse Model for Dengue Virus Vaccine Testing **73**:783–786.

41.	**Sarathy V V.**, **Infante E**, **Li L**, **Campbell GA**, **Wang T**, **Paessler S**, **Beatty PR**, **Harris E**, **Milligan GN**, **Bourne N**, **Barrett ADT**. 2015. Characterization of lethal dengue virus type 4 (DENV-4) TVP-376 infection in mice lacking both IFN-??/?? and IFN-?? receptors (AG129) and comparison with the DENV-2 AG129 mouse model. J Gen Virol **96**:3035–3048.

42.	**Milligan GN**, **Sarathy V V.**, **Infante E**, **Li L**, **Campbell GA**, **Beatty PR**, **Harris E**, **Barrett ADT**, **Bourne N**. 2015. A dengue virus type 4 model of disseminated lethal infection in AG129 mice. PLoS One **10**:1–21.

43.	**Milligan GN**, **Sarathy V V.**, **White MM**, **Greenberg MB**, **Campbell GA**, **Pyles RB**, **Barrett ADT**, **Bourne N**. 2017. A lethal model of disseminated dengue virus type 1 infection in AG129 mice. J Gen Virol.

44.	**Lin YL**, **Liao CL**, **Chen LK**, **Yeh CT**, **Liu CI**, **Ma SH**, **Huang YY**, **Huang YL**, **Kao CL**, **King CC**. 1998. Study of Dengue virus infection in SCID mice engrafted with human K562 cells. J Virol **72**:9729–9737.

45.	**Mota J**, **Rico-Hesse R**. 2009. Humanized mice show clinical signs of dengue

fever according to infecting virus genotype. J Virol **83**:8638–45.

46. **Mota J**, **Rico-Hesse R**. 2011. Dengue virus tropism in humanized mice recapitulates human dengue fever. PLoS One **6**:2–11.

47. **Prestwood TR**, **Morar MM**, **Zellweger RM**, **Miller R**, **May MM**, **Yauch LE**, **Lada SM**, **Shresta S**. 2012. Gamma Interferon (IFN-) Receptor Restricts Systemic Dengue Virus Replication and Prevents Paralysis in IFN- / Receptor-Deficient Mice. J Virol **86**:12561–12570.

48. **Orozco S**, **Schmid MA**, **Parameswaran P**, **Lachica R**, **Henn MR**, **Beatty R**, **Harris E**. 2012. Characterization of a model of lethal dengue virus 2 infection in C57BL/6 mice deficient in the alpha/beta interferon receptor. J Gen Virol **93**:2152–2157.

49. **Halstead SB**, **Shotwell H**, **Casals J**. 1973. Studies on the pathogenesis of dengue infection in monkeys. I. Clinical laboratory responses to primary infection. J Infect Dis **128**:7–14.

50. **Halstead SB**, **Shotwell H**, **Casals J**. 1973. Studies on the pathogenesis of dengue infection in monkeys. II. Clinical laboratory responses to heterologous infection. J Infect Dis **128**:15–22.

51. **Onlamoon N**, **Noisakran S**, **Hsiao H-M**, **Duncan A**, **Villinger F**, **Ansari AA**, **Perng GC**. 2010. Dengue virus–induced hemorrhage in a nonhuman primate model. Blood **115**:1823–1834.

52. **Thomas SJ**, **Rothman AL**. 2015. Trials and Tribulations on the Path to Developing a Dengue Vaccine. Am J Prev Med **49**:S334–S344.

53. **Whitehead SS**, **Durbin AP**, **Pierce KK**, **Elwood D**, **McElvany BD**, **Fraser EA**, **Carmolli MP**, **Tibery CM**, **Hynes NA**, **Jo M**, **Lovchik JM**, **Larsson CJ**, **Doty EA**, **Dickson DM**, **Luke CJ**, **Subbarao K**, **Diehl SA**, **Kirkpatrick BD**. 2017. In a randomized trial, the live attenuated tetravalent dengue vaccine TV003 is well-tolerated and highly immunogenic in subjects with flavivirus exposure prior to vaccination. PLoS Negl Trop Dis **11**:1–19.

54. Dengue Vaccine Registered in 19 Countries _ Sanofi Pasteur _ Dengue Info.

55. **Guy B**, **Lang J**, **Saville M**, **Jackson N**. 2015. Vaccination Against Dengue: Challenges and Current Developments INTRODUCTION: DENGUE DISEASE AND QUESTIONS TO BE ADDRESSED DURING VACCINE DEVELOPMENT **18**:1–18.

56. **Halstead SB**, **Russell PK**. 2016. Protective and immunological behavior of chimeric yellow fever dengue vaccine. Vaccine **34**:1643–1647.

57. **Mantel N**, **Girerd Y**, **Geny C**, **Bernard I**, **Pontvianne J**, **Lang J**, **Barban V**. 2011. Genetic stability of a dengue vaccine based on chimeric yellow fever/dengue viruses. Vaccine **29**:6629–6635.

58. **Higgs S**, **Vanlandingham DL**, **Klingler KA**, **McElroy KL**, **McGee CE**, **Harrington L**, **Lang J**, **Monath TP**, **Guirakhoo F**. 2006. Growth characteristics of chimerivax-den vaccine viruses in Aedes aegypti and Aedes albopictus from Thailand. Am J Trop Med Hyg **75**:986–993.

59. **Balas C**, **Kennel A**, **Deauvieau F**, **Sodoyer R**, **Arnaud-Barbe N**, **Lang J**, **Guy B**. 2011. Different innate signatures induced in human monocyte-derived dendritic cells by wild-type dengue 3 virus, attenuated but reactogenic dengue 3 vaccine virus, or attenuated nonreactogenic dengue 1-4 vaccine virus strains. J Infect Dis

203:103–108.

60. **Guirakhoo F**, **Weltzin R**, **Chambers TJ**, **Zhang ZX**, **Soike K**, **Ratterree M**, **Arroyo J**, **Georgakopoulos K**, **Catalan J**, **Monath TP**. 2000. Recombinant chimeric yellow fever-dengue type 2 virus is immunogenic and protective in nonhuman primates. J Virol **74**:5477–85.

61. **Guirakhoo F**, **Pugachev K**, **Zhang Z**, **Myers G**, **Levenbook I**, **Draper K**, **Lang J**, **Ocran S**, **Mitchell F**, **Parsons M**, **Brown N**, **Brandler S**, **Fournier C**, **Barrere B**, **Rizvi F**, **Travassos A**, **Nichols R**, **Trent D**, **Monath T**. 2004. Safety and efficacy of chimeric yellow Fever-dengue virus tetravalent vaccine formulations in nonhuman primates. J Virol **78**:4761–75.

62. **Guy B**, **Guirakhoo F**, **Barban V**, **Higgs S**, **Monath TP**, **Lang J**. 2010. Preclinical and clinical development of YFV 17D-based chimeric vaccines against dengue, West Nile and Japanese encephalitis viruses. Vaccine **28**:632–649.

63. **Guirakhoo F**, **Kitchener S**, **Morrison D**, **Forrat R**, **McCarthy K**, **Nichols R**, **Yoksan S**, **Duan X**, **Ermak TH**, **Kanesa-Thasan N**, **Bedford P**, **Lang J**, **Quentin-Millet M-J**, **Monath TP**. 2014. Live Attenuated Chimeric Yellow Fever Dengue Type 2 (ChimeriVax^{TM}-DEN2) Vaccine: Phase I Clinical Trial for Safety and Immunogenicity: Effect of Yellow Fever Pre-immunity in Induction of Cross Neutralizing Antibody Responses to All. Hum Vaccin **2**:60–67.

64. **Capeding MR**, **Tran NH**, **Hadinegoro SRS**, **Ismail HIHM**, **Chotpitayasunondh T**, **Chua MN**, **Luong CQ**, **Rusmil K**, **Wirawan DN**, **Nallusamy R**, **Pitisuttithum P**, **Thisyakorn U**, **Yoon IK**, **Van Der Vliet D**, **Langevin E**, **Laot T**, **Hutagalung Y**, **Frago C**, **Boaz M**, **Wartel TA**, **Tornieporth NG**, **Saville M**, **Bouckenooghe A**. 2014. Clinical efficacy and safety of a novel tetravalent dengue vaccine in healthy children in Asia: A phase 3, randomised, observer-masked, placebo-controlled trial. Lancet **384**:1358–1365.

65. **Villar L**, **Dayan GH**, **Arredondo-García JL**, **Rivera DM**, **Cunha R**, **Deseda C**, **Reynales H**, **Costa MS**, **Morales-Ramírez JO**, **Carrasquilla G**, **Rey LC**, **Dietze R**, **Luz K**, **Rivas E**, **Montoya MCM**, **Supelano MC**, **Zambrano B**, **Langevin E**, **Boaz M**, **Tornieporth N**, **Saville M**, **Noriega F**. 2014. Efficacy of a Tetravalent Dengue Vaccine in Children in Latin America. N Engl J Med **372**:141103114505002.

66. **Ferguson NM**, **Rodríguez-Barraquer I**, **Dorigatti I**, **Mier-y-Teran-Romero L**, **Laydon DJ**, **Cummings DAT**. 2016. Benefits and risks of the Sanofi-Pasteur dengue vaccine: Modeling optimal deployment. Science (80-) **353**:1033–1036.

67. **Huang CY-H**, **Butrapet S**, **Tsuchiya KR**, **Bhamarapravati N**, **Gubler DJ**, **Kinney RM**. 2003. Dengue 2 PDK-53 virus as a chimeric carrier for tetravalent dengue vaccine development. J Virol **77**:11436–47.

68. **Bhamarapravati N**, **Yoksan S**, **Chayaniyayothin T**, **Angsubphakorn S**, **Bunyaratvej A**. 1987. Immunization with a live attenuated dengue-2-virus candidate vaccine (16681-PDK 53): Clinical, immunological and biological responses in adult volunteers. Bull World Health Organ **65**:189–195.

69. **Kinney RM**, **Butrapet S**, **Chang G-JJ**, **Tsuchiya KR**, **Roehrig JT**, **Bhamarapravati N**, **Gubler DJ**. 1997. Construction of Infectious cDNA Clones for Dengue 2 Virus: Strain 16681 and Its Attenuated Vaccine Derivative, Strain PDK-53. Virology **230**:300–308.

70. **Osorio JE**, **Huang CYH**, **Kinney RM**, **Stinchcomb DT**. 2011. Development of DENVax: A chimeric dengue-2 PDK-53-based tetravalent vaccine for protection against dengue fever. Vaccine **29**:7251–7260.

71. **Brewoo JN**, **Kinney RM**, **Powell TD**, **Arguello JJ**, **Silengo SJ**, **Partidos CD**, **Huangy CYH**, **Stinchcomb DT**, **Osorio JE**. 2012. Immunogenicity and efficacy of chimeric dengue vaccine (DENVax) formulations in interferon-deficient AG129 mice Joseph. Vaccine **30**:1513–1520.

72. **Durbin AP**, **Karron RA**, **Sun W**, **Vaughn DW**, **Reynolds MJ**, **Perreault JR**, **Thumar B**, **Men R**, **Lai CJ**, **Elkins WR**, **Chanock RM**, **Murphy BR**, **Whitehead SS**. 2001. Attenuation and immunogenicity in humans of a live dengue virus type-4 vaccine candidate with a 30 nucleotide deletion in its 3′-untranslated region. Am J Trop Med Hyg **65**:405–413.

73. **Troyer JM**, **Hanley KA**, **Whitehead SS**, **Strickman D**, **Karron RA**, **Durbin AP**, **Murphy BR**. 2001. A live attenuated recombinant dengue-4 virus vaccine candidate with restricted capacity for dissemination in mosquitoes and lack of transmission from vaccinees to mosquitoes. Am J Trop Med Hyg **65**:414–419.

74. **Durbin AP**, **Whitehead SS**, **McArthur J**, **Perreault JR**, **Blaney, Jr. JE**, **Thumar B**, **Murphy BR**, **Karron RA**. 2005. rDEN4Δ30, a Live Attenuated Dengue Virus Type 4 Vaccine Candidate, Is Safe, Immunogenic, and Highly Infectious in Healthy Adult Volunteers. J Infect Dis **191**:710–718.

75. **Men R**, **Bray M**, **Clark D**, **Chanock RM**, **Lai C-J**. 1996. Dengue Type 4 Virus Mutants Containing Deletions in the 3J Noncoding Region of the RNA Genome: Analysis of Growth Restriction in Cell Culture and Altered Viremia Pattern and Immunogenicity in Rhesus Monkeys. J Virol **70**:3930–3937.

76. **Durbin AP**, **Kirkpatrick BD**, **Pierce KK**, **Elwood D**, **Larsson CJ**, **Lindow JC**, **Tibery C**, **Sabundayo BP**, **Shaffer D**, **Talaat KR**, **Hynes NA**, **Wanionek K**, **Carmolli MP**, **Luke CJ**, **Murphy BR**, **Subbarao K**, **Whitehead SS**. 2013. A single dose of any of four different live attenuated tetravalent dengue vaccines is safe and immunogenic in flavivirus-naive adults: A randomized, double-blind clinical trial. J Infect Dis **207**:957–965.

77. **Schmitz J**, **Roehrig JT**, **Barrett A**, **Hombach J**. 2011. Next generation dengue vaccines: A review of the preclinical development pipeline. Vaccine **29**:7276–7284.

78. **Clements DE**, **Coller BG**, **Lieberman MM**, **Ogata S**, **Harada KE**, **Putnak JR**, **Ivy JM**, **Mcdonell M**, **Gary S**, **Peters ID**, **Leung J**, **Weeks-levy C**, **Nakano ET**, **Humphreys T**. 2010. Development of a Recombinant Tetravalent Dengue Virus Vaccine: Immunogenicity and Efficacy Studies in Mice and Monkeys. Vaccine **28**:2705–2715.

79. **Coller BG**, **Clements DE**, **Bett AJ**, **Sagar SL**, **ter Meulen JH**. 2011. The development of recombinant subunit envelope based vaccines to protect against dengue virus induced disease. Vaccine **29**:7267–7275.

80. **Beckett CG**, **Tjaden J**, **Burgess T**, **Danko JR**, **Tamminga C**, **Simmons M**, **Wu SJ**, **Sun P**, **Kochel T**, **Raviprakash K**, **Hayes CG**, **Porter KR**. 2011. Evaluation of a prototype dengue-1 DNA vaccine in a Phase 1 clinical trial. Vaccine **29**:960–968.

81. **Julander JG**. 2016. Animal models of yellow fever and their application in

clinical research. Curr Opin Virol **18**:64–69.

82. **Monath TP**, **Vasconcelos PFC**. 2015. Yellow fever. J Clin Virol **64**:160–173.

83. **Frierson JG**. 2010. The yellow fever vaccine: a history. Yale J Biol Med **83**:77–85.

84. **Theiler BYMAX**, **Smith HH**. 1937. The effect of prolonged cultivation in vitro upon the pathogencity of yellow fever virus.

85. **Beck A**, **Tesh RB**, **Wood TG**, **Widen SG**, **Ryman KD**, **Barrett ADT**. 2014. Comparison of the live attenuated yellow fever vaccine 17D-204 strain to its virulent parental strain Asibi by deep sequencing. J Infect Dis **209**:334–44.

86. **Pugachev K V**, **Guirakhoo F**, **Ocran SW**, **Mitchell F**, **Parsons M**, **Penal C**, **Girakhoo S**, **Pougatcheva SO**, **Arroyo J**, **Trent DW**, **Monath TP**. 2004. High fidelity of yellow fever virus RNA polymerase. J Virol **78**:1032–8.

87. **Sukupolvi-Petty S**, **Austin SK**, **Engle M**, **Brien JD**, **Dowd KA**, **Williams KL**, **Johnson S**, **Rico-Hesse R**, **Harris E**, **Pierson TC**, **Fremont DH**, **Diamond MS**. 2010. Structure and Function Analysis of Therapeutic Monoclonal Antibodies against Dengue Virus Type 2. J Virol **84**:9227–9239.

88. **Meier KC**, **Gardner CL**, **Khoretonenko M V.**, **Klimstra WB**, **Ryman KD**. 2009. A mouse model for studying viscerotropic disease caused by yellow fever virus infection. PLoS Pathog **5**.

89. **Thibodeaux BA**, **Garbino NC**, **Liss NM**, **Piper J**, **Blair CD**, **Roehrig JT**. 2012. A small animal peripheral challenge model of yellow fever using interferon-receptor deficient mice and the 17D-204 vaccine strain. Vaccine **30**:3180–3187.

90. **Erickson a. K**, **Pfeiffer JK**. 2015. Spectrum of disease outcomes in mice infected with YFV-17D. J Gen Virol 1328–1339.

91. **Tesh RB**, **Guzman H**, **da Rosa AP**, **Vasconcelos PF**, **Dias LB**, **Bunnell JE**, **Zhang H**, **Xiao SY**. 2001. Experimental yellow fever virus infection in the Golden Hamster (Mesocricetus auratus). I. Virologic, biochemical, and immunologic studies. J Infect Dis **183**:1431–1436.

92. **Mcarthur MA**, **Suderman MT**, **Xiao S**, **Barrett ADT**, **Mutebi J**. 2003. Molecular Characterization of a Hamster Viscerotropic Strain of Yellow Fever Virus Molecular Characterization of a Hamster Viscerotropic Strain of Yellow Fever Virus **77**:1462–1468.

93. **Monath TP**. 2008. Treatment of yellow fever. Antiviral Res **78**:116–124.

94. **Fan Z**, **Li W**, **Lee SR**, **Meng Q**, **Shi B**, **Bunch TD**, **White KL**, **Kong IK**, **Wang Z**. 2014. Efficient gene targeting in golden Syrian hamsters by the CRISPR/Cas9 system. PLoS One **9**:1–9.

95. **Toth K**, **Lee SR**, **Ying B**, **Spencer JF**, **Tollefson AE**, **Sagartz JE**, **Kong IK**, **Wang Z**, **Wold WSM**. 2015. STAT2 Knockout Syrian Hamsters Support Enhanced Replication and Pathogenicity of Human Adenovirus, Revealing an Important Role of Type I Interferon Response in Viral Control. PLoS Pathog **11**:1–22.

96. **Guirakhoo F**, **Zhang Z**, **Chambers TJ**, **Delagrave S**, **Arroyo J**, **Barrett ADT**, **Monath TP**. 1999. Immunogenicity, Genetic Stability, and Protective Efficacy of a Recombinant, Chimeric Yellow Fever-Japanese Encephalitis Virus (ChimeriVax-JE) as a Live, Attenuated Vaccine Candidate against Japanese Encephalitis. Virology **257**:363–372.

97. **Chambers TJ**, **Nestorowicz A**, **Mason PW**, **Rice CM**. 1999. Yellow fever/Japanese encephalitis chimeric viruses: construction and biological properties. J Virol **73**:3095–101.

98. **Arroyo J**, **Guirakhoo F**, **Fenner S**, **Zhang ZX**, **Monath TP**, **Chambers TJ**. 2001. Molecular basis for attenuation of neurovirulence of a yellow fever Virus/Japanese encephalitis virus chimera vaccine (ChimeriVax-JE). J Virol **75**:934–942.

99. **Monath TP**, **Soike K**, **Levenbook I**, **Zhang ZX**, **Arroyo J**, **Delagrave S**, **Myers G**, **Barrett ADT**, **Shope RE**, **Ratterree M**, **Chambers TJ**, **Guirakhoo F**. 1999. Recombinant, chimaeric live, attenuated vaccine (ChimeriVax(TM)) incorporating the envelope genes of Japanese encephalitis (SA14-14-2) virus and the capsid and nonstructural genes of yellow fever (17D) virus is safe, immunogenic and protective in non-hum. Vaccine **17**:1869–1882.

100. **Arroyo J**, **Guirakhoo F**, **Fenner S**, **Zhang ZX**, **Monath TP**, **Chambers TJ**. 2001. Molecular basis for attenuation of neurovirulence of a yellow fever Virus/Japanese encephalitis virus chimera vaccine (ChimeriVax-JE). J Virol **75**:934–42.

101. **Monath TP**, **McCarthy K**, **Bedford P**, **Johnson CT**, **Nichols R**, **Yoksan S**, **Marchesani R**, **Knauber M**, **Wells KH**, **Arroyo J**, **Guirakhoo F**. 2002. Clinical proof of principle for ChimeriVax^{TM}: Recombinant live, attenuated vaccines against flavivirus infections. Vaccine **20**:1004–1018.

102. **Monath TP**, **Guirakhoo F**, **Nichols R**, **Yoksan S**, **Schrader R**, **Murphy C**, **Blum P**, **Woodward S**, **McCarthy K**, **Mathis D**, **Johnson C**, **Bedford P**. 2003. Chimeric live, attenuated vaccine against Japanese encephalitis (ChimeriVax-JE): phase 2 clinical trials for safety and immunogenicity, effect of vaccine dose and schedule, and memory response to challenge with inactivated Japanese encephalitis antigen. J Infect Dis **188**:1213–1230.

103. **Arroyo J**, **Miller C**, **Catalan J**, **Myers GA**, **Ratterree MS**, **Trent DW**, **Monath TP**. 2004. ChimeriVax-West Nile Virus Live-Attenuated Vaccine : Preclinical Evaluation of Safety , Immunogenicity , and Efficacy. J Virol **78**:12497–12507.

104. **Monath TP**, **Liu J**, **Kanesa-Thasan N**, **Myers G a**, **Nichols R**, **Deary A**, **McCarthy K**, **Johnson C**, **Ermak T**, **Shin S**, **Arroyo J**, **Guirakhoo F**, **Kennedy JS**, **Ennis F a**, **Green S**, **Bedford P**. 2006. A live, attenuated recombinant West Nile virus vaccine. Proc Natl Acad Sci U S A **103**:6694–6699.

105. **Biedenbender R**, **Bevilacqua J**, **Gregg AM**, **Watson M**, **Dayan G**. 2011. Phase II, randomized, double-blind, placebo-controlled, multicenter study to investigate the immunogenicity and safety of a West Nile virus vaccine in healthy adults. J Infect Dis **203**:75–84.

106. **De Filette M**, **Ulbert S**, **Diamond MS**, **Sanders NN**. 2012. Recent progress in West Nile virus diagnosis and vaccination. Vet Res **43**:16.

107. **Iyer A V.**, **Kousoulas KG**. 2013. A review of vaccine approaches for West Nile virus. Int J Environ Res Public Health **10**:4200–4223.

108. **Lauring AS**, **Andino R**. 2010. Quasispecies Theory and the Behavior of RNA Viruses. PLoS Pathog **6**:e1001005.

109. **Vignuzzi M**, **Stone JK**, **Arnold JJ**, **Cameron CE**, **Andino R**. 2006. Quasispecies Diversity Determines Pathogenesis through Cooperative Interactions Within a

Viral Population. Nature **439**:344–348.

110. **Domingo E**. 1998. Quasispecies and the implications for virus persistence and escape. Clin Diagn Virol **10**:97–101.
111. **Domingo E**, **Martín V**, **Perales C**, **Grande-Pérez A**, **García-Arriaza J**, **Arias A**. 2006. Viruses as quasispecies: Biological implications. Curr Top Microbiol Immunol **299**:51–82.
112. **Domingo E**, **Sheldon J**, **Perales C**. 2012. Viral Quasispecies Evolution. Microbiol Mol Biol Rev **76**:159–216.
113. **Pugachev K V.**, **Guirakhoo F**, **Trent DW**, **Monath TP**. 2003. Traditional and novel approaches to flavivirus vaccines. Int J Parasitol **33**:567–582.
114. Illumina_Sequencing_Introduction.Pdf.
115. **Ammerman N**, **Beier-Sexton M**, **Azad A**. 2008. Growth and Maintenance of Vero Cell Lines. Curr Protoc Microbiol **Appendix-4**:1–10.
116. **Rossi SL**, **Nasar F**, **Cardosa J**, **Mayer S V.**, **Tesh RB**, **Hanley KA**, **Weaver SC**, **Vasilakis N**. 2012. Genetic and phenotypic characterization of sylvatic dengue virus type 4 strains. Virology **423**:58–67.
117. **Domingo E**. 2001. Quasispecies: Concepts and Implications for Virology.
118. **Sarathy V V.**, **Milligan GN**, **Bourne N**, **Barrett ADT**. 2015. Mouse models of dengue virus infection for vaccine testing. Vaccine **33**:7051–7060.
119. **Pitcher TJ**, **Sarathy V V.**, **Matsui K**, **Gromowski GD**, **Huang CY-H**, **Barrett ADT**. 2015. Functional analysis of dengue virus (DENV) type 2 envelope protein domain 3 type-specific and DENV complex-reactive critical epitope residues. J Gen Virol **96**:288–293.
120. **Barrett ADT**, **Higgs S**. 2007. Yellow Fever: A Disease that Has Yet to be Conquered. Annu Rev Entomol **52**:209–229.

VITA

Courtney P. Cromer was born on November 13, 1990 to Robin and Paige Parker in Altamonte Springs, Florida. Soon after, she moved to Sikes, Louisiana, where she was raised and attended high school in Dodson, Louisiana. In 2009, she moved to Shreveport, Louisiana to attend Louisiana State University in Shreveport. While attending university, she worked as a student ambassador in the Admissions and Records office, as well as a student worker at the Biomedical Research Institute. In 2013, she obtained a Bachelor's of Science degree in Cellular and Molecular Biology. In August of 2014, she moved to Galveston, Texas to attend graduate school at University of Texas Medical Branch. In April of 2017, she married Walter E. Cromer, Ph.D.

Education

B.S., May 2013, Louisiana State University in Shreveport, Shreveport, Louisiana

Publications

Chaitanya GV, Cromer WE, **Parker CP**, Couraud PO, Romero IA, Weksler B, Mathis JM, Minagar A, Alexander JS. A Recombinant Inhibitory Isoform of Vascular Endothelial Growth Factor164/165 Aggravates Ischemic Brain Damage in a Mouse Model of Focal Cerebral Ischemia. *Am J Pathol.* 2013 Jul 29. pii: S0002-9440(13)00422-7. doi: 10.1016/j.ajpath.2013.06.009.

Christopher P. Monceaux, Traci L. Testerman, Moheb Boktor, Paul Jordan, Patrick Adegboyega, David J. McGee, Merilyn H. Jennings, **Courtney P. Parker**, Shelly Gupta, Ping Yi, Vijay C. Ganta, Haidy Galous, Kenneth Manas, J. Steven Alexander. *Helicobacter* infection decreases basal colon inflammation, but increases disease activity in experimental IBD. *OJGas.* 3.3: 177-189

Permanent address: 4402 Wild Rose Hill Lane, Richmond, Texas 77469

This dissertation was typed by Courtney Parker Cromer.